The utility of LiDAR for landscape biodiversity assessment

A thesis submitted in fulfilment of the requirements for
the degree of Doctor of Philosophy in Applied Science

Naoko Miura
M.Sc. and LL.B.

School of Mathematical and Geospatial Sciences
College of Science, Engineering and Technology
RMIT University
August 2010

DECLARATION

I certify that except where due acknowledgement has been made, the work is that of the author alone; the work has not been submitted previously, in whole or in part, to qualify for any other academic award; the content of the thesis is the result of work which has been carried out since the official commencement date of the approved research program; any editorial work, paid or unpaid, carried out by a third party is acknowledged; and, ethics procedures and guidelines have been followed.

Signature:

Name: Naoko Miura

Date:

ACKNOWLEDGEMENTS

First of all, I would like to acknowledge all the support and advice from my primary supervisor, Prof. Simon Jones. I would not have completed this research without his patient and encouraging support. I am also grateful to my second supervisor, Assoc. Prof. Chris Bellman for his valuable comments on my thesis.

I would like to thank RMIT University for the financial support via its RUIS scholarship scheme. I am also thankful to the Australian Commonwealth Environment Research Fund "Landscape Logic" Project for its support and the provision of the initial data, and to the State Emergency Service and the Commonwealth Natural Disaster Mitigation Programme for the provision of the additional data.

I would like to acknowledge Prof. Tony Norton (University of Tasmania), Mr. James Shaddick (Cradle Coast NRM) and Dr. Karyl Michaels (University of Tasmania) for their support in the fieldwork. I am grateful to Assoc. Prof. Jorg Hacker and Mr. Wolfgang Lieff (Airborne Research Australia), and Dr. Holger Eichstaedt (Digital Mapping Australia) for their advice on LiDAR datasets. I would also like to thank Mr. Rodney Deakin (RMIT) for his invaluable assistance and the RMIT Remote Sensing Group for their support, especially those who helped me with the field data collection (Dr. Kathryn Sheffield, Grant Dickins, Dr. Danielle Martin, Yin Lee and Alex Lechner).

I really appreciate my family and all my friends for their support here in Melbourne and in Japan. I would not have survived difficult times without their kind and strong support. Thank you!

TABLE OF CONTENTS

LIST OF TABLES

LIST OF FIGURES

LIST OF ABBREVIATIONS

AVIRIS	Airborne Visible/Infrared Imaging Spectrometer
CBD	Convention on Biological Diversity
CC	Canopy cover (FCS category 4)
CHM	Canopy Height Model
CLIPSO	Cloud Aerosol Lidar and Infrared Pathfinder Satellite Observations
CWD	Coarse Woody Debris
DBH	Diameter at Breast Height
DEM	Digital Elevation Model
DGPS	Differential Global Positioning System
D_H	Vertically dense canopy of high trees (FCS category 8)
DSM	Digital Surface Model
DTM	Digital Terrain Model
EMR	Electromagnetic Radiation
EVC	Ecological Vegetation Class
FCS	Forest Characterisation Scheme
fPAR	fraction of Photosynthetically Active Radiation
FRI_C	First return intensity in Canopy stratum
FRI_G	First return intensity in Ground stratum
GLAS	Geoscience Laser Altimeter System
GPE	Gaussian Pulse Estimation
GPF	Gaussian Pulse Fitting
GPS	Global Positioning System
ICESat	Ice, Cloud, and land Elevation Satellite
IMU	Inertial Measurement Unit
LAI	Leaf Area Index
Laser	Light amplification by stimulated emission of radiation
LiDAR	Light Detection and Ranging
LRI_C	Last return intensity in Canopy stratum
LRI_G	Last return intensity in Ground stratum
MODIS	Moderate Resolution Imaging Spectroradiometer
NDVI	Normalized Difference Vegetation Index
O_G	Opening above the ground (FCS category 1)
O_L	Opening above low vegetation (FCS category 2)
O_M	Opening above medium vegetation (FCS category 5)
POS	Position and Orientation System
PRF	Pulse Repetition Frequency
RMSE	Root Mean Square Error
Rader	Radio Detection and Ranging
RTK	Real Time Kinematic
SPOT-5	Satellite Pour l'Observation de la Terre
TIN	Triangular Irregular Network
TOF	Time of Flight
VCA	Vegetation Condition Assessment
V_H	Presence of high trees (FCS category 7)
V_L	Presence of understorey vegetation (FCS category 3)
V_M	Presence of mid-storey vegetation (FCS category 6)
WGS84	World Geodetic System 1984

ABSTRACT

Since the UN Convention on Biological diversity (CBD) held in Rio de Janeiro in 1992, conservation of biodiversity has been recognised internationally as critically important for sustainability. Forest structure variables have been recognized as a surrogate of biodiversity. In Australia, existing vegetation monitoring methods also assess forest structure variables. However, these assessments require costly fieldwork, are often logistically difficult and to a large degree qualitative. Light Detection and Ranging (LiDAR) is an active sensing technology. There is well documented evidence of the utility of LiDAR to extract forest structure variables and potential to compliment traditional ecological survey methods.

In this thesis, the potential of LiDAR to inform landscape biodiversity assessments was investigated. The objectives of this research are to examine how LiDAR discrete return and full waveform systems can be used to recover forest structure information, how LiDAR intensity can be used for biodiversity assessment and whether the utility of LiDAR can compliment traditional ecological survey methods. Experiments using LiDAR discrete return and full waveform systems were conducted. An eight category forest characterisation scheme (FCS) derived from a LiDAR full waveform system was proposed and validated using field derived variables. Intensity variables derived from a LiDAR full waveform system were explored to determine their utility. The applicability of the proposed scheme was also examined by comparing two independent LiDAR full waveform datasets of the same area and by comparing the LiDAR derived FCS to commonly used field-based biodiversity metrics.

From these surveys, it was concluded that conventional discrete return systems can be used

to recover forest structure information for forests with an ecologically simple structure (i.e. single tree species with no mid- and understorey vegetation except grass and relatively flat terrain). Vertically stratified LiDAR intensity, using range information, has potential to recover canopy cover, grass cover and the amount of fallen trees. The combination of LiDAR intensity mean and standard deviation can be used to differentiate forest structural types; sparse canopy with few fallen trees or dense canopy with many fallen trees.

The LiDAR full waveform system experiment demonstrated that the FCS, which was created using pulse types and heights of a full waveform LiDAR, allows for quantification of gaps (above bare ground, low vegetation and medium vegetation), canopy cover and its vertical density as well as the presence of various canopy strata (low, medium and high). Regression analysis showed all LiDAR derived variables were good predictors of field recorded variables (e.g. $R^2 = 0.86$, $P < 0.05$ between LiDAR derived canopy cover and field derived canopy cover). The FCS clearly showed the potential of full waveform LiDAR to provide information on the complexity of habitat structure.

The exploratory analysis of intensity derived from a LiDAR full waveform system displayed the potential of intensity variables (the standard deviation of intensity and the intensity version of FCS) to recover forest structure variables, however it was noted that the analysis using intensity variables could be site specific. It was also noted that the selection of sensor with appropriate wavelength for the study would be critical to use intensity information. Further study is required to account for the utility of intensity variables.

In terms of the applicability of the FCS, a multiple dataset comparison showed that the FCS was resilient when recovering canopy cover, openings above the ground and medium

vegetation, and presence of mid-storey vegetation and high trees, however it was less so when recovering openings above low vegetation, the presence of understorey vegetation and vertical canopy density of high trees. These last categories were considered to be affected by the difference in the pulse repetition frequency. Obtaining sufficient multiple returns by setting an appropriate pulse repetition frequency is the key to maintaining good performance of the scheme. The FCS was also found to be incompatible with commonly used field-based biodiversity metrics due to the qualitative and subjective measurements used in field-based metrics. Refinement in field methodology would be necessary for measuring structural variables to maximise the utility of FCS in their metrics.

This study demonstrated how LiDAR technology (conventional discrete return system and full waveform systems) can be used to derive forest structure information for landscape biodiversity assessment. The method proposed in this study is versatile, repeatable and quantitative, which can provide useful information to inform decisions and conservation strategies.

CHAPTER 1 INTRODUCTION

This thesis investigates the potential of Light Detection and Ranging (LiDAR) to inform landscape biodiversity assessments. In this thesis, biodiversity is defined in accordance with the UN Convention on Biological Diversity (CBD) (Articles 7, 8 & 9). This states that biodiversity is understood in terms of the variety of species, genetic differences and ecosystems, and in a landscape context, in terms of landscape diversity and natural habitat (Secretariat of the Convention on Biological Diversity, 2000). The aim of this thesis is to develop a methodology to measure a surrogate of biodiversity to inform decisions made at a landscape scale, using airborne LiDAR data, field survey data and existing environmental information.

Since the UN CBD, held in Rio de Janeiro in 1992, conservation of biodiversity has been recognised internationally as critically important for sustainability. The CBD cited forest biodiversity as the most rich of all terrestrial systems holding the vast majority of the world's terrestrial species (Secretariat of the Convention on Biological diversity, 2005). A range of national and international initiatives have been established and commitments were made by governments for the maintenance of biodiversity through the sustainable management of forest ecosystems (McElhinny, 2002). For example, in Canada, a number of criteria such as biological diversity and ecosystem condition and productivity, and indicators such as area of forest, by type and age class, and wetlands in each ecozone, have been developed through the Canadian Council of Forest Ministers Framework of Criteria and indicators for sustainable forest management released in 1995. This provides a science-based framework to define and measure Canada's progress in the sustainable management

of its forests (Canadian Council of Forest Ministers, 2003). In Finland, National Forest Programme 2015, which is financed by seven government ministries and private sectors, has been proposed to provide new competitive forest products and services with an increase in the use of domestic wood and an improvement in forest biodiversity (Secretariat of the Convention on Biological Diversity, 2010). As such measurements are required at all levels of government from the international scale to the local scale to maintain biodiversity and the effectiveness of any management invention (Ahern et al., 2003). At the landscape level, a robust, practical way of defining and measuring biodiversity is a priority for managers (Noss, 1990).

Forest structure information has been recognised as a surrogate of biodiversity (e.g. Mac Nally et al., 2001; Noss, 1990). Many authors have noted the association between biodiversity and measures of the variety and/or complexity of arrangement of structural components within an ecosystem (e.g. Mac Nally et al., 2001; Sullivan et al., 2001). Furthermore, the habitat complexity of a forest structure can be used to predict the occurrence of some species, since such information provides locally specific descriptions of faunal habitat (Catling and Burt, 1995; Jorgensen, 2002; Psyllakis and Gillingham, 2009; Tanabe et al., 2001; Verschuyl et al., 2008; Watson et al., 2001). In Australia, vegetation condition monitoring is mandated at the state level. These vegetation condition monitoring assessments are recognised as biodiversity management tools and assess forest structure information. However, these assessments require costly fieldwork and laborious processes that presently involve site visits and point based measurements of botanical and ecological variables. They are also to a large degree qualitative. An efficient and cost-effective total sampling assessment tool to compliment these survey methods would be ideal.

LiDAR is an active sensor technology that propagates its own source of Electromagnetic Radiation (EMR) and the timed difference between pulse generation and return allows for the measurement of the range distance between sensor and the illuminated object. Compared with 2D information derived from passive remote sensing technology, LiDAR can provide highly accurate 3D information. The potential for using LiDAR data for deriving forest attributes at the level of the forest stand has been widely studied in forestry (e.g. Lefsky et al., 1999a; Næsset, 2002; Nelson et al., 1984). There is an increasing interest in applying this technology to ecological research (e.g. Goetz et al., 2007; Vehmas et al., 2009). In particular, the potential of LiDAR for extracting forest structure information for biodiversity assessment and in complimenting traditional survey methods is apparent.

This thesis explores the potential of LiDAR technology for biodiversity assessments. LiDAR sensors used in this thesis include a conventional discrete return system and the latest full waveform systems. Although the latest systems are more powerful and capable of providing detailed information, they have not been widely used in biodiversity research and such systems are far less common than conventional discrete return systems. For example, large areas in Australia have already been surveyed using conventional discrete return systems. Therefore, examining the potential of the conventional system could provide practical utility, and exploring the latest systems could show the potential of LiDAR for land management agencies and natural resource management groups. The information which can be derived from LiDAR data includes intensity of backscattered pulses as well as 3D information of the objects. However, to date, the utility of LiDAR intensity has been limited due to difficulties with calibration and associated problems in its interpretation. The utility of intensity information is another issue to explore for determining how we can use LiDAR technology for biodiversity assessments.

The objective of this research is to develop a robust, quantifiable and repeatable method able to assess biodiversity. In particular, the ability of LiDAR to recover forest structure information is modelled. To address these aims, the following research questions are posed.

Research questions are:

1. What, if any, forest structure information can be extracted from data produced by a LiDAR discrete return system?

2. Does a LiDAR full waveform system provide additional or higher quality forest structure information?

3. Can LiDAR intensity values be used to recover forest structure information?

4. Can the utility of LiDAR compliment traditional ecological survey methods?

In this thesis, following chapters are presented. Chapter 1 provides context and a broad overview of the thesis, and presents the objectives of this research. Chapter 2 presents a literature review of how forest structure has been attributed and used for biodiversity assessments including existing field assessment methods in Australia. Previous work using passive remotely sensed methods is summarised. LiDAR technology is also reviewed and discussed in the context of its potential for extracting forest structure information. Chapter 3 evaluates the utility and potential of conventional discrete return systems for biodiversity assessment. The work presented in this chapter addresses research questions 1 and 3. Chapter 4 provides a background for a LiDAR full waveform system experiment describing the study area, the LiDAR data used and the fieldwork protocols developed specifically for this LiDAR experiment. Chapter 5 examines whether LiDAR full

waveform system data can provide more detailed forest structure information relative to conventional discrete return systems. An eight category of forest characterisation scheme derived from LiDAR data is proposed to characterise the ecological structure of a dry Eucalypt forest landscape and validated using field derived variables. This work addresses research question 2. Chapter 6 explores the utility of the return intensity derived from a LiDAR full waveform system. The intensity variables are examined to determine whether they can give more insights into intensity response of full waveform data from forested landscape and enhance the potential of LiDAR data to recover forest structure variables. The work reported in this chapter addresses research question 3. Chapter 7 assesses the applicability of the previously proposed LiDAR based forest characterisation scheme. The robustness of the proposed scheme is examined by comparing two independently acquired LiDAR datasets of the same area. The scheme is also tested for compatibility with commonly used field-based biodiversity metrics. The work exhibited in this chapter addresses research questions 2 and 4. Chapter 8 summarises and discusses the work presented in this thesis, and presents concluding commentary on the utility of LiDAR for landscape biodiversity assessment.

CHAPTER 2 LITERATURE REVIEW

2.1 Introduction

Conservation of biodiversity has been recognised internationally as critically important for sustainability since the UN Convention on Biological diversity (CBD) in 1992 as stated in Chapter 1. Many authors have recognized forest structure information as surrogates of biodiversity (e.g. Noss, 1990). In this chapter, the details are presented how forest structure has been recognised and used for biodiversity assessment including existing field assessment methods in Australia. The previous work using passive remotely sensed methods is also discussed. Finally, Light Detection and Ranging (LiDAR) technology is reviewed and discussed its potential for extracting forest structure information.

2.2 Forest structure as an index of biodiversity

2.2.1 Forest structure

Forests are complex spatial structures. The often intricate architecture of the plant species they contain creates an environment that is difficult to characterise, record and study analytically. Forest structure, the architectural arrangement of plant material, has received less attention than species composition in terms of description and/or classification, yet diagnostically structure is considered just as important in characterising a forest as its composition (Florence, 1996; Spies, 1998; Stone and Porter, 1998). Early attempts at modelling structure proposed a vertical stratification suggesting forests had two photic

zones (Richards, 1939). It was argued that two highly different environments for biotic existence were evident: a euphotic layer (or canopy stratum) which intercepts sunlight directly and the oligophotic layer (or understorey stratum) which intercepts sunflecks, scattered and transmitted radiation. Longman and Jenik (1987) and Klinge et al. (1975), amongst others, expanded this vertical stratification concept to describe three, or more vertical layers. Other researchers (e.g. Cain et al., 1956; Grubb et al., 1963) report problems in the identification of strata however, and some authors (e.g. Gordon et al., 1974) have even discredited the notion of distinct layers in forests altogether. The fact remains however that from the perspective of energy capture, such delineation has merit.

Structural analysis of individual trees within forests was recognized as an ecologically useful tool for the assessment of plant interaction by Hallé et al. (1978). This approach to assess gross morphological diversity was based on the idea that each individual species has a precise and genetically determined growth plan, i.e. architectural model, which development stage is represented as the architecture of the plant. Morphological analysis is important since morphology is the visible representation of the growth success of a tree species in the highly competitive environment of the forest (Tomlinson, 1983). For example, morphological analysis such as profiling of a forest (Fig. 2-1) can provide critical information for studies of physiology of trees, production ecology and faunal distribution (Tomlinson, 1983). Some features of forest structure, such as horizontal distribution of vegetation, have also been considered to have relationship with environmental factors (Bourgeron, 1983). Webb et al. (1970) found that the structural features of forests, such as the type of tree branching and the bark characteristics, are related with altitudinal gradient and efficient tools for the classification of vegetation in eastern Australia. The ecological significance of forest structure was also presented by Franklin et al. (1981). These authors characterised old-growth coniferous forests and distinguished them from young-growth

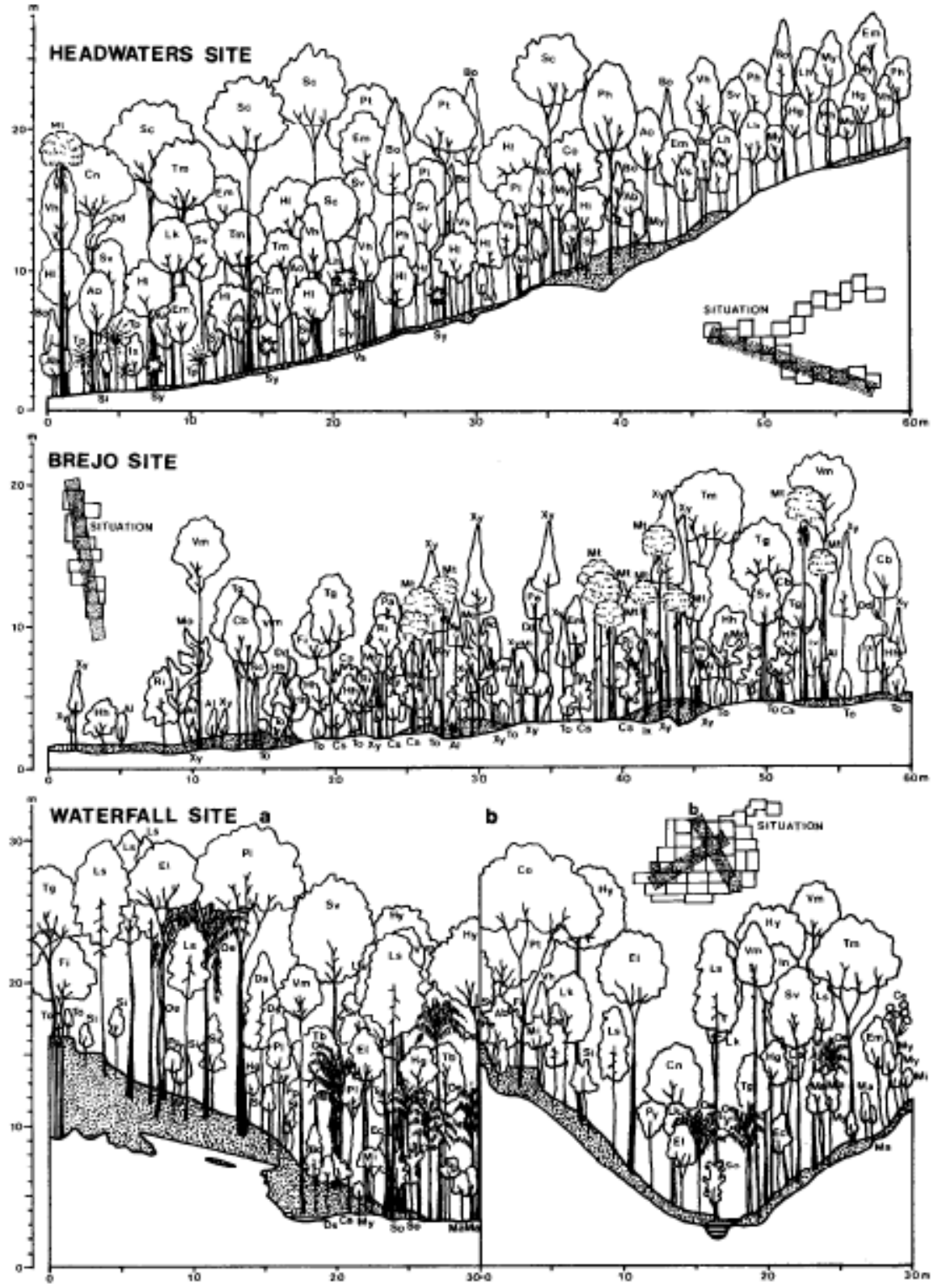

Figure 2-1 Example of forest profile diagrams. Diagrams were obtained from transects of 5 m width (Oliveira-Filho et al., 1990 p. 111).

forests in terms of species composition, function (rate and paths of energy flow and nutrient and water cycling) and structure. They identified four structural components; large live trees, large snags (standing remnant of a dead tree), large logs on land and large logs in streams, as key diagnostic indicators of old-growth forests. Gutiérrez et al. (2009) similarly suggested that old-growth forests have a distinctive structural variability as well as floristic diversity. This analogy was also used by Noss (1990) who suggested that vegetation condition, when assessed in the context of biodiversity, should be considered in terms of: structure, composition, and function. Spies (1998) described the essential attributes of forest structure as structural type, size, shape, and spatial distribution (vertical and horizontal) of components (summarised in Table 2-1) and examined their roles and importance to the functioning and diversity of ecosystems. For example, foliage layering or vertical foliage distribution is a component of forest structure that plays important roles in absorption of solar radiation, the microclimate of the forest and in providing wildlife habitat. Many authors have noted the association between biodiversity and measures of the variety and/or complexity of arrangement of structural components within an ecosystem (e.g. Mac Nally et al., 2001; Sullivan et al., 2001). Furthermore, the habitat complexity of a forest structure can be used to predict the occurrence of some species, since such information provides locally specific descriptions of faunal habitat (Catling and Burt, 1995; Jorgensen, 2002; Psyllakis and Gillingham, 2009; Tanabe et al., 2001; Verschuyl et al., 2008; Watson et al., 2001).

Most forest stand structure descriptors are traditionally based on measures easily obtainable from the ground level (e.g. Diameter at Breast Height (DBH), stem density or ground assessed canopy cover). General descriptions such as ‘patchy’, ‘dense’, ‘multi-storied’ offer a useful picture suggesting a horizontal and vertical organization but may not

Table 2-1 Components of forest structure (After Spies, 1998).

1. Foliage	**5. Wood Tissues**	**9. Forest Floor and Organic Layers**
Leaf area	Volume	Depth
Vertical distribution	Biomass	Decay state
Leaf shape, density	Type (e.g. sapwood, heartwood)	**10. Pit and Mound Topography**
Canopy gaps and horizontal pattern	**6. Standing Dead Trees**	Area
2. Tree Crowns	Diameter	Height/depth
Shepe	Height	**11. Roots**
Length	Decay state	Size
Life form (e.g. decidous,	Volume, mass	Density, decay state
coniferous)	Cavities	Biomass
Diameter, area, density	**7. Fallen Trees**	Spatial pattern
Position in stands	Diameter	**12. Soil Structure**
Branch characteristics	Height	Aggregations
Cavities, breakage, decay	Decay state	Organic matter distribution
3. Tree Bark	Volume, mass	**13. Landscape Structure**
Texture	**8. Shrub, Herb, and Moss Layers**	Stand/patch type distribution
Thickness	Biomass, volume	Patch size
4. Tree Boles	Height	Patch shape
Diameter	Life form	Habitat connectivity
Height	Spatial pattern	Edge density
Cavities, breakage, decay		
Gaps and spatial pattern		
Age distribution		

be competent for many operational uses (Stone and Porter, 1998). The most utilised tool to assess vertical stratification of forests is the profile-diagram (e.g. Davis and Richards, 1933). An example is shown in Fig. 2-1. The vertical structure of stands is represented by illustration drawing the stand naturalistically along real transects (e.g. Lamprecht, 1969) or as idealized and standardized profile (e.g. Holdridge, 1970). Profiles are very informative, however, the main use is the illustrative characterisation of actual stand structure and limited to qualitative understanding (Brunig, 1983). In ecological studies, quantitative data of forest structure are critical for research such as habitat modelling, however, the data are often qualitative, merely descriptive (Jorgensen, 2002). The early attempt to quantitatively measure vertical structure was presented by Klinge (1973). The author assessed the proportion of the basal area in each vertical layer of the canopy: the emergent trees of the A layer, main canopy trees B layer, the C layer and the ground layers D and E. The issue of

such methods is the time-consuming data collection, which leads a lack of analysis of pattern and variances between plots and transects (Brunig, 1983). Rapid, repeatable and quantitative measurement tools to assess vertical forest structure are desired. Currently, appraisal or scoring methods for structural complexity require a laborious process that involves site visits and many logistically expensive point based measurements. An automated or semi-automated method, which could rapidly and quantitatively assess forest structure with high-area coverage yet reduce the manpower, would be ideal.

There is much anecdotal evidence that such a technique is required. For example, Watson et al. (2001) measured the vegetation structural complexity of remnant patches including area and isolation to test the effects of loss of habitat structure, increased isolation and loss of habitat area on woodland birds. The authors calculated a habitat complexity score modified from the one developed by Catling and Burt (1995) assessing the percent cover for the different forest components; canopy, tall shrubs, low shrubs, ground herbage, logs and fallen branches and litter, and found that the mean habitat complexity score of each remnant explained a significant portion of the deviance of presence/absence for 20 bird species. This method has been used to develop and strengthen conservation strategies but is prohibitively time-consuming to apply at a large area or landscape level. If a technique could automate this process then significant advantage in terms of conservation planning would be realised.

2.2.2 Existing assessment methods for forest structure

In Australia, vegetation condition monitoring is mandated at the state level. Various methods to assess vegetation condition have been published (e.g. Eyre et al., 2006;

Freudenberger, 1999; Gibbons et al., 2004; Parks et al., 2003). These methods are ground-based and also assessing the forest structure information. In this section, vegetation condition monitoring methods in Victoria, Tasmania and New South Wales are reviewed since the vegetation community and their monitoring methods are relevant to this study.

The 'Habitat Hectares' (Parks et al., 2003) approach in the state of Victoria is a method which assesses vegetation condition by comparing it to the same vegetation type in the absence of major ecosystem changes and aims to identify an integrated view of the habitat for all the indigenous species that can be expected in a site. This consists of seven components for the site condition (large trees, tree/canopy cover, understorey strata, lack of weeds, recruitment, organic litter and logs) and three components for the landscape context assessments (patch size, neighbourhood and distance to core area). Vegetation communities and their interactions with each other and other biophysical or anthropogenic systems are mapped using Ecological Vegetation Class (EVC) (Department of Sustainability and Environment, 2004). The assessment area or unit is one stand, which is the combination of one vegetation type and condition state, within a native vegetation patch. The assessed structural variables, which are large trees, tree/canopy cover, understorey strata, organic litter and logs, account for 50 % of over all habitat score. Particularly, the component of understorey strata has the highest weighting (25 %). This is based on the assertion that understorey components can be useful indicators of site disturbance and are important for recognising and verifying future improvements in site condition (Parks et al., 2003).

The condition of native vegetation is also assessed in Tasmania using a similar methodology, Tasmanian Vegetation Condition Assessment (VCA), which is based on the above mentioned 'Habitat Hectares' approach (Parks et al., 2003). The same variables (large trees, tree/canopy cover, understorey life forms, lack of weeds, recruitment, organic

litter and logs) are visually assessed and compared to TASVEG, which is an integrated vegetation map for Tasmania, vegetation community benchmarks to give scores for the site condition and landscape contexts, which yield the final habitat score (Michaels, 2006).

The 'Biometric' tool (Gibbons et al., 2004) in New South Wales assesses native vegetation condition as terrestrial biodiversity at the scale of the patch, paddock or property. This aims to provide a quantitative assessment of either positive or negative impacts to terrestrial biodiversity of management activities. Nested 20 x 50 m and 20 x 20 m plots are established within relatively homogeneous or discrete zones for assessments. Measured variables include indigenous plant species richness, native over-storey cover, native mid-storey cover, native ground cover (grasses, shrubs and other), exotic plant cover, the number of trees with hollows, proportion of over-storey species occurring as regeneration, the total length of fallen logs and the number of stems in specified diameter classes. These measurements are compared against benchmarks and scored to produce site values.

In the following sub-sections, the methods for measuring each structural variable out of assessed variables in the above mentioned vegetation condition assessments are detailed.

2.2.2.1 Large trees

The number of large trees (alive and dead) is assessed in 'Habitat Hectares' (Parks et al., 2003) and TASVEG VCA (Michaels, 2006). Large trees can be a representative of remnant native vegetation and are important habitat features since they provide food resources and habitats to many organisms. Such trees are often old and difficult to replace once they are lost (Parks et al., 2003). In these two assessment methods, a large tree is defined by DBH,

which is measured at 1.5 m in 'Habitat Hectares' and at 1.3 m in TASVEG VCA above the ground. The assessment procedure is basically the same between these two methods. First, the large tree DBH and expected number of large trees/ha are referred to the community benchmark. In the assessment area or zone which is the combination of one vegetation type and condition state within a native vegetation patch, the number of large trees/ha is estimated and compared to the community benchmark. Then the result is placed in the appropriate category in the table (Table 2-2). Finally, the health of large trees is assessed estimating canopy cover in the three categories; more than 70 %, between 30 and 70 % and less than 30 %. The final score for large trees is determined from the table (Table 2-2). The assessments could be subjective since the number of large trees/ha and the category of canopy cover in an entire assessment area are based on the assessor's visual estimation. Referring to the community benchmark to calculate a score would be a time-consuming in the fieldwork.

Table 2-2 Criteria and scores for the number of large trees for 'Habitat Hectares' (Parks et al., 2003) and TASVEG VCA (Michaels, 2006) (After Michaels, 2006).

Large trees	Canopy Health (%)		
	>70%	30-70%	<30%
None present	0	0	0
>0 to 20% of the benchmark number of large trees/ha	3	2	1
>20% to 40% of the benchmark number of large trees/ha	4	3	2
>40% to 70% of the benchmark number of large trees/ha	6	5	4
>70% to 100% of the benchmark number of large trees/ha	8	7	6
≥ the benchmark number of large trees/ha	10	9	8

2.2.2.2 Canopy cover

This variable is assessed in 'Habitat Hectares' (Parks et al., 2003), TASVEG VCA (Michaels, 2006) and 'Biometric' (Gibbons et al., 2004). The first two methods utilise the

same approach. Tree canopy cover is defined as those canopy tree species reaching more than 80 % of mature height in these methods. The projective foliage cover of canopy trees is estimated using the image guideline of different levels of projective foliage cover (Walker and Hopkins, 1990) in an assessment area. Projective foliage cover is averaged over the area. This is compared to the benchmark percentage cover (EVC and TASVEG, respectively) and scored according to the health of the canopy (Table 2-3). The health of the canopy is assessed in the same way as the health of the large tree in 'Habitat Hectares' and TASVEG VCA. This assessment requires a laborious process that an assessor firstly needs to identify the canopy tree species to measure canopy cover referring to the benchmark tree height. Then the projective foliage cover is estimated using the image guideline and the average foliage cover over the area is computed. Finally the value is compared with the bench mark tree cover. The assessed foliage cover could be subjective and biased since the location and the number of assessment points in the area depend on the site and assessors.

In 'Biometric' (Gibbons et al., 2004), native over-storey is defined as the tallest woody stratum present above 1 m from the ground. Therefore different vegetation communities have different over-storey vegetation such as the tree layer for a woodland community and the tallest shrub layer for a shrubland community. The percent foliage cover is estimated directly overhead using the image guideline (Walker and Hopkins, 1990) at 10 points along a 50 m transect within a 20 x 50 m plot. Final foliage cover is calculated as a mean within a plot. This is compared to the benchmark and scored for Site value (Table 2-4). This method could be also subjective since the "tallest woody stratum" is site dependant and prone to observer bias.

Table 2-3 Criteria and scores for tree canopy cover for 'Habitat Hectares' (Parks et al., 2003) and TASVEG VCA (Michaels, 2006) (After Michaels, 2006).

Tree canopy cover	Canopy Health (%)		
	>70%	30-70%	<30%
<10% of the benchmark tree cover	0	0	0
<50% or >150% of the benchmark tree cover	3	2	1
≥50% or ≤150% of the benchmark tree cover	5	4	3

Table 2-4 Scoring methods for vegetation cover and logs in BioMetric (After Gibbons et al., 2004).

Variable	Score in BioMetric			
	0	1	2	3
Native over-storey cover	0-10% or >200% of benchmark	10-50% or 100-150% of benchmark	50-100% or 150-200% of benchmark	Within benchmark
Native mid-storey cover	0-10% or >200% of benchmark	10-50% or 100-150% of benchmark	50-100% or 150-200% of benchmark	Within benchmark
Native ground cover (grasses)	0-10% or >200% of benchmark	10-50% or 100-150% of benchmark	50-100% or 150-200% of benchmark	Within benchmark
Native ground cover (shrubs)	0-10% or >200% of benchmark	10-50% or 100-150% of benchmark	50-100% or 150-200% of benchmark	Within benchmark
Native ground cover (other)	0-10% or >200% of benchmark	10-50% or 100-150% of benchmark	50-100% or 150-200% of benchmark	Within benchmark
Lack of exotic plant cover	>66%	33-66%	5-33%	0-5%
Total length of fallen logs	0-10% of benchmark	0-50% of benchmark	50-100% of benchmark	≥benchmark

2.2.2.3 Mid-storey and understorey cover

Understorey vegetation is very important since the greatest richness and diversity of plant species are almost always found in a variety of shrub and herb strata, and they can be useful indicators of site disturbance (Parks et al., 2003). The definition of understorey vegetation is slightly different between vegetation assessment methods, however all the methods basically assess the indigenous plant species between canopy layer and the ground.

'Habitat Hectares' (Parks et al., 2003) and TASVEG VCA (Michaels, 2006) define

Table 2-5 Criteria and scores for understorey lifeform for 'Habitat Hectares' (Parks et al., 2003) and TASVEG VCA (Michaels, 2006) (After Michaels, 2006).

Understorey lifeform Category 1	Category 2	Score
All strata and life forms effectively absent		0
Up to 50% of life forms present		5
≥50% -90% of life forms present	Of those present ≥50% substantially modified	10
	Of those present <50% substantially modified	15
≥90% of life forms present	Of those present ≥50% substantially modified	15
	Of those present <50% substantially modified	20
	Of those present, none substantially modified	25

understorey vegetation as 'understorey' which includes all indigenous species present under canopy trees (e.g. sub-canopy tree, tall shrub, small shrub, immature trees, herbs and mosses). The assessment procedure includes two steps. First the range of lifeforms present are recognised and compared to those expected (i.e. benchmark understorey life forms), and then the diversity and cover within each lifeform (i.e. degree of modification) are assessed and scored (Table 2-5). This assessment is more qualitative rather than quantitative since the focus is species diversity and its modification.

'Biometric' (Gibbons et al., 2004) defines understorey vegetation as 'mid-storey' which contains all native vegetation between the over-storey stratum and 1 m in height. Unlike 'Habitat Hectares' (Parks et al., 2003) and TASVEG VCA (Michaels, 2006), vegetation less than 1 m in height is assessed in different categories as ground cover (see Section 2.2.2.5 Ground cover). Percentage of foliage cover in mid-storey stratum is assessed in one of the two ways. 1) Visually estimate per cent foliage cover in a 20 m x 20 m plot. 2) Visually estimate per cent foliage cover at 10 points along the 50 m transect within a 20 m x 50 m plot and average the total per cent. This is compared to the benchmark and scored for Site value (Table 2-4). This method assesses understorey vegetation more quantitatively

compared to ‘Habitat Hectares’ (Parks et al., 2003) and TASVEG VCA (Michaels, 2006). However, what is assessed as mid-storey is not clear and could be subjective since the definition of the over-storey stratum is site and assessor dependant (see Section 2.2.2.2 Canopy cover).

2.2.2.4 Weed cover

Weeds are a threat to native vegetation species since they can successfully compete and may change the site condition. In ‘Habitat Hectares’ (Parks et al., 2003) and TASVEG VCA (Michaels, 2006), weed cover includes all introduced species and non-indigenous native weed species, and is assessed by the averaged total projective foliage cover across the area and the proportion of this cover due to high threat weeds. Categories of weed foliage cover and their scores are slightly different between these two vegetation condition assessments (Table 2-6 and 2-7). Similar to the assessment of canopy cover (Section 2.2.2.2), the location and the number of assessment point in the area depend on the site and assessors. The assessment could be biased.

‘Biometric’ (Gibbons et al., 2004) defines weed cover as ‘Exotic plant cover’, which are vascular plants not native to Australia. The assessment method is similar to ‘Habitat Hectares’ (Parks et al., 2003) and TASVEG VCA (Michaels, 2006), which uses the total per cent foliage cover of all extotics in all strata within 20 m x 20 m plot or at 50 points along a 50 m transect within 20 m x 50 m plot. This is compared to the benchmark and scored for Site value (Table 2-4).

Table 2-6 Criteria and scores for weed cover for 'Habitat Hectares' (After Parks et al., 2003).

Weed cover	High threat weeds (%)		
	None	≤50%	>50%
>50% cover of weeds	4	2	0
25-50% cover of weeds	7	6	4
5-25% cover of weeds	11	9	7
<5% cover of weeds	15	13	11

Table 2-7 Criteria and scores for weed cover for TASVEG VCA (After Michaels, 2006).

Weed cover	High threat weeds (%)		
	None	≤50%	>50%
>75% cover of weeds	0	0	0
25-75% cover of weeds	4	2	0
10-25% cover of weeds	7	6	4
5-10% cover of weeds	11	9	7
<5% cover of weeds	15	13	11

2.2.2.5 Ground cover

'Habitat Hectares' (Parks et al., 2003) and TASVEG VCA (Michaels, 2006) do not utilise vertical stratification under canopy trees. Most ground cover components except organic litter and logs (see Section 2.2.2.6 Logs) are included in understorey lifeforms (see Section 2.2.2.3 Mid-storey and understorey cover). In these two vegetation condition assessments, organic litter is defined as dead organic material and both fine and coarse plant debris less than 10 cm diameter on the ground. The percentage cover of the organic litter in the area is estimated and compared to the benchmark. The final score is determined according to the proportion of this litter comprised of material from native species. Categories of litter cover are slightly different between the two assessments (Table 2-8 and 2-9).

In 'Biometric' (Gibbons et al., 2004), ground components, which include all native

vegetation below 1 m in height, are assessed separately for grasses, shrubs and other. It is defined that grasses as native grasses, shrubs as native woody vegetation and other as non-woody native vegetation that is not grass. Percentage cover of these components is estimated either one of the two ways. 1) Visually estimate per cent cover in a 20 m x 20 m plot. 2) Visually estimate per cent cover at 10 points along the 50 m transect within a 20 m x 50 m plot and average the total per cent. This is compared to the benchmark and scored for Site value (Table 2-4).

Table 2-8 Criteria and scores for organic litter cover for 'Habitat Hectares' (After Parks et al., 2003).

Organic litter cover	Organic litter cover due to native species (%)	
	≥50%	<50%
<10% of the benchmark organic litter cover	0	0
<50% or >150% of the benchmark organic litter cover	3	2
≥50% or ≤150% of the benchmark organic litter cover	5	4

Table 2-9 Criteria and scores for organic litter cover for TASVEG VCA (After Michaels, 2006).

Organic litter cover	Organic litter cover due to native species (%)	
	≥50%	<50%
<10% of the benchmark organic litter cover	0	0
<50% of the benchmark organic litter cover	3	2
≥50% of the benchmark organic litter cover	5	4

2.2.2.6 Logs

In 'Habitat Hectares' (Parks et al., 2003), TASVEG VCA (Michaels, 2006) and 'Biometric' (Gibbons et al., 2004), logs are assessed as the total length of fallen trees that have at least 10 cm diameter (and 0.5 m long for 'Biometric' (Gibbons et al., 2004)). This is compared to the benchmark and scored. Criteria and scores for log assessments are summarised in Table 2-10 for 'Habitat Hectares' (Parks et al., 2003) , in Table 2-11 for TASVEG VCA

(Michaels, 2006) and in Table 2-4 for 'Biometric' (Gibbons et al., 2004). 'Habitat Hectares' (Parks et al., 2003) and TASVEG VCA (Michaels, 2006) do not set up a fixed area plot to survey, however, it is recommended for logs components to be assessed in one or more 0.1 ha sample areas (e.g. 20 m x 50 m rectangle or 18 m radius circle) as 'Biometric' (Gibbons et al., 2004) assesses logs in a 20 m x 50 m plot. Dead cut stumps of a height less than 0.5 m for 'Habitat Hectares' (Parks et al., 2003) and 1.3 m for TASVEG VCA (Michaels, 2006), which are assigned a default length of 0.5 m per stump, are included in log assessments.

All of the above mentioned assessments require costly fieldwork. The assessment process is often time-consuming and laborious referring to the bench mark and identifying the appropriate categories in the field. In terms of measuring forest structural components, they are to a large degree qualitative and subjective. An efficient and cost-effective assessment tool, which can be carried out in objective and quantitative way, to compliment these survey methods is necessary.

Table 2-10 Criteria and scores for logs for 'Habitat Hectares' (After Parks et al., 2003).

Total length of logs	Proportion of log length more than half of the bench mark large tree DBH	
	≥25%	<25%
<10% of the benchmark length	0	0
<50% or >150% of the benchmark length	3	2
≥50% or ≤150% of the benchmark lenght	5	4

Table 2-11 Criteria and scores for logs for TASVEG VCA (After Michaels, 2006).

Total length of logs	Proportion of log length more than half of the bench mark large tree DBH	
	≥25%	<25%
<10% of the benchmark length	0	0
<50% of the benchmark length	3	2
≥50% of the benchmark length	5	4

2.3 Passive remote sensing methods for forest structure

Remote sensing data derived from satellite and airborne sensors is superior to field survey data in terms of high-spatial coverage, near simultaneous acquisition, repeated regional accounting and cost. To date, most natural resource remote sensing has been undertaken using passive sensing technologies, mainly in the visible/shortwave infrared red portions of the electro-magnetic spectrum. The Normalised Difference Vegetation Index (NDVI) computed from these portions of the electro-magnetic spectrum is one of the most widely used techniques to make quantitative estimates of vegetation properties (e.g. Liang, 2004; Tucker, 1979). The attempts to estimate forest structure using 2D information has been reported. For example, Lévesque and King (1999) examined airborne multispectral digital camera images to identify the type of forest canopy, individual tree crown structure and health information analysing semivariograms at the tree spatial information of the images; 0.25 m, 0.5 m and 1.0 m. The results showed that 1 m pixel semivariograms were best related to forest canopy closure, stem density and a visually derived tree stress index, and 0.5 m pixel semivariograms were related better to tree crown size and tree height at the canopy level, while 0.25 m pixel semivariograms were well related to tree crown closure at the tree crown level. However, it was noted that the study was done in a very homogeneous forest stand with basically one overstorey species and small ranges of forest structural parameters. Therefore, the algorithm used in this study might not be applicable to more complex forest stands such as natural forests. Muinonen et al. (2001) investigated the aerial photo, which was scanned, orthorectified and resampled to a 0.8 m pixel size, to estimate forest stand characteristics. As the result of combining the information on variograms with image interpretation by using a nonparametric method based on a distance-weighted mean of most similar neighbors, the stand volume was estimated with the root mean square error (RMSE) of 27.67 m^3/ha (17.9 %) and a bias of -0.97 m^3/ha (-0.63%). However, this

technique requires a priori information of the forest stand borders. It was also reported that the calibration problem originated from imaging geometry might become bottleneck in aerial photo image analysis due to a central projection of the photographed area (i.e. objects such as trees bend away from the centre of the image and this may have impact on the spatial indicator attributes).

In the studies using high spatial resolution satellite imagery, Lamonaca et al. (2008) examined a multi-resolution segmentation of a QuickBird image to determine whether it can detect the spatial heterogeneity in forest structure: trees spatial distribution, tree sizes, tree species mingling and occurrence of forest canopy gaps, and presented promising results. These authors also reported that the geometric and heterogeneity of QuickBird imagery was most closely related with the tree species mingling, which is a quite understandable outcome. Song (2007) estimated the mean tree crown diameter on a stand basis with an Ikonos image, using the disc scene model that the ratio of image variances at two spatial resolutions is determined by the scene structure only. The author found the ratio of image variances at 2 m and 3 m spatial resolutions best estimated conifer tree crown diameter, however, it did not work well for hardwood stands because of the continuity in canopy structure. These two studies showed the potential of multispectral high spatial resolution imagery to extract forest structure. However the biophysical parameters were limited to horizontal structure in these studies.

In the studies using larger spatial resolution imagery than QuickBird and Ikonos, Wolter et al. (2009) extended the Song (2007) approach from stand-level to pixel-level estimation of mean crown diameter and other forest structural attributes (bole diameter at breast height, tree height, crown closure, vertical length of live crown and basal area) with SPOT-5 data. The authors reported better performance of the model for conifers compared to the model

for hardwoods, and attributed it to greater overall contrast between the sunlit and shaded components of conifer canopies in the image. This implies that the results could be affected under different illumination conditions. Furthermore, the authors compared the results of the partial least squares regression model used in the study with similar parameter estimates made using LiDAR data. It was reported the SPOT-5 results were better than their LiDAR derived counterparts in terms of R^2 and/or RMSE for conifer and hardwood canopy diameter and bole diameter at breast height. On the other hand, LiDAR derived models outperformed SPOT in tree height, canopy closure, vertical length of live crown and basal area estimation, particularly for hardwood. This study displayed the prospective use of multispectral imagery for estimation of forest structure, however LiDAR would be more precise particularly when the attributes are measured in mixed species forests. Another example of using SPOT images to detect forest structure was presented by de Wasseige and Defourny (2002). These authors analysed the spatial variation in an image and bi-directional reflectance distribution function (Jupp and Walker, 1997) of three tropical forest sites, where forest structure and species composition are different from each other, using a time-series of six SPOT-HRVIR images including various viewing zenith angles and under various illumination conditions. In this study, a single geometric-optical gap model explained more than 80 % of the variability of near-infrared red reflectance standard deviation as a function of the viewing zenith angle, which was directly related to the structure of the forest. However, a very specific configuration of sensor observation, such as near-nadir viewing zenith angle, solar zenith angle higher than 20 º and solar azimuth angle aligned with one of the four directions of the grid, were required for this forest structure detection. This would restrict analysis over limited areas. Lathrop Jr and Pierce (1991) examined the relationship between ground-based canopy transmittance and Landsat Thematic Mapper near-infrared/red radiance ratio data for estimating forest

canopy structure in Montana. The results indicated that both ground-based canopy transmittance and satellite-based measurements responded to the same general trends in forest canopy structure. These authors, however, reported that there was still significant amount of unexplained variation in the relationship between ground-based canopy transmittance and Landsat Thematic Mapper near-infrared/red ratio, which could be affected by differences in species' canopy geometry, stand canopy closure, slope/sun angle interactions and background reflectance. Significant difference in scale of the two measurements (e.g. the ceptometer at 9 m^2 and the Landsat Thematic Mapper at 900 m^2) were also stated as another problem. Similar problems were reported by Gemmell and Varjo (1999) in their study for testing the inversion of a forest reflectance model (FLIM; Rosema et al., 1992) to estimate cover and crown transmittance in a boreal forest of Finland using Landsat Thematic Mapper data. Marsden et al. (2009) examined the relationships between NDVI time-series of the Moderate Resolution Imaging Spectroradiometer (MODIS) and stand structural characteristics; stem volume, dominant height and mean annual increment, over even-aged forest plantations. The authors concluded that cumulative NDVI was a good predictor of stem volume and dominant height. This would be useful application in forestry for large plantation areas. However, it would be difficult to apply for other purposes such as ecological application, due to the low spatial resolution (250 m) and limited forest attributes.

In summary, passive remote sensing technology can offer some biophysical parameters of forest structure, however they are limited to either horizontal parameters or homogeneous species.

2.4 LiDAR

Active remote sensing technology refers to a sensor system that supplies its own source of energy. Light Detection and Ranging (LiDAR) is an active sensor technology that illuminates the object using the sensor unit and measures the range distance between sensor and the illuminated object. LiDAR instruments utilise light amplification by stimulated emission of radiation (laser) as illumination source. LiDAR instruments include laser ranging, laser profiling and laser scanning instruments on various platforms such as terrestrial and airbourne. The application of this technology for extracting forest structure information is promising. The basic LiDAR technology and systems are reviewed as well as their various applications.

2.4.1 LiDAR technology

Laser scanning is a relatively new technology. After the invention of laser in the early 1960s, it was developed through the 1970s and 1980s with an early NASA system and other attempts in the USA and Canada (Ackermann, 1999). NASA contributed a great deal in LiDAR technology and applications from the 1960's starting with the development of ground-based satellite ranging systems for studying crustal dynamics and plate tectonics (Einaudi et al., 2004). However, a lack of supporting technologies delayed the application of laser scanning technology for topographic mapping until early 1990s. By then, direct geo-referencing technology, the Global Positioning System (GPS), facilitated the development of commercial airborne laser profiling and scanning systems for topographic mapping (HyyppÃ et al., 2008). By the mid-1990s, the commercial availability of a medium/high performance Inertial Measurement Unit (IMU) along with GPS enabled

integrated GPS/IMU geo-reference systems provided airborne platform position and attitude data at an accuracy of 4-7 cm and 20-60 arc-seconds, respectively (Petrie and Toth, 2009a). Airborne laser scanning has developed very rapidly since then, delivering highly accurate geo-referenced three-dimensional points, and adopted for various uses such as forest inventory and feature extraction in urban areas.

In terms of the basic principles, laser scanners evolved from laser profilers, which in turn were upgraded from laser ranging instruments: laser rangers or laser rangefinders. A comprehensive review of these technologies is provided in Petrie and Toth (2009a). In the following sub-sections, much of this material has been collected and the discussion around the elements of the technology has been focused, which are useful in the context of this research.

2.4.1.1 Laser ranging

Laser ranging measures the distance or range based on the precise measurement of time. One of the main methods is the timed pulse or the time-of-flight (TOF) method. A very short but intense pulse of laser radiation is emitted by the laser ranging instrument to illuminate the object and the reflected pulse is returned from the object to the instrument. The laser ranging instrument calculates the precise time interval that has passed between the emitted pulse from the instrument and the returned pulse reflected from the object. This is expressed as follows.

$$R = v \cdot t / 2 \qquad (2\text{-}1)$$

Where, R denotes the slant distance or range, v denotes the speed of electromagnetic radiation, which is a known value, and t denotes the measured time interval.

In this method, if a series of reflections is returned back to the sensor from a specific object such as a tree, the time taken for each of the returned pulses, such as the first and last pulses, is measured. The complete waveform of the entire return signal can be also measured as an alternative. The actual length of the pulse emitted by the laser ranging has a significant effect on how multiple returns can be delivered or differentiated, since the measuring resolution is determined by the length of the emitted pulse. For a given energy, if the pulse duration is shorter, the pulse power becomes higher, which results in smaller pulse detection error (Baltsavias, 1999). The pulse repetition frequency (PRF), which is how frequently a pulse is emitted by the laser source, may also have an impact on multiple return properties, since laser systems from the early 2000s increased their PRF at the cost of reducing the energy of the emitted pulse, thus the ranging accuracy was decreased because of the less distinct signal-to-noise ratio (Næsset, 2009). It is noted that up-to-date laser supplies are more powerful with the increased power supply on an aircraft, therefore this is not an issue for the latest systems as of 2009 (Petrie and Toth, 2009a).

Another method of laser ranging is the phase comparison technique, which utilises a continuous beam of laser radiation, referred to as a CW laser, instead of discrete pulses. The range value is computed by comparing the transmitted and received versions of the sinusoidal wave pattern and calculated the phase difference between them. A digital pulse counting technique is generally used for this phase measurement, which gives the fractional part of the total distance ($\Delta\lambda$). The integer number of wavelengths (M) is fixed

by altering the modulation pattern and added to the fractional values to deliver the final slant range (R).

$$R = \left(M\lambda + \Delta\lambda\right)/2 \qquad (2\text{-}2)$$

Where, M denotes the integer number of wavelengths, λ denotes the known value of the wavelength and $\Delta\lambda$ denotes the fractional part of the wavelength = $(\varphi/2\pi) \cdot \lambda$, where φ is the phase angle.

This method is often used in short-range terrestrial laser scanners due to the limited power of the CW laser. The signal strength is lost as the distance to objects is increased. The actual operation in airborne and spaceborne is rare (Heritage and Large, 2009; Petrie and Toth, 2009a).

2.4.1.2 Laser Profiling

Laser profiling utilises a reflectorless ranger and measures the distance to a series of closely spaced points along a line on the ground. This provides a two-dimensional profile or vertical section from the ground up. When a terrestrial laser ranger is used, the terrain profile is measured by a series of steps with the successive measured distances and vertical angles (V) to each sampled point (Fig. 2-2(a)). With the digitally recorded and stored data, the profile of the terrain along the line can be obtained as follows (Fig. 2-2(b)).

$$D = R\cos V \qquad (2\text{-}3)$$

Where, D denotes horizontal distance, R denotes the measured slant range and V denotes the measured vertical angle.

$$\Delta H = R \sin V \qquad (2\text{-}4)$$

Where, ΔH denotes the difference in height between the laser ranger and the point being measured.

When an airborne or spaceborne platform is used for a simple laser profiler, the laser ranger is pointed vertically toward the ground providing a rapid series of measurements of the distances to the ground from the successive positions of the moving platform. If the positions and altitudes of the platform at these successive positions in the air or in space can be obtained utilising a GPS/IMU system for an airborne platform or a star-tracker for a spaceborne platform, the corresponding ranges measured at these points enable the calculation of their ground elevation values. The terrain profile along the flight line can be delivered (Petrie and Toth, 2009a).

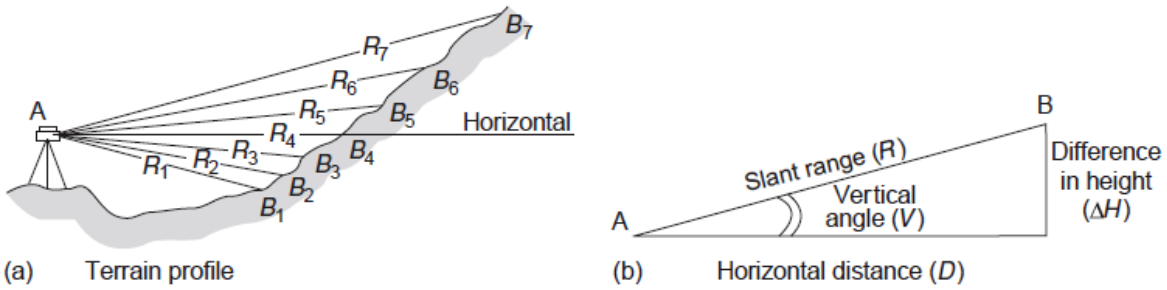

Figure 2-2 (a) Measurement of slant ranges (R) and vertical angles by a rangefinder located at A to a series of successive points located along a line on the ground to form a profile. (b) The measured slant ranges (R) and vertical angles (V) are used to compute the horizontal distances and differences in height between the rangefinder at A and each of the ground objects at B. (Petrie and Toth, 2009a p.6)

2.4.1.3 Laser Scanning

An additional scanning mechanism such as a rotating mirror or prism enabled a laser profiler to be upgraded to a laser scanner, increasing the point density of the sample thereby providing detailed topographic features of an area. A terrestrial or ground-based

laser scanner moves in two directions; the vertical motion caused by the rotating mirror or prism and a controlled motion in the azimuth direction given by a motor drive. This measures a series of profiles around the vertical axis of the laser ranger, which gives the position and elevation data. Thus, a 3D model of the terrain and the objects on the ground are formed. An airborne or spaceborne laser scanner measures a series of profiles in the direction perpendicular to the flight line as the platform moves forward providing the second dimension. The angular rotation values for the reflective mirror or prism are continuously and precisely obtained using an angular encoder. This provides the additional profiles of the terrain to be measured by the laser ranger in cross-track direction, and supplements the longitudinal profile being measured in the along-track direction of the flight line. Through a series of these profiles, the locations and elevations of a mesh of points, which are called a LiDAR point cloud, are produced for an area of the terrain (Large and Heritage, 2009; Petrie and Toth, 2009a).

2.4.1.4 Other features of LiDAR technology

Other features of LiDAR technology to understand include the laser beam. It is particularly important in successful data acquisitions. The laser beam or pulse spreads to illuminate a circular area when it reaches the ground or the object on the ground. The diameter of the circular area is called the footprint. If the ground is uneven elevation, the return signal will be the average of the mixture of reflectance within a footprint. If the scan angle is fixed, the footprint becomes larger as the range increases (Goodwin et al., 2006). Therefore, to obtain useful signal with high flying heights, the beam divergence should be decreased and the transmitted power and the receiver optics dimensions increased (Baltsavias, 1999).

Another significant aspect that one should consider in terms of the ranging performance is

the laser beam reflectance. The reflectance is defined as the ratio of the incident radiation on a specific surface to the reflected radiation from that surface. When the strength of the reflected radiation is too weak to detect, the range needs to be reduced. Therefore, the backscattering properties of the object are important. For a diffuse reflector object, the reflected radiation is scattered into a hemispherical pattern (Fig. 2-3). The maximum reflection occurs perpendicular to the target plane with the intensity decreasing to each side. Furthermore, the reflectance of the target is different in accordance with the laser wavelength (Baltsavias, 1999; Petrie and Toth, 2009a). Thus, one should select the appropriate laser wavelength for the object measured. The reflectance of laser radiation is also affected by the angle that the object makes with the incident pulse or beam. When an airborne laser scanner is used to measure the terrain, the highly reflective surface on the ground that is not at right angles to the incident laser pulse or beam will not return the pulse to the laser ranger due to reflecting its radiation off to the side. In case of a forest canopy, the emitted laser pulse in nadir direction will be able to penetrate the gaps in the canopy and the return signal from the ground below the canopy can travel back to the

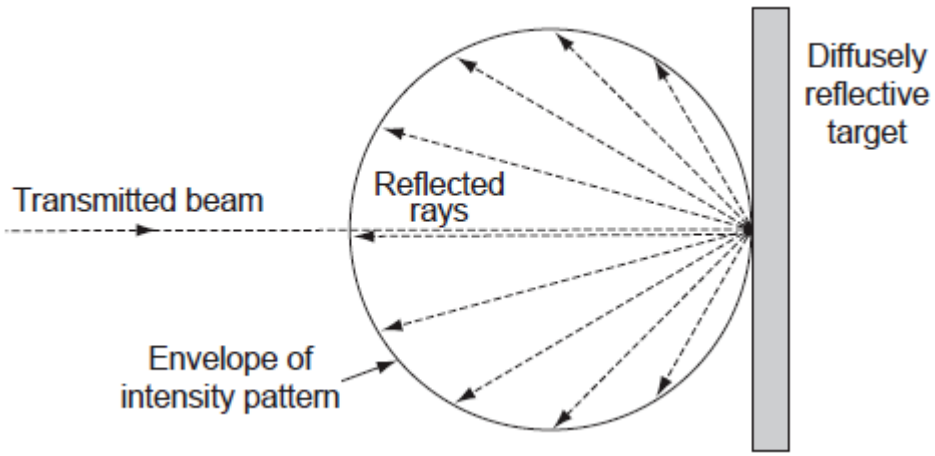

Figure 2-3 Reflectivity of a diffuse target (Petrie and Toth, 2009a p.23).

sensor. However, this penetration will decrease significantly as the scan angles are increased away from the nadir direction (Holmgren et al., 2003).

2.4.2 Positioning of LiDAR

The laser scanning data is 2-Dimensional without the position and orientation of the laser system being known according to a coordinate system. To archive 3-Dimensional position of the points and accurate range measurements, an airborne laser scanning system needs components both in the airborne and the ground segments (Fig. 2-4). The airborne segment comprises an airborne platform, a laser scanner and a Position and Orientation System (POS). The ground segment includes GPS reference stations and the processing hardware and software for synchronization and registration which is carried out off-line. While a laser scanner samples the line-of-site slant ranges with respect to the laser coordinate system, a POS independently stores GPS data including carrier phase information and orientation data from the IMU. The IMU defines the roll, pitch and yaw of the scanner and the angle encoder determines the angular position of the scanner mechanism deflecting the laser beam. Simultaneously, the ground GPS stations store GPS data and GPS carrier phase data at known earth fixed positions for later off-line computing of differential GPS (DGPS) positions of the airborne platform. An integrated POS consisting of a DGPS and an IMU allows the positional accuracy to be computed with centimetre to decimetre accuracy and its orientation to be determined better than one-hundredth of a degree. Since the position and orientation data is stored as a function of GPS time as well as the laser scanner data is stored with timestamps derived from the received GPS signal, the POS data and the laser data can be synchronised. The synchronisation enables the laser vector for each sampled ground point to be directly transformed into an earth fixed coordinate system such as

World Geodetic System 1984 (WGS84). Thus geocoded laser data is obtained. The accuracy of the data is depends on the accuracy of POS. With the latest system, the accuracy better than 10 cm in 3-Dimensional space is possible (Wehr, 2009; Wehr and Lohr, 1999).

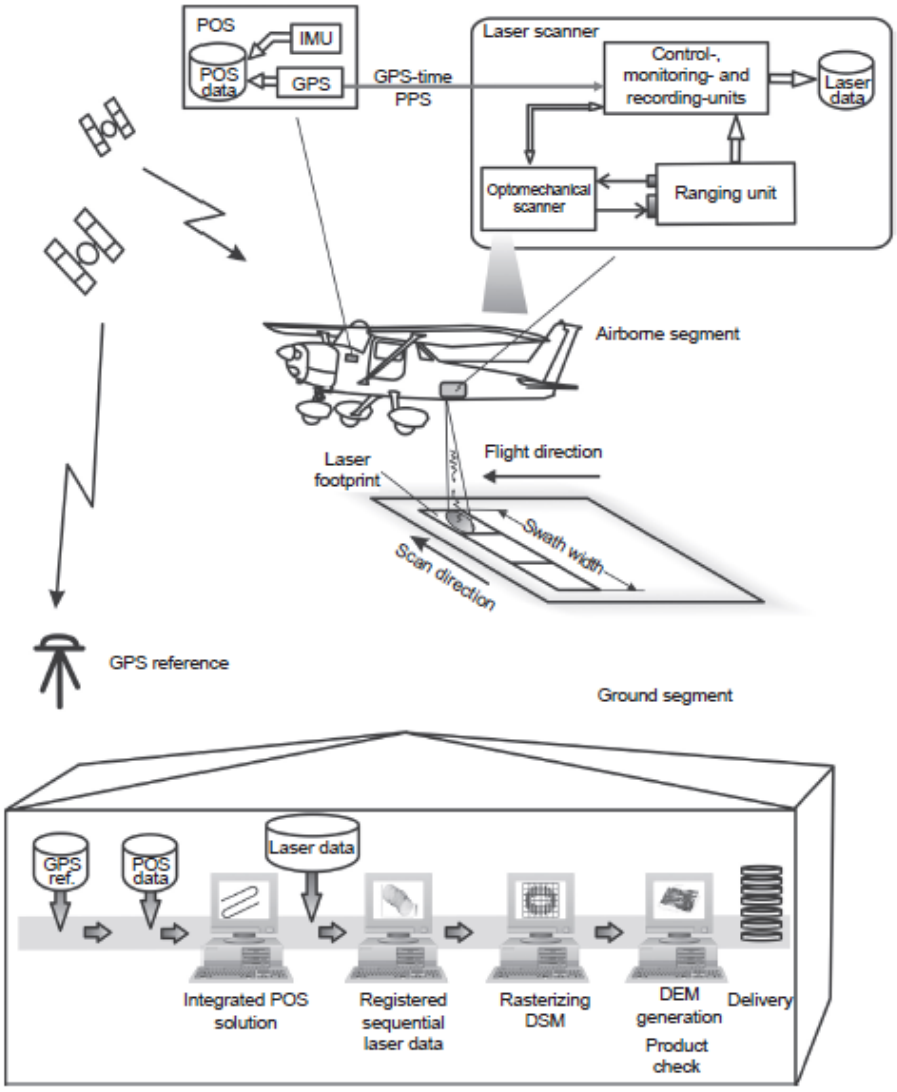

Figure 2-4 LiDAR system (airborne and ground segment) (Wehr, 2009 p.131).

2.4.3 Platform for LiDAR technology

Platforms on which to mount laser rangers include terrestrial instruments, spaceborne

satellites and airborne fixed wing airplanes and helicopters. Terrestrial or ground-based laser rangers have been well adopted in land and engineering surveying for the last 30 years and used for various applications such as measuring topographic mapping, complex industrial facilities, open-cast mines and the facades of buildings within urban areas operated either from a static position such as being mounted on a tripod on the ground, or a dynamic platform such as a van or truck (Large and Heritage, 2009; Petrie and Toth, 2009b). Spaceborne laser rangers are limited mainly by the large distances (100 – 1000 km) implied when using an Earth-orbiting satellites. This requires the use of a high power laser. Current spaceborne laser profilers include the Geoscience Laser Altimeter System (GLAS) aboard the Ice, Cloud, and land Elevation (ICESat) satellite launched in 2003, which was designed to measure ice-sheet topography and associated temporal changes, as well as cloud and atmospheric properties by NASA. Cloud Aerosol Lidar and Infrared Pathfinder Satellite Observations (CLIPSO) is a joint NASA (USA) and CNES (France) satellite launched in 2006 to supply a unique set of atmosphere vertical profiles measured by a Lidar on-board a satellite.

Airborne laser scanners have become wide-spread, being used today in many applications such as topographic mapping, forest inventory and urban planning. Many commercial and research laser scanners are aboard either on a fixed-wing airplane or a helicopter. An airplane flies faster than a helicopter, at approximately 200 km/h, and can cover large areas quickly. On the other hand, the helicopter has more flexibility in its flight, and therefore, is better suited for flying over particular areas such as power lines and steep slopes on mountains (Airborne Laser Survey Working Group, 2004).

2.4.4 LiDAR Systems

Current airborne laser scanning systems have two major configurations, discrete return systems and full waveform systems. In the following sub-sections, these two systems are detailed.

2.4.4.1 Discrete return system

The LiDAR discrete return system has been commercially available from mid-1990s. An essential feature of the system is the number of returns that can be recorded per emitted laser pulse. Assuming that the emitted laser pulse is entirely coherent with phased emission of photons of light at an almost constant known energy state, this supposition is used to set the threshold for recording of return energy (Heritage and Large, 2009). In this system, returns are identified with distinct peaks in amplitude, which exceed a detection threshold that triggers data recording. Earlier systems recorded only one return by setting the threshold to record either the highest detected distinct peak or the lowest peak. Later systems recorded two returns (both the highest and lowest peak), and then multiple returns up to a maximum of five returns. The instrument dead-time, the time that is necessary in-between two returns for them to be recorded as separate returns is another important property in this system. This time can be translated into the vertical distance, which is related to the duration of the emitted laser pulse, and is at least half the pulse length of the emitted pulse. For example, an airborne laser scanning utilising a laser pulse of 10 ns, which is equivalent to approximately 3 m, in length, the minimum detectable spacing that can be measured by one laser shot would be 1.5 m. This is often explained by the lack of returns between the lower part of a vegetation canopy and the ground (Danson et al., 2009).

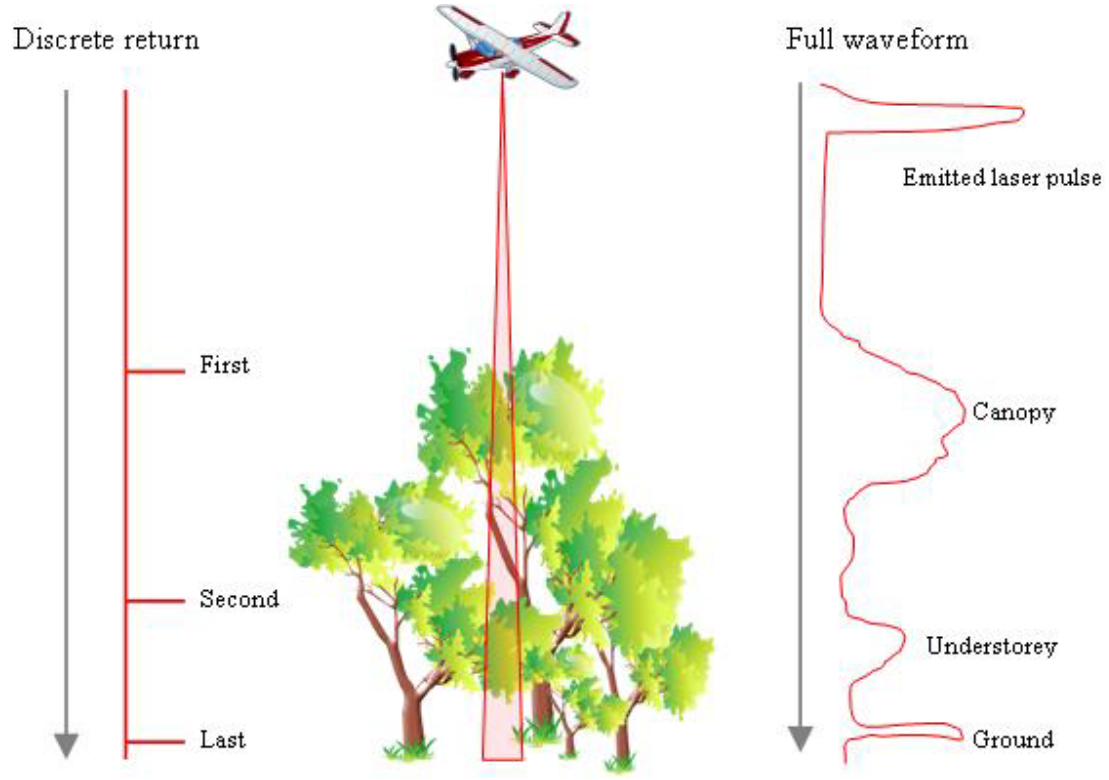

Figure 2-5 Illustration of discrete return system and full waveform system, recording emitted laser pulses and returned signals from multiple surfaces of vegetation canopy.

Fig. 2-5 illustrates the laser ranging methods of the discrete return system and full waveform system. Recent systems (e.g. Optech ALTM 1225 and successive systems) can also record the return amplitude or intensity associated with each discrete return, which can be used to differentiate targets. It is noted that the intensity is affected by the wavelength and energy of the transmitted pulse, the distance to the target, the reflectance of the target, the transmission of the atmosphere, the area of the receiver aperture, the throughput efficiency of the receiver, the sensitivity of the detector and the amplification gain applied to the detector output if analog detection is selected (Harding, 2009). Generally, small footprints (<1 m) are favoured in intercepting multiple surfaces, which enables high-resolution mapping of topography and canopy structure. Compared to the full waveform

system, an advantage of the discrete system is smaller volume of recorded data, however a disadvantage is the highly instrument-dependant representations of multiple returns. The ability to identify separate returns from closely spaced surfaces depends on instrument parameters such as the laser pulse width, detector sensitivity and response time, the system signal to noise performance, the detection threshold and the ranging electronics implementation. Therefore, one should be aware that measurements of canopy variables such as height, canopy depth or the distribution of understorey vegetation and gaps using different discrete return systems are not always the same (Harding, 2009).

2.4.4.2 Full waveform system

The LiDAR full waveform system is a new system which emerged in mid-2000s. The innovative feature of this system is to record the full waveform of an emitted pulse, which enables full characterisation of the vertical structure of the target. In the full waveform system, both the transmitted pulse shape and the received pulse shape are digitized and recorded. This is the result of digitization of the waveform with an analog-to-digital converter (Fig. 2-6). When this system is used for distributed objects such as vegetation canopies, vertically distributed multiple surfaces are illuminated by a single laser pulse and a complex shape of the received signal can be digitized (Fig. 2-5). The signal represents the height distribution of illuminated surfaces weighted by the spatial distribution of laser energy within the footprint and the reflectivity of the surfaces at a given laser pulse wavelength (Harding, 2009; Harding et al., 2001). The pulse shape is an important feature as it can provide information about different surface attributes. Typical surface attributes to extract from a full waveform signal include range, elevation variation and reflectance, corresponding to the waveform attributes of time, width and amplitude. To extract the

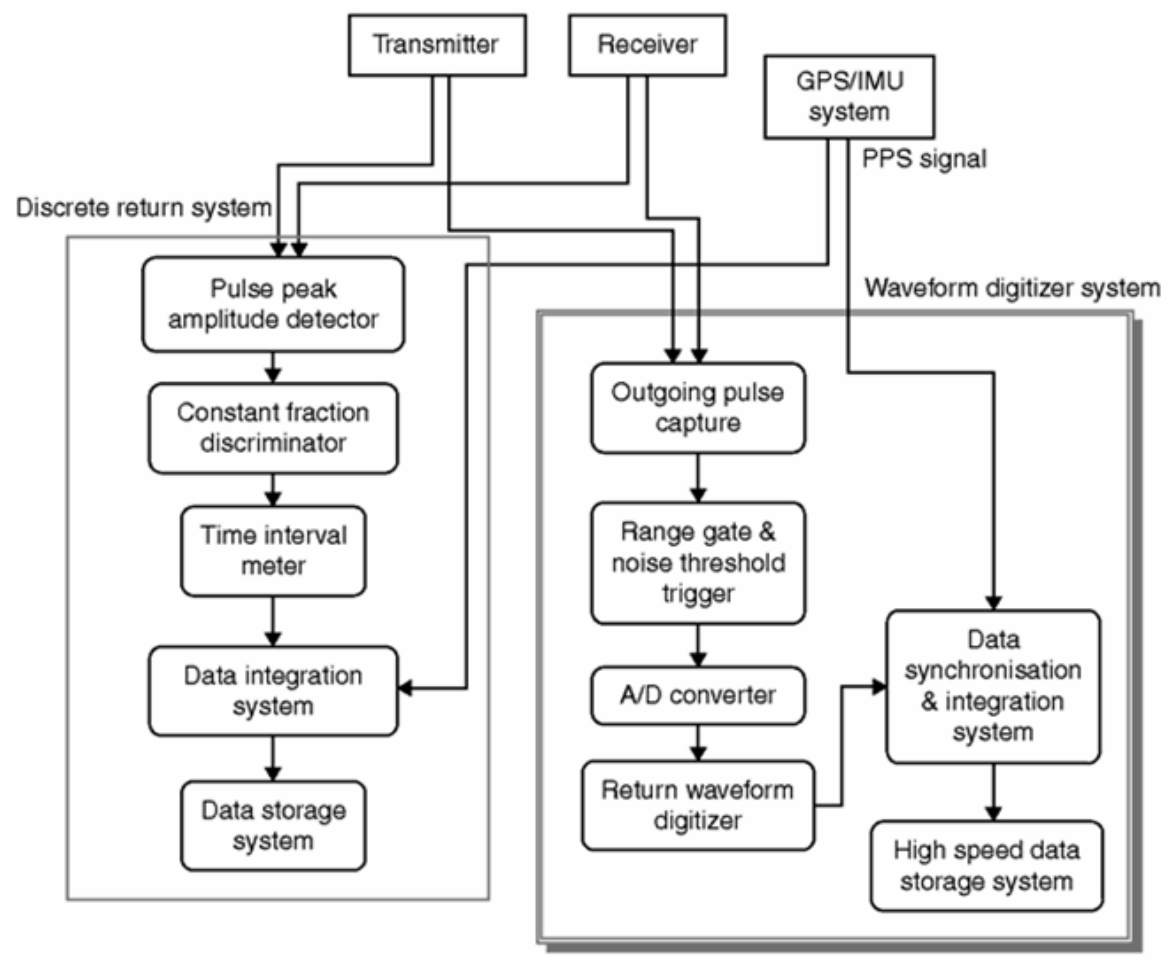

Figure 2-6 Example of the waveform digitizer system developed by Optech Inc. of Canada and the Unit for Landscape Modelling, University of Cambridge (Devereux and Amable, 2009 p.57).

attributes, one needs to be aware that the received waveform is dependent on the transmitted waveform, the impulse response of the receiver, the spatial distribution of the laser pulse beam and the geometric and reflectance properties of the illuminated surface. The width of the pulse can be used to measure the elevation variation of the surface since a rough surface will broaden the reflected laser pulse. Furthermore, the broadening of the pulse results in spreading of the reflected photons over a greater amount of time, which reduces the peak amplitude. Therefore, the pulse width and amplitude need to be known to estimate the elevation variation or reflectance attributes of a surface. The range to a surface can be determined in various schemes such as peak detection, leading edge ranging,

constant fraction detection, centre of gravity detection and Gaussian decomposition and deconvolution. It is noted that the different processes may impact the shape of the waveform (Stilla and Jutzi, 2009).

2.4.5 LiDAR Applications

LiDAR, especially airborne laser scanning has become wide-spread, being used today in many applications such as topographic mapping, forest inventory and urban planning. In this section, topographic mapping, forestry and ecological application of airborne laser scanning are reviewed and discussed.

2.4.5.1 DEM (Digital Elevation Model)

Assessing topographic features is the largest area of application for airborne laser scanning. After the first commercial projects to acquire terrain data in Europe in mid-1990s (Pfeifer and Mandlburger, 2009), survey companies aggressively started using this emerging technology to obtain a Digital Elevation Model (DEM) otherwise called a Digital Terrain Model (DTM), which is derived from a Digital Surface Model (DSM) using filtering techniques (Flood and Gutelius, 1997). Fig. 2-7 illustrates an example of original point cloud derived from laser scanning data, created DSM and DTM. DSM includes any objects such as buildings, clouds and vegetation in the path of the laser pulse. To determine the terrain surface from laser scanning data, filtering is necessary to eliminate those points that are not on the terrain surface (Lefsky et al., 2002). Numerous filter algorithms such as the "Morphological Filter" (Vosselman, 2000) and progressive densification (Axelsson, 1999)

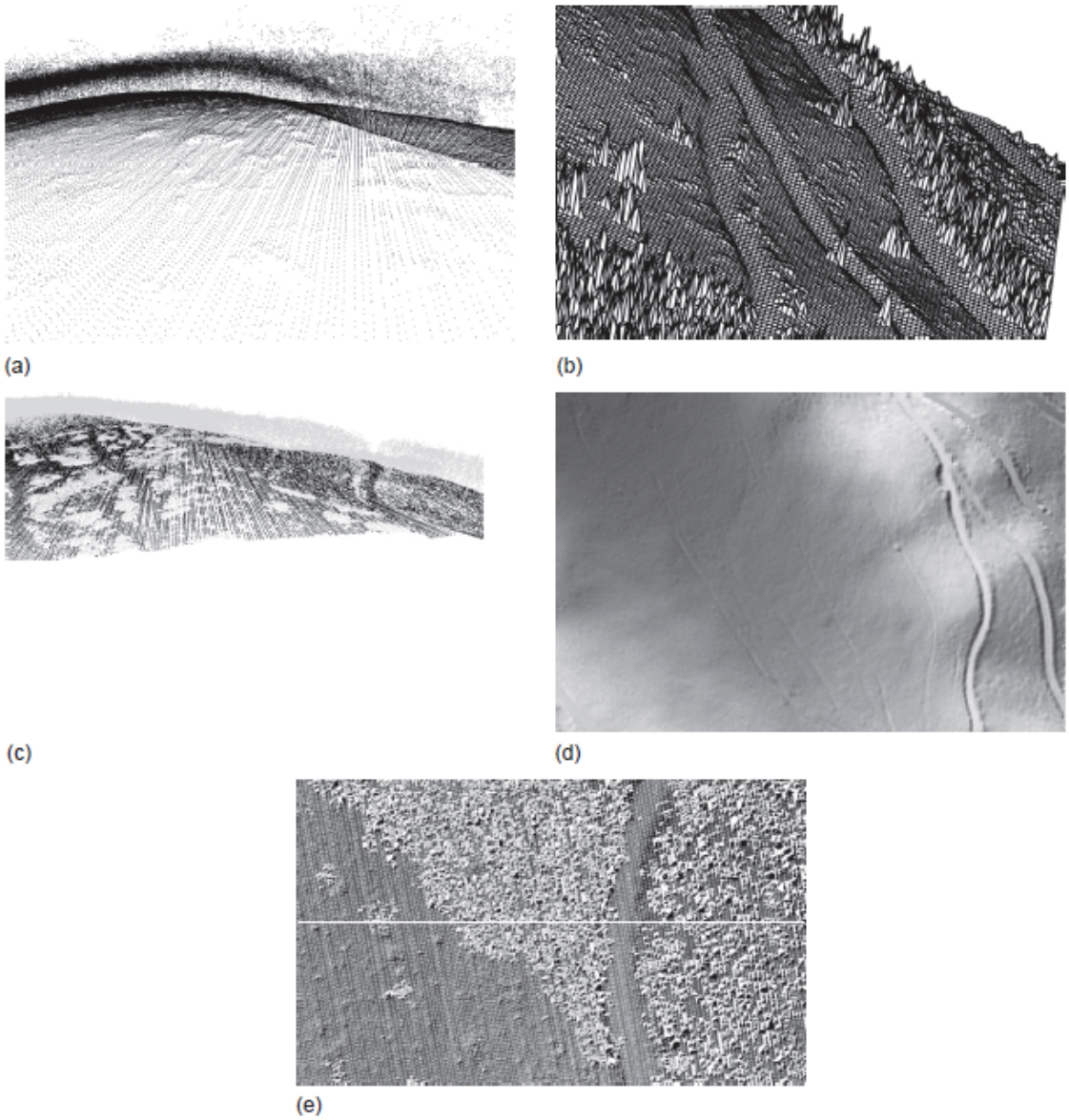

Figure 2-7 Example of original point cloud, DSM and DTM (Pfeifer and Mandlburger, 2009 p.313). (a) Original point cloud in perspective view from the side. (b) DSM of the same dataset. (c) Classified point set: ground points (black) and off-terrain points (gray). (d) Z-coding superimposed to shading of the DTM, plan view. (e) A shaded view of a DSM detail together with the original points and a profile of 85 m length.

have been reported. Compared with the traditional survey and photogrammetric techniques to determine the terrain, data acquisition of airborne laser scanning can be performed at night time (independent of sun position) and over difficult areas such as forests where the ground is not visible (e.g. Kraus and Pfeifer, 1998), and wetland and coastal dune where is low relief and texture (e.g. Irish and Lillycrop, 1999), with high accuracy and cost-

performance. Therefore, traditional methods are gradually being replaced by airborne laser scanning (Flood and Gutelius, 1997; Lefsky et al., 2002; Pfeifer and Mandlburger, 2009).

2.4.5.2 Forestry

The concept of producing forest stand profiles with laser profilers was introduced around 1980 (e.g. Nelson et al., 1984; Schreier et al., 1985). A background to the application of airborne laser scanning in forestry can be found in HyyppÃ et al. (2009). Numerous papers have documented the utility of LiDAR for the estimation of forest attributes in forestry. Recent studies are summarised in Table 2-12 which shows derived forest attributes with used LiDAR sensors and authors of the work. Since the primary interest in forestry is the assessment of timber volume, airborne laser scanning started being applied to estimating biomass and stand structure (e.g. Lefsky et al., 1999a; Lefsky et al., 1999b; Means et al., 1999; Nelson et al., 1988). In the following sub-sections, forest attributes derived from airborne laser scanning is detailed.

2.4.5.2.1 Tree height

Tree height and related attributes are the major area of airborne laser scanning, since it can measure the tree height with high accuracy. The most commonly used technique to extract tree height is the canopy height model (CHM) approach (e.g. Hill and Thomson, 2005; Hopkinson et al., 2008; Yu et al., 2004). This creates a DSM relevant to tree tops by classifying the highest returns and interpolating missing points, and then subtracts the DTM from the corresponding DSM. Consequently, the tree height is expressed as a mean

height. To obtain individual tree top height, the segmentation of individual trees is necessary, which usually requires high resolution data (e.g. Persson et al., 2002). For estimating height related attributes, computing percentiles of the distribution of laser canopy heights is another major approach (e.g. Næsset, 2002). In this method, canopy height metrics utilise quantiles equivalent to the 0, 10, 20, …, 90 percentiles of the first return laser canopy heights and corresponding statistics. Canopy density metrics use corresponding proportions of both the first and last returns above the 0, 10, 20, …, 90 quantiles to total number of laser returns. In terms of the accuracy of the estimation of tree height, Persson et al. (2002) reported an RMSE of 0.63 m for Norway spruce and Scots pine dominated forests and Hirata et al. (2009) demonstrated RMSE of 0.65 m for moderate thinning (30.4 %) Japanese cypress forests. In the studies of estimating forest growth based on the tree height, Yu et al. (2008) obtained the mean height growth with R^2 value of 0.86 and standard deviation of residuals of 0.15 m. It has been reported that tree height is underestimated by airborne laser scanning (e.g. Nelson et al., 1988; Persson et al., 2002). The tree height will be underestimated if the tree top and/or the ground are not detected by the sensor (HyyppÃ et al., 2008). Therefore, a sufficient density of laser pulses with sufficient energy to return signals is required to detect the tree top and penetrate the canopy to ground level (Lefsky et al., 2002).

2.4.5.2.2 Biomass

Measuring biomass has been another major area of interests in forestry since it measures tree materials that can be utilised as a source of energy. It is also becoming globally important in terms of carbon sequestration in forests. Most of previous studies using airborne laser scanning to estimate biomass have been conducted in temperate forests

Table 2-12 Recent studies using airborne/spaceborne LiDAR for forest attributes.

Forest attributes	LiDAR sensor (Airborne/*Spaceborne*)	Other sensor data used	Recent study
LAI	Optech ALTM 1233		Solberg et al. (2009)
	Leica ALS 40		Zhao and Popescu (2009)
	Falcon II		Morsdorf et al. (2006)
	Optech ALTM 3100C		Solberg et al. (2006)
	Optech ALTM 1210		Roberts et al. (2005)
	TopoSys-II		Riaño et al. (2004)
Tree height (including height metrics and height profile)	Optech ALTM 30		Falkowski et al. (2009)
	Optech ALTM 3100		Hirata et al. (2009)
	Riegl LMS-Q560		Müller et al. (2009)
	Optech ALTM 3100		Ørka et al. (2009)
	Leica ALS 40		Zhao et al. (2009)
	Optech ALTM 1225, 2050, 3100		Hopkinson et al. (2008)
	TopoSys-I, II		Yu et al. (2008)
	GLAS		Simard et al. (2008)
	GLAS		Rosette et al. (2008)
	GLAS, LVIS		Sun et al . (2008)
	Optech ALTM 2033	Aerial photograph	Packalén and Maltamo (2007)
	LVIS		Goetz et al. (2007)
	Terra Remote Sensing's instrument		Coops et al. (2007)
	Optech ALTM 3100C		Næsset and Nelson (2007)
	LVIS		Anderson et al. (2006)
	Optech ALTM 1210		Bradbury et al. (2005)
	LVIS		Hyde et al. (2005)
	SLICER		Lefsky et al. (2005)
	Optech ALTM 1210		Roberts et al. (2005)
	TopoSys-I		Yu et al. (2004)
	TopoSys-I		Riano et al. (2003)
	TopEye		Brandtberg et al. (2003)
	Aeroscan lidar system		Zimble et al. (2003)
	TopEye		Persson et al. (2002)
	Optech ALTM 1210		Næsset (2002)
	SLICER		Harding et al. (2001)
Biomass	Leica ALS 40		Zhao et al. (2009)
	Leica ALS 50 Phase II		Kim et al. (2009)
	GLAS		Simard et al. (2008)
	TopoSys-I, II		Yu et al. (2008)
	Optech ALTM 1210, 1233, 3100, Leica ALS 50-I		Næsset and Gobakken (2008)
	LVIS	AVIRIS	Anderson et al. (2008)
	Optech ALTM 3025		Goodwin et al. (2007)
	TopEye	SPOT	Wallerman and Holmgren (2007)
	Optech ALTM 2033	Aerial photograph	Packalén and Maltamo (2007)
	LVIS		Anderson et al. (2006)
	Spectrum mapping, LLC DATIS II		van Aardt et al. (2006)
	LVIS		Hyde et al. (2005)
	TopoSys-I		Riano et al. (2003)
	Optech ALTM 1210		Næsset (2002)
Stem number	Optech ALTM 2033	Aerial photograph	Packalén and Maltamo (2007)
	Optech ALTM 1210		Næsset (2002)

Forest attributes	LiDAR sensor (Airborne/*Spaceborne*)	Other sensor data used	Recent study
Stem diameter	LVIS	AVIRIS	Anderson et al. (2008)
	LVIS		Anderson et al. (2006)
Stem density	TopEye	SPOT	Wallerman and Holmgren (2007)
Basal area	LVIS	AVIRIS	Anderson et al. (2008)
	Optech ALTM 2033	Aerial photograph	Packalén and Maltamo (2007)
	Optech ALTM 1210		Næsset (2002)
Canopy cover (including volume profile/density)	Optech ALTM 2050, 3100		Hopkinson and Chasmer (2009)
	Optech ALTM 30		Falkowski et al. (2009)
	Optech ALTM 3100		Ørka et al. (2009)
	Optech ALTM 3025		Goodwin et al. (2007)
	Terra Remote Sensing's instrument		Coops et al. (2007)
	Falcon II		Morsdorf et al. (2006)
	LVIS		Hyde et al. (2005)
	SLICER		Lefsky et al. (2005)
	TopoSys-II		Riaño et al. (2004)
	TopoSys-I		Riano et al. (2003)
Crown shape	Optech ALTM 3100		Kato et al. (2009)
	Optech ALTM 3100		Hirata et al. (2009)
	Optech ALTM 1210		Roberts et al. (2005)
	TopEye		Brandtberg et al. (2003)
	TopEye		Persson et al. (2002)
Understorey vegetation	Optech ALTM 3100		Vehmas et al. (2009)
	TopoSys Falcon		Maltamo et al. (2005)
Coarse woody debris (CWD)	Optech ALTM 3100		Pesonen et al. (2008)
	Aeroscan lidar system		Seielstad and Queen (2003)
Tree species	Optech ALTM 3100		Ørka et al. (2009)
	TopEye MkII	Multi-spectral image by digital camera	Holmgren et al. (2008)
	TopEye		Brandtberg (2007)
	Optech ALTM 1020		Moffiet et al. (2005)
	TopEye		Holmgren and Persson (2004)
	TopEye		Brandtberg et al. (2003)

dominated by deciduous tree species and the estimation is based on a strong relationship between above-ground biomass components and amount of foliage, which can be detected by laser pulses (Næsset and Gobakken, 2008). One major approach to estimating biomass is to use the percentile of canopy height distribution as a predictor and determine the regression with related in-situ measurements (e.g. Næsset and Gobakken, 2008; Yu et al., 2008; Zhao et al., 2009).

2.4.5.2.3 LAI

Leaf area index (LAI) is generally defined as the one-sided leaf area per unit of ground area (e.g. Chen and Black, 1992; Danson et al., 2009; Watson, 1947). In the studies using airborne laser scanning, effective LAI (e.g. Solberg et al., 2006) or LAI proxy (e.g. Morsdorf et al., 2006) is often computed since these include the area of stems and branches, which are intercepted by the laser pulses as well as leaves. The theory of Beer-Lambert Law in chemistry, which states that the absorbance of a light beam transmitted and sent through the solution is determined by the concentration and path length in the solution, has been often applied to the transmission of laser pulses through the canopy, i.e. gap fraction (e.g. Gower et al., 1999; Riaño et al., 2004; Solberg et al., 2006; Zhao and Popescu, 2009). In this theory, LAI is determined by the transmission of laser pulses through the canopy and an extinction coefficient that depends on the foliage inclination angle distribution and the reflectivity of the foliage (Solberg et al., 2006). A major approach for estimations of LAI involves examining LiDAR metrics and regression analysis with related in-situ LAI values measured by hemispherical photographs or other optical sensors such as LAI2000 of LI-COR, Inc. (e.g. Morsdorf et al., 2006; Riaño et al., 2004; Solberg et al., 2009; Solberg et al., 2006; Zhao and Popescu, 2009). Riaño et al. (2004) estimated LAI using 50, 75, and 95 percentile of heights, average height, maximum height and percentage of canopy hits as LiDAR predictive variables in oak and Scots pine forests in Spain. These authors found that the percentage of canopy hits was the best estimator. Zhao and Popescu (2009) examined various LiDAR metrics such as laser penetration metrics (return number-based ratio), height-related metrics and foliage-density proxies for estimation of LAI in a pine-dominant eastern Texas forest. These authors concluded that laser penetration metrics with logarithm models were more effective than height-related metrics.

2.4.5.2.4 Canopy cover

Canopy cover has also been a focus for LiDAR based forestry assessments. Canopy cover is the inverse of gap fraction and also called as fractional cover in some studies (e.g. Hopkinson and Chasmer, 2009; Morsdorf et al., 2006). For example, Næsset (1997) showed the potential of LiDAR to estimate fractional cover. Fractional cover was derived from LiDAR as the ratio of canopy returns to the total number of returns per unit area. Similar methods utilising the point density of LiDAR returns to estimate fractional cover were presented in other studies (Coops et al., 2007; Hopkinson and Chasmer, 2007; 2009; Morsdorf et al., 2006; Riaño et al., 2004; Solberg et al., 2006) and showed promising results. Hopkinson and Chasmer (2007; 2009) also incorporated the intensity of LiDAR returns into their algorithm. These authors estimated canopy fractional cover calculating the ratio of the sum of all canopy level return intensities to the sum of total return intensity, and achieved a high correlation with fractional cover recovered from ground-based digital hemispherical photography.

2.4.5.2.5 Crown shape

To obtain information on crown shape, the segmentation of individual trees is required. Roberts et al. (2005) used interpolated canopy surface models from a LiDAR point cloud and identified the location of individual trees by assuming that the pixel related to the top of a tree will be higher than surrounding pixels. These authors then estimated crown diameter by identifying the crown edge in each cardinal direction from the located tree top pixel in the canopy surface model. It was reported that crown diameter derived from LiDAR was underestimated due to asymmetrical shape of crowns with irregular edges,

although the comparison with field measured crown diameters achieved R^2 value of 0.55. Hirata et al. (2009) located individual tree crowns from a LiDAR derived digital canopy model by the watershed segmentation method and the identification rates achieved were 95.3% for heavy thinning (the thinning ratio of the basal area, 38%), 89.2% for moderate thinning (30.4%) and 60% for no thinning, respectively. Kato et al.(2009) developed a 'wrapped surface reconstruction' method to capture tree crown formation. In this method, an individual tree was identified either by a marker controlled segmentation method or by a density or height variance dependent segmentation method from LiDAR derived digital canopy height models. Then, crown surface points were selected and 'wrapped' using Radial Basis Functions and an isosurface algorithm (Angel, 2003). In their study, the comparison between tree crown parameters derived from the wrapped surface and ground-based variables reported a R^2 value of 0.80 for coniferous trees and 0.75 for deciduous trees in crown width, R^2 value of 0.92 for coniferous trees and 0.53 for deciduous trees in crown base, R^2 value of 0.72 for coniferous trees and 0.51 for deciduous trees in height of the lowest branch, and R^2 value of 0.84 for coniferous trees and 0.89 for deciduous trees in crown volume.

2.4.5.2.6 Stem and basal area

In the recent studies of estimating basal area and stem related attributes such as stem number and its diameter, synthetic use of LiDAR data and other optical sensor data has been reported. Packalén and Maltamo (2007) estimated stem number, basal area and basal area median diameter for Scots pine, Norway spruce and deciduous trees using the combination of LiDAR derived height distribution variables, which include percentiles of canopy height and proportions of canopy hits, and spectral and textural features from aerial

photographs in a multivariate non-parametric k-MSN approach. These authors found that the RMSEs for basal area estimation were 27.05 % for pine trees and 31.30 % for spruce trees, which were acceptable, compared to a conventional field inventories in Finland. They also reported that the estimated stem numbers were even better than those of conventional field inventories. Wallerman and Holmgren (2007) combined LiDAR derived height distribution variables with the four SPOT-5 HRG spectral bands to predict forest stand variables in a managed forest dominated by Scots pine, Norway spruce and birch. These authors achieved RMSE of 19 % (1145 st ha^{-1}) for estimation of stem density and RMSE of 19 % (0.195 m) for mean diameter. Anderson et al. (2008) used integrated datasets of high spectral resolution imagery (Airborne Visible/Infrared Imaging Spectrometer; AVIRIS) and waveform LiDAR to estimate basal area, above-ground biomass and quadratic mean stem diameter in a experimental forest in the US. Canopy height, the height of median energy, the relative height at 25 % energy and the relative height at 75 % energy derived from waveform data and 24 AVRIS bands variables were compared with field derived variables in a stepwise mixed linear regression analysis. These authors concluded that the integrated datasets estimated the forest measurements better than the use of either data set alone.

2.4.5.2.7 Tree species

LiDAR data has been also used to discriminate between coniferous and deciduous tree species (Ørka et al., 2009) and individual tree species (Brandtberg, 2007; Brandtberg et al., 2003; Holmgren and Persson, 2004; Holmgren et al., 2008; Moffiet et al., 2005). Most of studies utilise tree shape and intensity information derived from LiDAR data. This is based on the concept that these information are different between tree species. Holmgren and

Persson (2004) classified Scots pine, Norway spruce and deciduous trees using LiDAR derived variables: proportion of canopy returns, standard deviation of the intensity of the returned pulses, mean intensity of the surface returns, proportion of first returns, proportion of surface hits, mean value of the parameters of the parabolic surface, relative standard deviation of laser heights and height percentile divided with the estimated tree height. These authors accomplished the classification accuracy of 95% with six of these variables. They also reported high classification accuracies were achieved by using the proportion of first returns and the standard deviation of the intensity. Holmgren et al. (2008) took the similar approach using the combination of LiDAR data and multi-spectral images and obtained an overall accuracy of 88 % to classify Norway spruce, Scots pine and deciduous trees. Ørka et al. (2009) analysed the differences in structural and intensity features between coniferous (Norway spruce) and deciduous (birch and aspen) trees and tested classification performance of the structural and intensity features. The highest classification accuracy of 88 % for large trees was achieved by combining eight variables: the kurtosis of the laser height distributions, maximum intensity from first returns, mean height, the skewness of the laser height distributions, crown density in 9^{th} layer from 1.3 m vantage point from single returns, coefficient of variation for the laser height values, crown density in 9^{th} layer from 1.3 m height and mean intensity from last returns. These authors reported that the return categories (first, single or last) were critical information to select the candidate feature for successful classification.

As described above, LiDAR based forest inventory studies show promising results. Recent forest inventory applications deal with various topics such as recreation, wildlife and watershed management in natural forests as well as plantation forests. However, the main focus is still on acquiring information on the volume and growth of trees, forest plots and stands (HyyppÃ et al., 2009). It should be also noted that many of them have been

conducted in Scandinavia or North America and have local or species specific methods. Careful consideration and modification would be necessary to apply their methods to other areas where other types of ecosystems exist.

2.4.5.3 Ecology

Compared to forest inventory studies, ecological applications require an assessment of complexity of habitat structure at a landscape scale. During the last decade, ecologists started recognising LiDAR as useful technology in providing valuable information for modelling relationships between landscape variables such as vegetation structure and organisms. LiDAR has great utility in this since it can offer data with high vertical resolution as well as sufficient area coverage required for valid statistical modelling (Müller et al., 2009). In the following sub-sections, forest attributes derived from LiDAR, which are particularly important in the ecological context, are detailed.

2.4.5.3.1 Vertical vegetation structure

Extracting vertical vegetation structure information is important but challenging in ecological applications since unlike managed forests, natural forests are more structurally complex, containing mixed vegetation species with different characteristics including ages. The individual tree approach is not realistic in such forests. The main approach is focused on identifying vegetation layers in forest stands using height information (e.g. Maltamo et al., 2005; Zimble et al., 2003). Zimble et al. (2003) used LiDAR derived tree height variance to differentiate single-storey and multi-storey vertical structural classes with a

97% accuracy. Riaño et al. (2003) used a cluster analysis of LiDAR height information to discriminate between overstorey and understorey canopies. Maltamo et al. (2005) tested the presence and the number of understorey trees by analysing the height distribution of LiDAR returns. These authors found that multi-layered stand structures can be recognised and quantified, however, the accuracy of the results varied greatly depending on the density of the dominant tree layer.

Understorey vegetation is another important attribute to identify. Vehmas et al. (2009) located the mature herb-rich forest stands, where are the main habitats for many endangered species, based on crown structure and vertical profile derived from LiDAR data.

2.4.5.3.2 Coarse woody debris (CWD)

Coarse woody debris (CWD) is important for nutrient cycling and habitation for species in forests. Small number of studies has been published to estimate the amount of CWD using LiDAR (e.g. Pesonen et al., 2008; Seielstad and Queen, 2003). In the study of fuel models in the closed-canopy conifer forests of the western United States, Seielstad and Queen (2003) showed the possibility of estimating CWD loads using a surface roughness metric and obstacle density, which was defined as the number of non-ground points less than 6 feet in height per square meter, normalized by the total number of ground and points greater than 6 feet. Pesonen et al. (2008) estimated downed dead wood volume using the predictive variables of canopy height distribution, cumulative proportional canopy densities, the laser pulse intensities accumulating in percentiles, the average intensity value of above-ground hits, the proportion of ground hits versus canopy hits and the average

height and standard deviation of the above-ground hits derived from first and last laser returns respectively. These authors found that the standard deviation of first return laser heights was the most significant variable in the models, and achieved the adjusted multiple correlation coefficient of 0.6099 with the combination of the standard deviation of first return laser heights and last return laser pulse intensity accumulating in 10^{th} percentile as predictors.

The vertical vegetation structure information derived from LiDAR has been used as a surrogate for habitat structure to predict population of a mammal (Nelson et al., 2005), bird's distribution and demography (Bradbury et al., 2005), bird's species richness and abundance (Goetz et al., 2007), chick mass (Hinsley et al., 2002) and bird's abundance and composition of assemblages (Müller et al., 2009). Hyde et al. (2005) characterised montane forest canopy structure; canopy height, canopy cover and biomass, as a prerequisite for large area habitat mapping for California spotted owls.

They showed the potential of LiDAR in integrating with ecological studies. More application of LiDAR for ecology is anticipated.

2.5 Conclusion

Conservation of biodiversity has been recognised internationally as critically important for sustainability. Measurements for the maintenance of biodiversity are required at all levels of government from the international scale to the local scale. At the landscape level, a practical way of defining and measuring biodiversity is necessary for managers. Forest structure has been internationally recognised as a surrogate of biodiversity since an

association is often found between biodiversity and measures of the variety and/or complexity of arrangement of structural components within an ecosystem. In Australia, forest structure variables are also measured in mandated vegetation monitoring systems. However, the current methods to assess forest structure information are often qualitative and require a laborious process that involves site visits and many logistically expensive point based measurements. An efficient and cost-effective assessment tool to compliment these survey methods is necessary. Remote sensing data derived from satellite and airborne sensors is superior to field survey data in providing high-spatial coverage, near simultaneous acquisition, repeated regional accounting and cost effectiveness. To date, most natural resource remote sensing has been undertaken using passive sensing technologies, which provide 2D information. Passive remote sensing technology can offer some biophysical parameters of forest structure, however these are often limited to either horizontal parameters or homogeneous species. LiDAR is an active sensor technology that illuminates the object using the sensor unit and measures the range distance between sensor and the illuminated target providing highly accurate 3D information of the objects. LiDAR has great potential in extracting forest structure information. Numerous papers have documented the utility of LiDAR, especially airborne laser scanning for the estimation of forest attributes in forestry applications and shown promising results. However, many of these studies have been conducted in Scandinavia or North America and have local or species specific methods. Careful consideration and modification would be necessary to apply their methods to other areas where other types of ecosystems exist. Ecologists also recently started recognising LiDAR as useful technology providing valuable information for modelling relationships between landscape variables such as vegetation structure and organisms. Ecological applications require an assessment of the complexity of habitat structure at a landscape scale. Innovative methods and more

application of LiDAR technology are anticipated in extracting forest structure information for biodiversity assessments.

CHAPTER 3 LIDAR DISCRETE RETURN SYSTEM EXPERIMENT

3.1 Introduction

The importance of forest structure information as a surrogate of biodiversity is widely acknowledged (Section 2.2). The application of LiDAR technology for extracting forest attributes was reviewed in Section 2.4.5.2 and Section 2.4.5.3. In this chapter, a LiDAR discrete return system experiment is conducted. Although the latest laser scanning systems can record several returns or a full waveform of returned signals, they have not been widely used in biodiversity research and such systems are far less common than conventional discrete return systems, which record only the first and last returns. This chapter evaluates the utility and potential of conventional discrete return systems for biodiversity assessment.

3.2 LiDAR intensity

LiDAR has been used to extract forest attributes such as canopy cover and biomass. The most commonly adopted approach is to use the height information derived from LiDAR data, computing, for example, percentiles of the distribution of laser pulses (Section 2.4.5.2.1). Some discrete return systems also record the intensity of the backscattered laser pulses. There have been few studies to date that utilise LiDAR intensity. This is because there is lack of calibration and the difficulty in interpreting the intensity information (see,

Section 2.4.4.1). However, the few studies that have utilised intensity information have shown promising results (e.g. Brandtberg et al., 2003; Means et al., 1999; van Aardt et al., 2006). The following is a comprehensive review of LiDAR intensity in extracting forest attributes to date.

Means et al. (1999) found that foliage biomass in coniferous forests was highly correlated with LiDAR derived metrics which included the sum of canopy intensity, ground intensity and canopy closure calculated from intensity. These authors found that tree foliage biomass was best predicted by a canopy intensity integration sum. Van Aardt et al. (2006) used intensity-based parameters such as mean and median intensity of return to estimate forest volume and above ground biomass in a mixed forest. Their results indicate that the number of returns and the intensity associated with each of these LiDAR interactions are necessary for effective modelling of biomass variations in structurally complex forests. For tree species classification, Brandtberg et al. (2003) note that the intensity of return 'maximum value', kurtosis and skewness, for individual leaf-off tree crowns, performed well for tree-based variables. These authors conclude that return intensity distributions were significantly different for different tree species. Holmgren and Persson (2004) tested a species classification algorithm, of Scots pine versus Norway spruce, at an individual tree level using two types of variables; those derived from the shape of trees resulting from a segmentation and variables derived directly from laser data. They achieved the highest classification accuracies by using the combination of six variables, but found that the proportion of first returns and the standard deviation of the return intensity provided a major contribution to successful species classification. This also suggested these variables could be used for estimation of tree species proportions on plots and in forest stands where the LiDAR returns are too few to allow identification of individual trees. Moffiet et al. (2005) examined how LiDAR intensity interacts with the forest canopy to produce

intensity return signals. Similarly to Van Aardt et al. (2006), these authors note that average LiDAR return intensity and intensity variation may be useful variables to assist with species discrimination. They also note intensity of return values can be affected by forest structure and the reflective properties of the vegetation. Hopkinson and Chasmer (2007; 2009) estimated canopy fractional cover calculating the ratio of the sum of all canopy level return intensities to the sum of total return intensity, and achieved a high correlation with fractional cover recovered from ground-based digital hemispherical photography. Pesonen et al. (2008) estimated downed dead wood volume (RMSE 51.6%) using the standard deviation in height distribution and laser pulse intensities accumulating in percentiles. Kim et al. (2009) estimated live and dead standing tree biomass and concluded intensity was key variable.

In this analysis, a conventional discrete return system is examined to determine whether it can extract forest structure information in an Australian Eucalyptus forest. In particular, the utility of LiDAR return intensity information is highlighted. Classification of forest structure types is also attempted using intensity information.

3.3 Study area

The study area for this experiment (Upper left S 35˚46', E 144˚52'; Lower right S 36˚0', E 145˚0') is situated in the Barmah Millewa Forest, located on the border of New South Wales (NSW) and Victoria (VIC) in Australia (Fig. 3-1). The area is a riparian complex which comprises approximately 70,000 ha of wetland and forests (Fig. 3-2). This system has a variety of land tenures including areas of national park and state forest reserves. In the latter, logging operations exist which can hinder the monitoring process. The area is

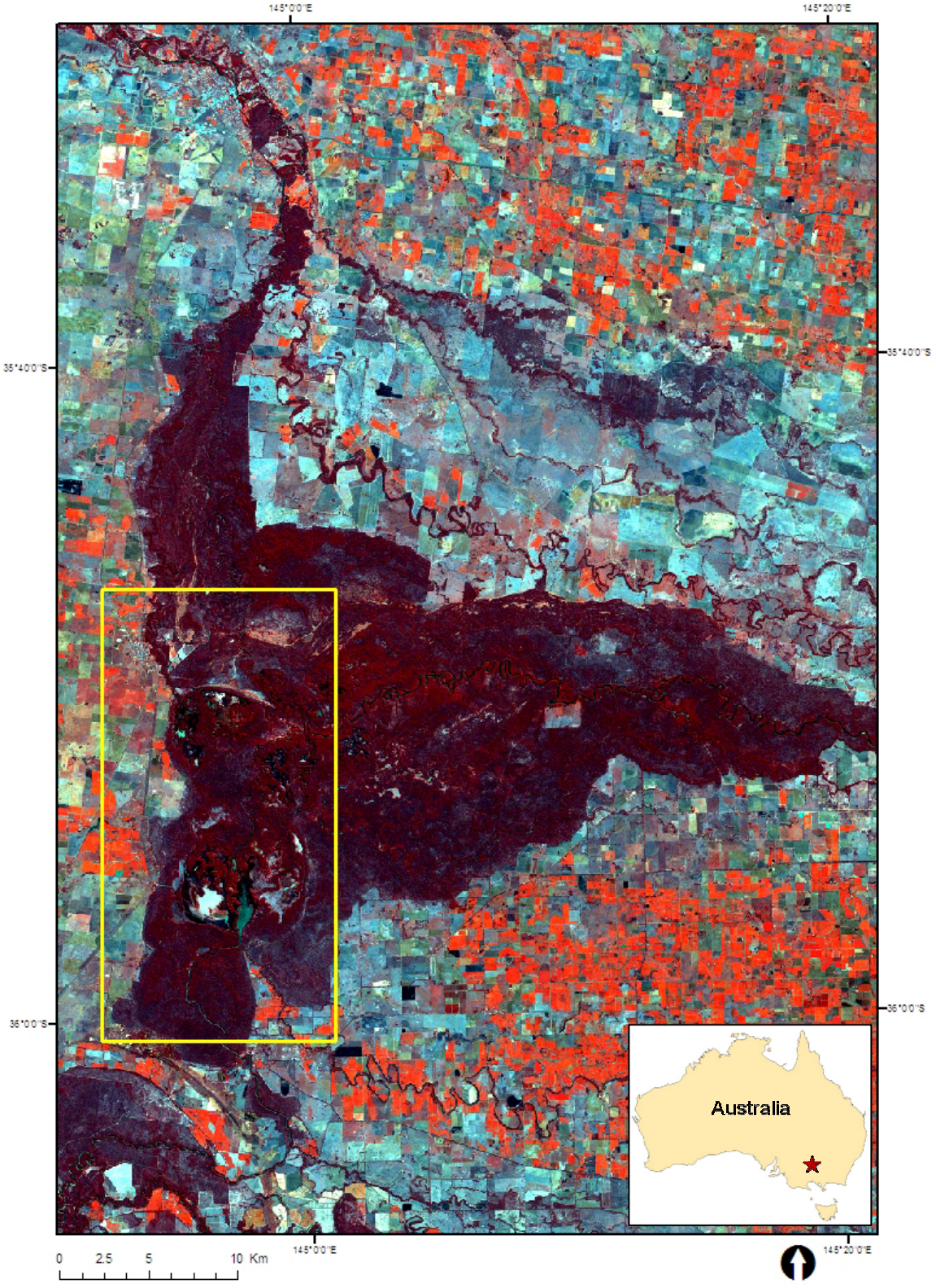

Figure 3-1 Study area is displayed in the rectangle on the satellite imagery; Landsat-7 ETM+ (Blue; band 1, Green; band 2, Red; band 4).

Figure 3-2 Photograph of study area. The area is a riparian complex which comprises approximately 70,000 ha of wetland and forests.

Table 3-1 LiDAR acquisition specifications.

Scanner Model	ALTM 1225 (now ALTM 3025)
Sampling intensity	11000 Hz and 12500 Hz
Flying height	1100 m
Laser swath width	800 m gross, 600 m net (25% overlap between swathes)
Laser wavelength	1.047 microns
Laser footprint	0.22 m
Vertical Accuracy	0.15 m (1 sigma)
ALS Internal precision	0.05 m
Acquisition Date	July 2001

important since it represents the largest remaining river red gum (*Eucalyptus camaldulensis ssp. obtusa Dehnh*) forest in the world (Bacon et al., 1993). This landscape contains important rare and endangered Flora and Fauna (Harris and Rawson, 1992). The Barmah-Millewa Forests are recognised as a significant habitat for migratory birds in international treaties such as the Ramsar convention, the Japan-Australia Migratory Birds Agreement and the China-Australia Migratory Birds Agreement (Chong, 2003). Conservation of biodiversity is therefore critical in this area.

3.4 Materials

3.4.1 LiDAR data

The LiDAR data used in this research was gathered in July 2001 and acquired by the Murray Darling Basin Commission, using ALTM, Optech airborne laser scanning system (small footprint and discrete return). Table 3-1 details the specifications of the sensor at the time of acquisition. The data provided comprises three data sets: First return pulse,

Last return pulse “ground” and Last return pulse “non-ground”. Each data set contains two variables: elevation information and an intensity of return value.

3.4.2 Field data

In July and September, 2005 a field survey was completed specifically to explore and validate the ecological content of the LiDAR dataset. The four year time difference between LiDAR acquisition date and field observation is unfortunate. However, the research team confirmed there was no major logging or wild fires during this period, and the forest condition was similar. Twenty five plots were positioned throughout the forest with a caveat of accessibility. Surveys were established as two hectare circular plots (Fig. 3-3, grey area). A plot was established by defining a centre point and taking a hand-held GPS (eTrex of GARMIN Corporation) measurement. This includes resident positional error of x y, ± 7 m on average. Tree height (m) was determined using a clinometer. Canopy and understorey cover (%) such as grass, leaf and bare ground, were assessed with the reference photography after the method of Walker and Hopkins (1990).

These measurements were conducted at the plot centre and three of the four peripheral points (Fig. 3-3, numbered 1-4). The quantity of fallen trees was also assessed over each plot in four classes; absent, 1-5 logs, 6-15 logs and more than 15 logs.

3.5 Methods

Data for the 2 ha plots was extracted from the three LiDAR point cloud data sets: (First

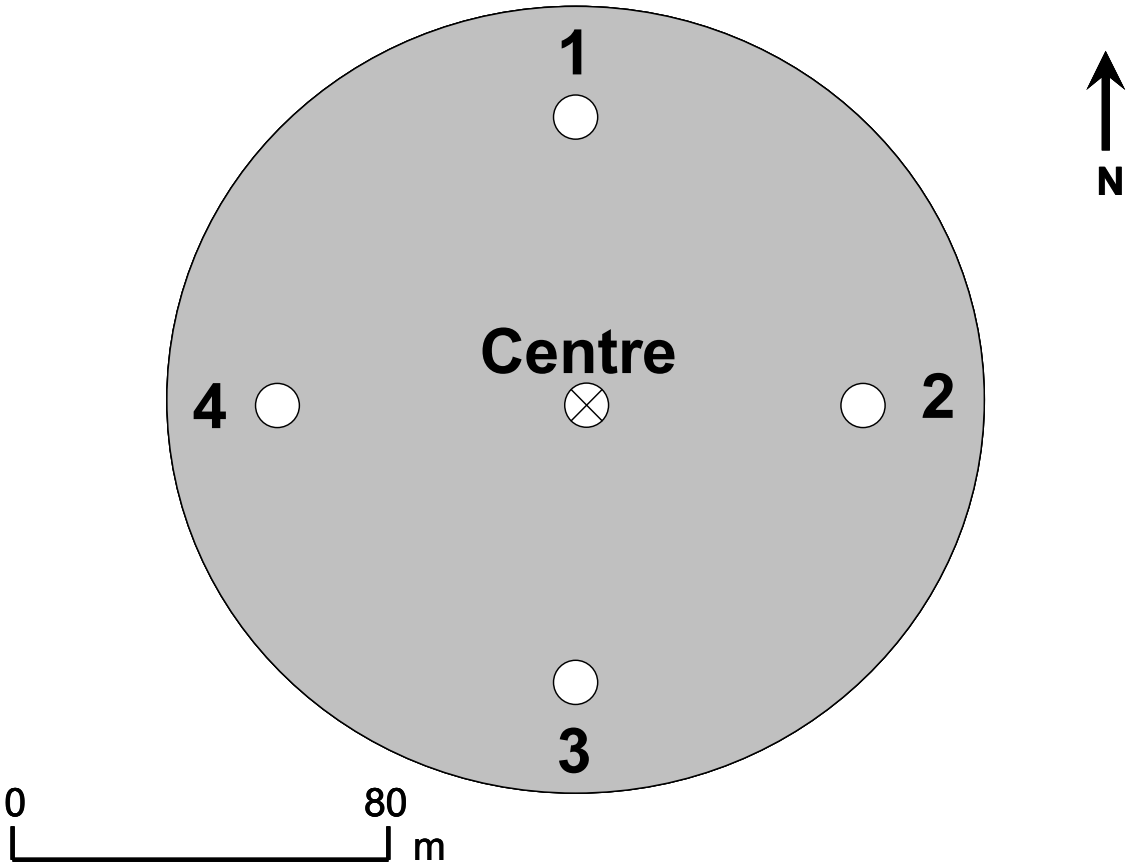

Figure 3-3 The grey area shows the survey area of the circular two hectare plot. Measurements of tree height, canopy cover, shrub cover, grass cover, leaf cover and bare ground cover were conducted at the plot centre and three of the four peripheral points (numbered 1-4). The quantity of fallen trees was assessed over each plot. Plot centre was located with a GPS. Tree height was measured with clinometers. Canopy and ground cover were assessed with the reference photography. The peripheral points were located approximately 60 m from the centre.

data - first pulse returns; Ground data - last pulse returns; and Non-ground data - last pulse returns). To account for positioning inaccuracies in locating the plot areas a 10 % area was added to each plot yielding an amended plot size of 2.2 ha (84 m radius circular plot (Fig. 3-3)). The first stage in processing was to group the three data sets (First data, Ground data and Non-ground data) into a single combined point cloud. This was then reclassified into two strata; Canopy and Ground. This was achieved using the maximum elevation value of the Ground dataset as a threshold (derived from Ground return statistics on a plot by plot basis -Fig. 3-4(b)). This was necessary since there were pronounced variations in ground elevation between plots which required a local definition of what constitutes ground.

Subsequently, the data in each stratum was reclassified into two groups; First return and Last return, to determine if there was any difference between these two interactions. This yielded four data sets that correspond to elevation and intensity information for two strata; canopy and ground, with First pulse returns and Last pulse returns recorded for each (Fig. 3-4(a)).

In order to assess the forest structure information content of the LiDAR data, the mean values for a range of ecological variables were calculated. Canopy, grass, leaf and bare-ground cover information were summed in each plot and presented as a mean. As the quantity of fallen trees was assessed over each plot in four classes; absent, 1-5 logs, 6-15 logs and more than 15 logs, these class values were used as a categorical variable.

For comparison with field data, mean LiDAR intensity and standard deviation of intensity were calculated for the classified groups; First return intensity in Canopy stratum (FRI_C), Last return intensity in Canopy stratum (LRI_C), First return intensity in Ground stratum (FRI_G) and Last return intensity in Ground stratum (LRI_G). These intensity values were utilised without any calibration. To examine the relationship between LiDAR data and collected ecological variables, the Pearson correlation coefficient was calculated to test the relationship between intensity values; mean intensity and standard deviation of intensity, and mean canopy cover, mean grass cover, mean leaf cover and mean bare-ground cover. The Pearson correlation coefficient estimates the degree of linear association between two variables in the parametric context (Sprent and Smeeton, 2001). The Spearman rank correlation coefficient, which is often referred to as Spearman's rho (Sprent and Smeeton, 2001), was used to evaluate the relationship between intensity values and the amount of fallen trees since the amount of fallen trees is an ordinal data.

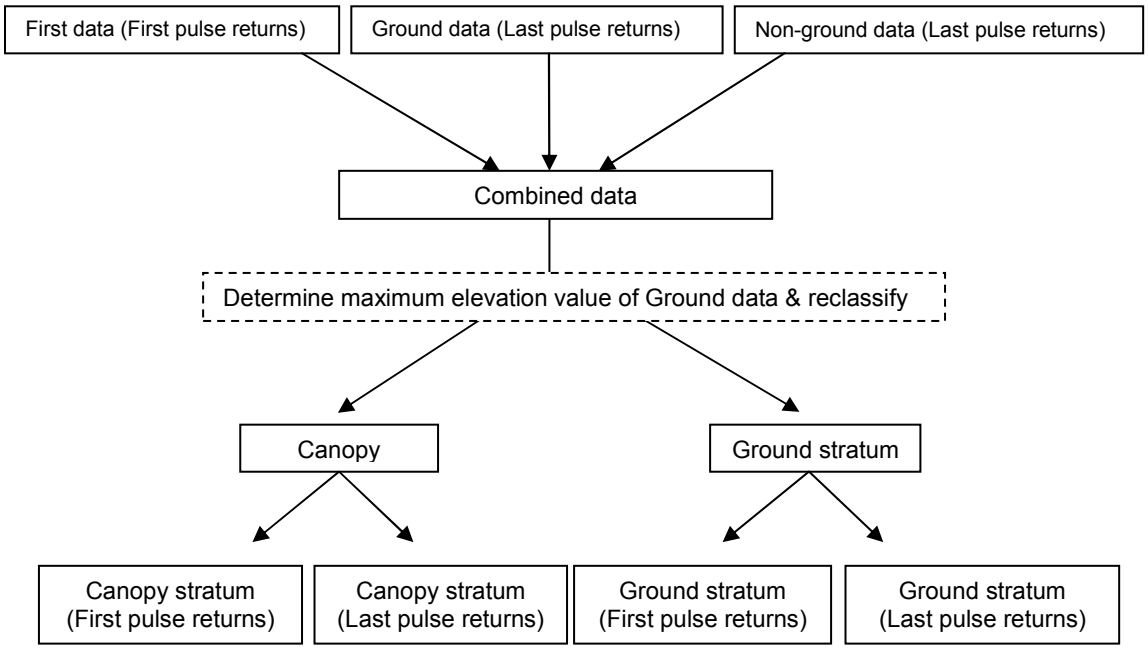

a) Flow chart

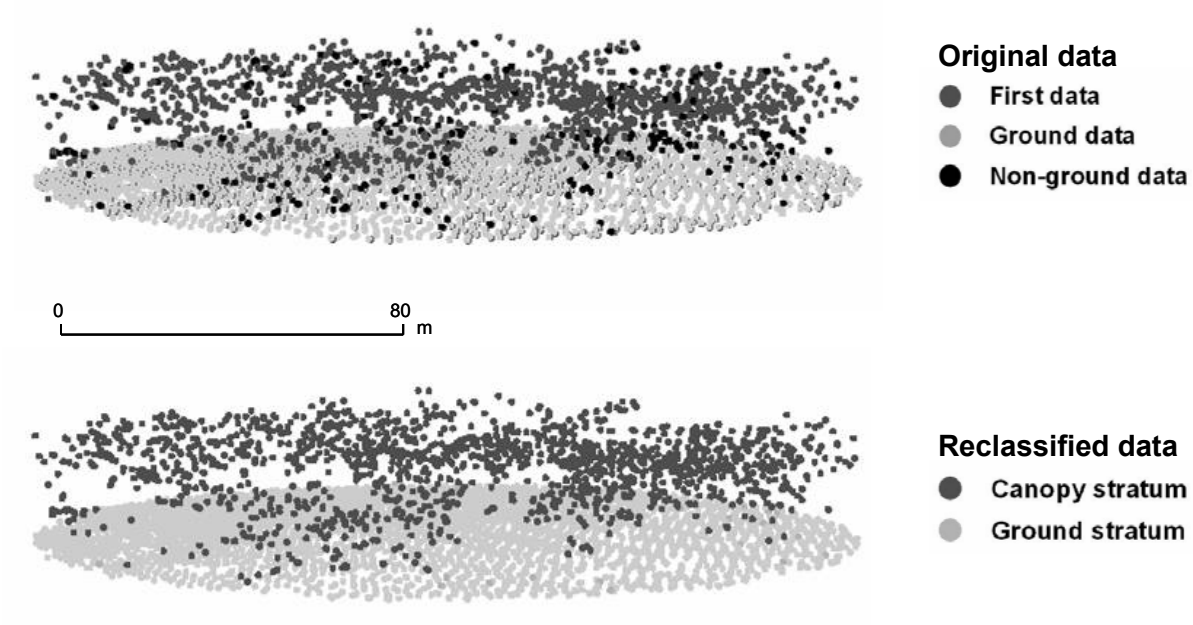

b) Example of LiDAR data within a two hectare plot

Figure 3-4 LiDAR data classification. a) Illustrates the algorithm of LiDAR data classification. LiDAR data was extracted within a two hectare plot. Original pre-processed data set; First data, Ground data and Non-ground data (b; upper diagram), were combined and reclassified into Canopy stratum and Ground stratum (b; below diagram) using maximum elevation value of Ground data as a threshold. This was calculated on a plot-by-plot basis. Then, these data were reclassified into two groups; First and Last pulse returns. Mean intensity and standard deviation of intensity were calculated in the classified groups; First return intensity in Canopy stratum (FRI_C), Last return intensity in Canopy stratum (LRI_C), First return intensity in Ground stratum (FRI_G) and Last return intensity in Ground stratum (LRI_G).

The combination of mean and standard deviation of intensity are also tested whether they can be an index to characterise the plot condition.

3.6 Results

The results of initial investigation of the standard deviation and mean intensity in different groups in each plot are presented in Fig. 3-5 and 3-6. They demonstrate some return intensity characteristics. LRI_G showed highest standard deviation in most plots, followed by LRI_C, FRI_C and FRI_G in this order (Fig. 3-5). Higher standard deviation of intensity was observed more in the last return (LRI_C and LRI_G) than in the first return (FRI_C and FRI_G) (Fig. 3-5). FRI_G exhibited highest mean intensity in most plots, followed by LRI_G, LRI_C and FRI_C in this order (Fig. 3-6). Mean intensity of the first return (FRI_G) is higher than the last return (LRI_G) in Ground stratum, however the value of FRI_C is lower than LRI_C in Canopy stratum (Fig. 3-6).

The results of comparison between LiDAR intensity variables and field variables are shown in Table 3-2. FRI_C exhibited a strong negative correlation with canopy cover ($R = 0.509$, $P < 0.01$) and a significant positive relationship with grass cover ($R = 0.620$, $P < 0.01$). FRI_G displayed a high positive association with canopy cover ($R = 0.580$, $P < 0.01$) and a strong positive correlation with the amount of fallen trees ($R = 0.698$, $P < 0.01$), which was shown in Table 3-3. The standard deviation of FRI_G displayed a negative correlation with canopy cover ($R = -0.519$, $P < 0.01$, Table 3-4) and the amount of fallen trees ($R = -0.686$, $P < 0.01$, Table 3-5). The results for LRI_C and LRI_G did not show significant relationship with field data (Table 3-2, 3-3, 3-4 and 3-5).

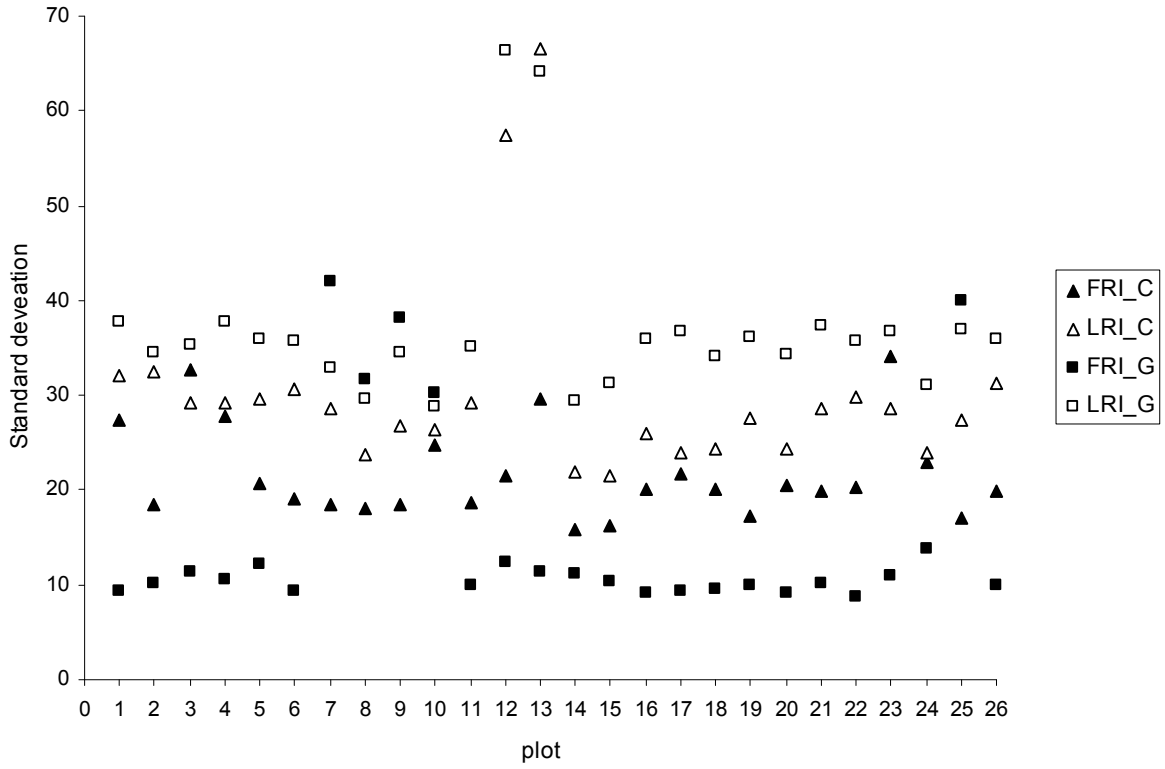

Figure 3-5 Standard deviation of intensity in different groups in each plot. Higher standard deviation of intensity was observed more in the last return (LRI_C and LRI_G) than in the first return (FRI_C and FRI_G).

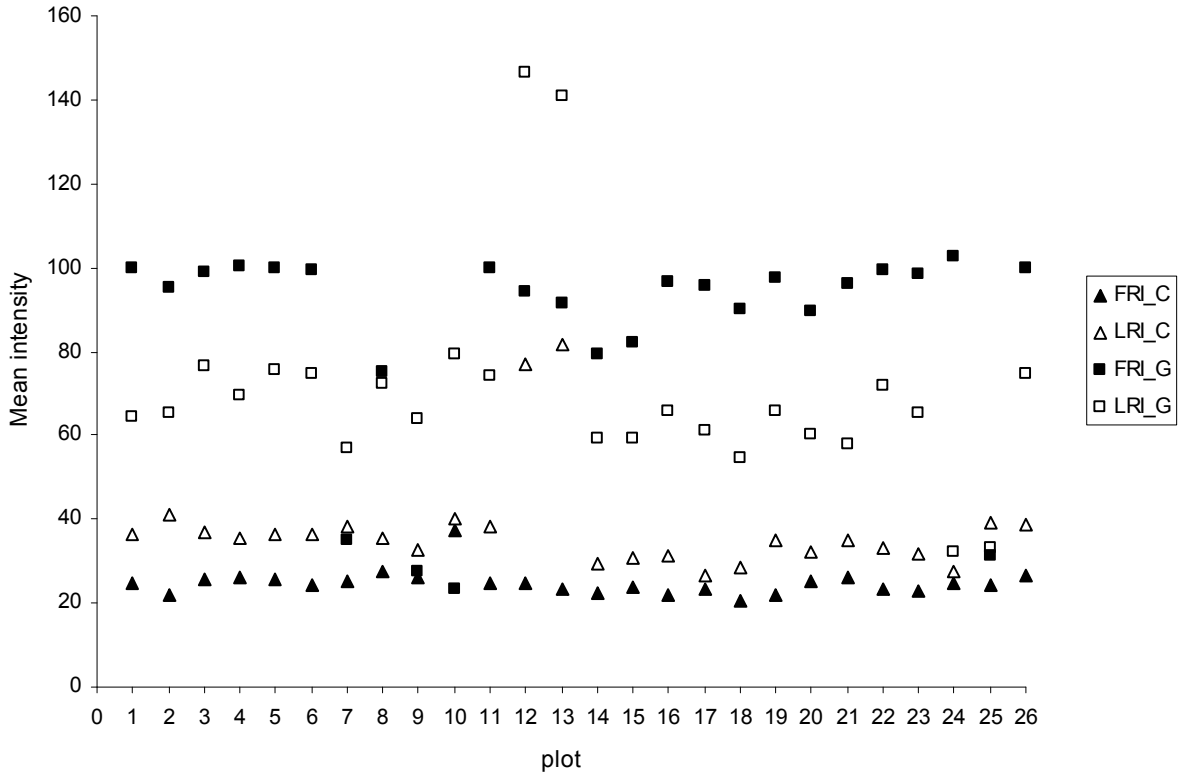

Figure 3-6 Mean intensity in different groups in each plot. Mean intensity of the first return (FRI_G) is higher than the last return (LRI_G) in Ground stratum, however the value of FRI_C is lower than LRI_C in Canopy stratum.

Table 3-2 Correlations between mean intensity; First return intensity in Canopy stratum (FRI_C), Last return intensity in Canopy stratum (LRI_C), First return intensity in Ground stratum (FRI_G) and Last return intensity in Ground stratum (LRI_G), and field data; mean canopy cover, mean grass cover, mean leaf cover and mean bare-ground cover in 25 plots.

		FRI_C	LRI_C	FRI_G	LRI_G
mean canopy cover	Pearson Correlation	-.509(**)	0.077	.580(**)	0.045
	Sig. (2-tailed)	0.009	0.713	0.002	0.829
	N	25	25	25	25
mean grass cover	Pearson Correlation	.620(**)	0.367	-.429(*)	.424(*)
	Sig. (2-tailed)	0.001	0.071	0.032	0.035
	N	25	25	25	25
mean leaf cover	Pearson Correlation	-.435(*)	-0.346	0.33	-0.355
	Sig. (2-tailed)	0.03	0.09	0.107	0.081
	N	25	25	25	25
mean bare-ground cover	Pearson Correlation	-0.309	-0.235	0.02	-.406(*)
	Sig. (2-tailed)	0.133	0.257	0.924	0.044
	N	25	25	25	25

** Correlation is significant at the 0.01 level (2-tailed).

* Correlation is significant at the 0.05 level (2-tailed).

Table 3-3 Correlation between mean intensity and the amount of fallen trees in four classes; absent, 1-5 logs, 6-15 logs and more than 15 logs.

			FRI_C	LRI_C	FRI_G	LRI_G
Spearman's rho	fallen trees	Correlation Coefficient	-.450(*)	-0.251	.698(**)	0.126
		Sig. (2-tailed)	0.024	0.225	0	0.549
		N	25	25	25	25

** Correlation is significant at the 0.01 level (2-tailed).

* Correlation is significant at the 0.05 level (2-tailed).

Table 3-4 Correlations between standard deviation of intensity and field data; mean canopy cover, mean grass cover, mean leaf cover and mean bare-ground cover in 25 plots.

		FRI_C STDEV	LRI_C STDEV	FRI_G STDEV	LRI_G STDEV
mean canopy cover	Pearson Correlation	0.085	0.134	-.519(**)	0.133
	Sig. (2-tailed)	0.686	0.522	0.008	0.526
	N	25	25	25	25
mean grass cover	Pearson Correlation	0.003	0.27	0.287	0.202
	Sig. (2-tailed)	0.988	0.192	0.164	0.332
	N	25	25	25	25
mean leaf cover	Pearson Correlation	-0.091	-0.319	-0.302	-0.241
	Sig. (2-tailed)	0.666	0.12	0.143	0.245
	N	25	25	25	25
mean bare-ground cover	Pearson Correlation	-0.037	-0.223	0.177	-0.189
	Sig. (2-tailed)	0.859	0.284	0.398	0.366
	N	25	25	25	25

** Correlation is significant at the 0.01 level (2-tailed).

Table 3-5 Correlation between standard deviation of intensity and the amount of fallen trees.

			FRI_C STDEV	LRI_C STDEV	FRI_G STDEV	LRI_G STDEV
Spearman's rho	fallen trees	Correlation Coefficient	0.301	0.288	-.686(**)	0.352
		Sig. (2-tailed)	0.144	0.163	0	0.084
		N	25	25	25	25

** Correlation is significant at the 0.01 level (2-tailed).

Table 3-6 Correlation between canopy cover and grass cover.

		mean grass cover	
mean canopy cover	Pearson Correlation	-0.542	(**)
	Sig. (2-tailed)	0.005	
	N	25	

** Correlation is significant at the 0.01 level (2-tailed).

Table 3-7 Correlation between canopy cover and sampled average tree height.

		mean canopy cover	
Sampled average tree height	Pearson Correlation	0.423	(*)
	Sig. (2-tailed)	0.035	
	N	25	

* Correlation is significant at the 0.05 level (2-tailed).

The combination of mean and standard deviation of intensity is presented in Fig. 3-7. It demonstrates the plots can be classified into three groups; group A, group B and group C, using FRI_G and standard deviation of FRI_G. Group A includes plots with low FRI_G and high standard deviation of FRI_G. Group B has plots with high FRI_G and low standard deviation of FRI_G. Group C has only one plot which has high FRI_G and high standard deviation of FRI_G. Fig. 3-8 shows the field measured canopy cover and fallen tree class for these groups. Plots in group A have lower canopy cover and fewer fallen trees. Higher canopy cover and many fallen trees are found in plots in group B. Group C shows in-between plot characteristics between group A and B: moderate canopy cover and fallen trees.

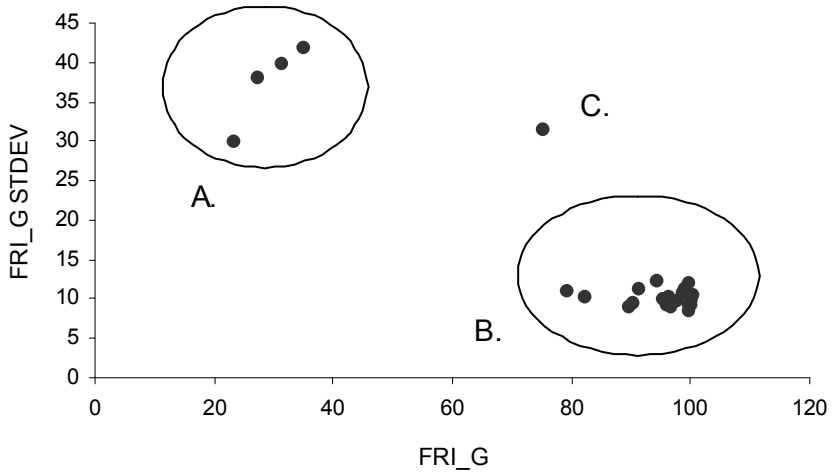

Figure 3-7 Scatter plot of first return intensity from ground stratum (FRI_G) and standard deviation of first return intensity from ground stratum (FRI_G STDEV). The sites can be classified into three groups; group A, group B and group C.

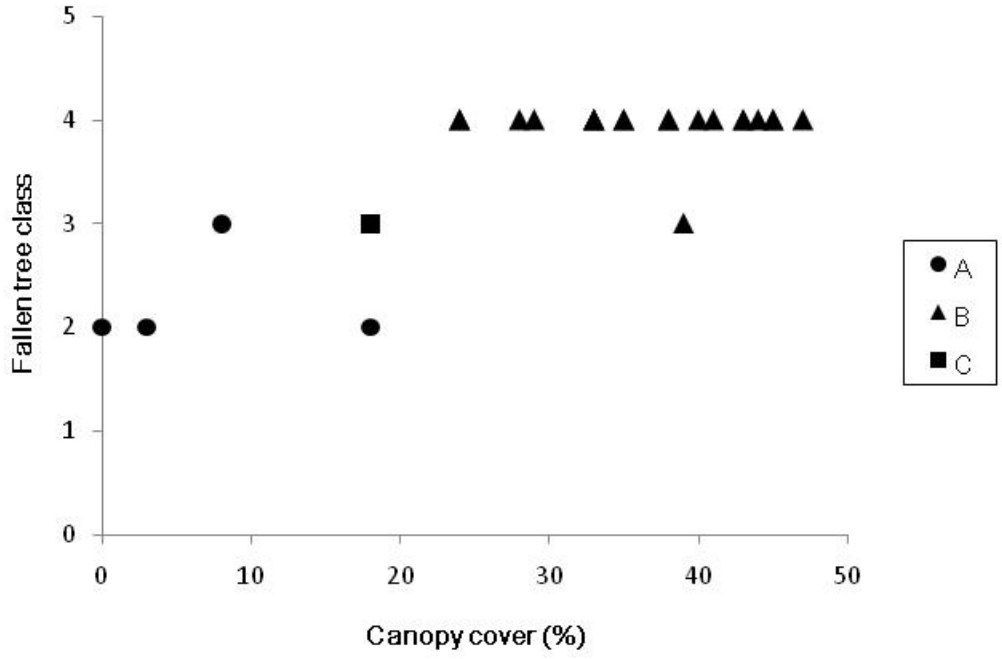

Figure 3-8 Field measured canopy cover and fallen tree class for group A, B and C.

3.7 Discussion

3.7.1 First return intensity in Canopy stratum (FRI_C)

FRI_C shows a strong negative correlation with canopy cover (Table 3-2). In other words, where canopy cover is high, first return intensity in the canopy stratum is low. The following scenario is hypothesised. At 1.047 μm, reflectance and transmittance components are the dominant radiation transfer processes (Bauer et al., 1986; Curran, 1985; Lillesand et al., 2004). However, emitted laser pulse is randomized on the interaction with the canopy layer due to small reflective areas and angles of leaves. Therefore weak pulses are often returned to the LiDAR sensor. On the other hand, where the canopy is present but with sparse foliage, laser pulses are much less likely to interact with canopy objects but when they do, the nature of the interaction is different. The pulse is more likely to interact with solid materials such as branches and boles, and stronger returned pulses therefore result.

FRI_C also displays a strong positive relationship with grass cover (Table 3-2). This provides strong anecdotal evidence since one would expect more grass growth where the canopy is sparse, if light is a limiting growth factor. In other words, grass does not grow thickly where canopy is dense, because the fraction of Photosynthetically Active Radiation (fPAR) is reduced. Although the correlation between mean leaf cover and FRI_C is only significant at the 0.05 level, a similar relationship was observed. Our field data also shows a negative relationship between canopy cover and grass cover (Table 3-6).

3.7.2 First return intensity in Ground stratum (FRI_G)

FRI_G also exhibits significant positive association with canopy cover (Table 3-2). It is hypothesised: where canopy cover is high, the first return intensity in the ground stratum is high. Our field data demonstrates a positive association between large trees and dense canopies (Table 3-7). Large fallen trees and debris are more likely to be on the ground and stronger ground return pulses result. FRI_G also shows a strong positive correlation with the amount of fallen trees (Table 3-3), which suggests where fallen trees are abundant, first return intensity in ground stratum is high. Again, it is hypothesised that when laser pulses hit solid materials such as logs and fallen trees, strong pulses are returned.

The standard deviation of FRI_G displays a negative correlation with canopy cover (Table 3-4) and the amount of fallen trees (Table 3-5). This can be explained as where canopy cover is high (fallen trees are abundant), the standard deviation of first return intensity in the ground stratum is low. The standard deviation of intensity is a measure of variation in intensity values. Assuming that each component on the ground has a distinct interaction with the laser pulse, standard deviation of FRI_G could be used as an index of heterogeneity of ground cover. A high standard deviation of FRI_G indicates heterogeneous ground cover, and lower standard deviation of FRI_G suggests homogeneous ground. Where the canopy is dense or fallen trees are abundant, ground is more likely homogeneous. Furthermore, this is an efficient way of using intensity data and avoiding calibration issues.

3.7.3 First return intensity and last return intensity

The results of the analysis revealed that the last return intensity for both canopy and

ground returns (LRI_C and LRI_G) does not show significant correlation with the field based ecological variables (Table 3-2 and 3-4). This fits with the results of Brandtberg et al. (2003) who report lower accuracy in classifying species when using last return information. Moffiet et al. (2005) explained that the last return intensity is affected by the pulse energy remaining within the portion of footprint as well as reflective surface properties. This can have a profound impact. In other words, the return is a result not just of the ground cover but also the amount of energy remaining in the pulse. In our study, this was explained by the standard deviation of intensity in each plot. A higher standard deviation of intensity was observed in the last return (LRI_C and LRI_G) as compared to the first return (FRI_C and FRI_G) (Fig. 3-5), indicating the last return has greater variation in intensity. This is especially salient since there is no species difference in Canopy stratum. We propose the difference in intensity variation between first return and last return in canopy stratum (FRI_C and LRI_C) could be due to the amount of pulse energy that remains to interact with the vegetation component in the canopy stratum. However, the results are contrary to this. Mean intensity of LRI_C is higher than FRI_C in all plots (Fig. 3-6). It is possible, but unlikely, that the emitted pulse is intercepted by a vegetation component initially, but the majority of pulse energy retained for the next vegetation interaction. As our data set can not identify whether FRI_C is singular or the first return out of two returns, we can not conclude if this is the case. It is also possible that the last return interacts with a solid material such as a branch or a large fallen tree on the ground, since most of LRI_C were found in lower level of Canopy stratum. This might explain why mean intensity in LRI_C was higher than FRI_C.

Identification of the return property for the ground returns is simpler. We can safely assume that FRI_G is singular return as it is the first return from the ground. The mean intensity of FRI_G is higher than LRI_G in most plots (Fig. 3-6). This is because FRI_G is the first

return and therefore did not lose any energy before it interacted with the ground, while the pulse energy of LRI_G was reduced after being partially intercepted by vegetation components in Canopy stratum.

3.7.4 Relationship between mean intensity and standard deviation of intensity

Mean intensity and standard deviation of intensity exhibit a strong correlation with some of ecological variables. Using FRI_G and standard deviation of FRI_G, it was demonstrated that the combination of these values can be an index to characterise the plot condition (Fig. 3-7). Using the scenario of FRI_G and standard deviation of FRI_G discussed in Section 3.7.2, the plots in group A are assumed to have sparse canopy and few fallen trees. The plots in group B would have dense canopy and many fallen trees. Field observations actually support this assumption (Fig. 3-8). All plots in group A have lower canopy cover and fewer fallen trees compared with plots in group B.

3.8 Conclusion

Conventional discrete (first and last) return systems are still more common and available to natural resource managers than the latest laser scanning systems such as full waveform LiDAR. In this chapter, a conventional discrete return system was examined to determine whether it can extract forest structure information. As a result of a LiDAR discrete return system experiment, it was concluded that conventional discrete return systems can be used to recover forest structure information for forests with an ecologically simple structure (i.e. single tree species with no mid- and understorey vegetation except grass and relatively flat

terrain). LiDAR intensity, vertically stratified using range information, has potential to recover canopy cover, grass cover and the amount of fallen trees. The combination of LiDAR intensity mean and standard deviation can be used to differentiate forest structural types; sparse canopy with few fallen trees or dense canopy with many fallen trees. Utilising standard deviation of intensity as a variable could be one solution in using intensity data since it avoids the intensity calibration issues. It was noted that first returns are better variables for analysis, since last returns were affected by the remaining energy in the pulse and did not show as significant correlation with field variables as the first returns. In terms of data preparation, it is recommended that LiDAR point data should be accompanied by information regarding its return properties such as singular returns or first of many returns since these properties could have the impact on the results.

CHAPTER 4 BACKGROUND FOR LIDAR FULL WAVEFORM SYSTEM EXPERIMENT

4.1 Introduction

The utility and potential of conventional discrete return systems for biodiversity were evaluated in Chapter 3. This chapter provides a background for a LiDAR full waveform system experiment, which will be presented in the following chapters, Chapter 5 and 6. The study area and the LiDAR data used are described. Fieldwork protocols developed specifically for this LiDAR experiment are also explained.

4.2 Study area

The study area for the LiDAR full waveform experiment (Upper left S 41.12º, E 146.45º; Lower right S 41.32º, E 146.58º) is located in the Rubicon catchment of the Cradle Coast Region of Tasmania, Australia and is approximately 20,000 ha (Fig. 4-1). The area is classified as *Eucalyptus amygdalina* coastal forest and woodland. The forests are dry sclerophyll communities dominated by *E. amygdalina* and have heathy, sedgy and shrubby understorey variants (Harris and Kitchener, 2005), and the forest structure varies (Fig. 4-2). In this area, the human population is growing in coastal towns such as Devonport, which is one of the two major centres in this region. Most people are employed in primary industries (agriculture, mining, forestry and fishing), manufacturing, retail and tourism. As

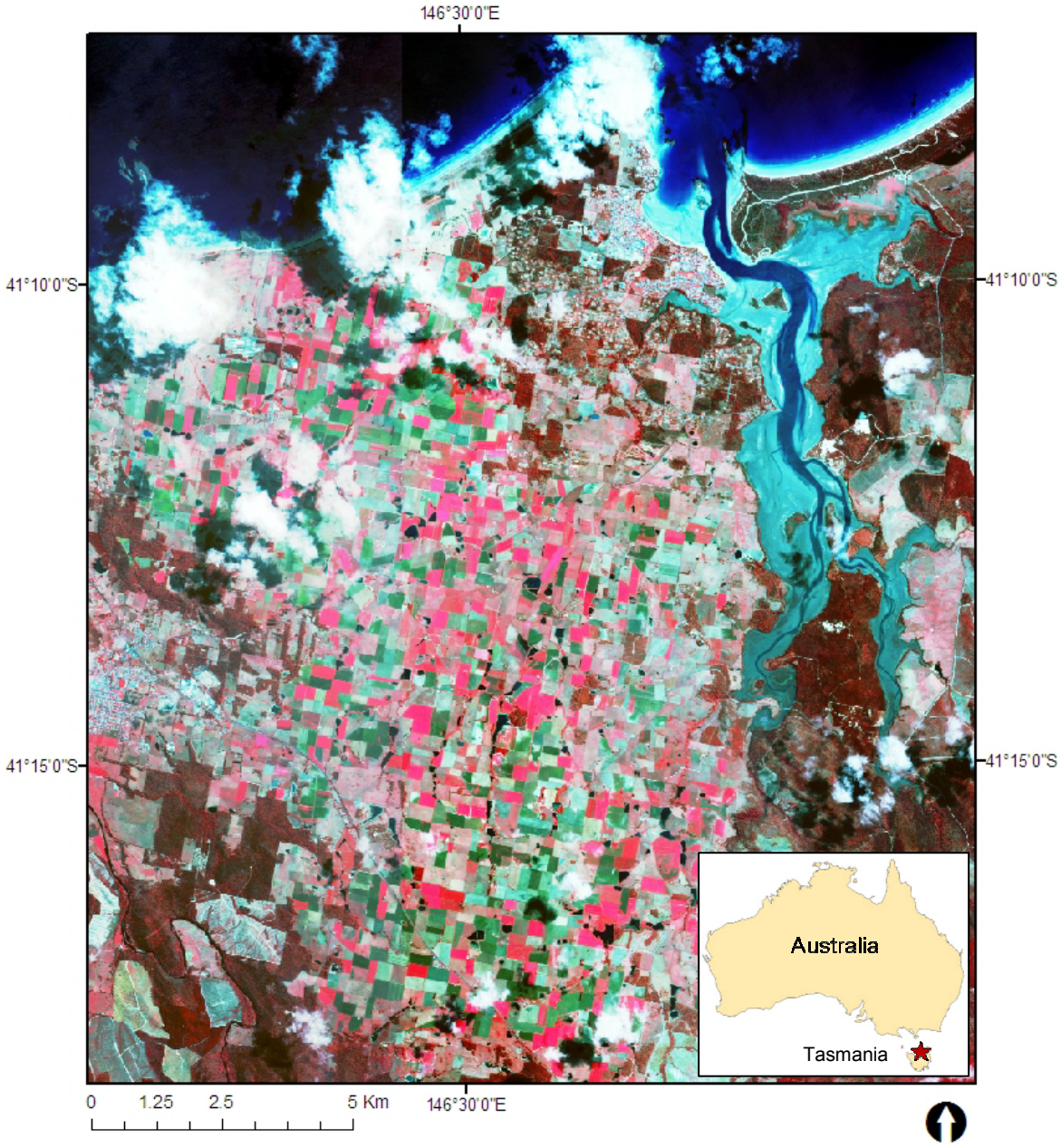

Figure 4-1 Study area is located in the Rubicon catchment of the Cradle Coast Region of Tasmania, Australia (SPOT 5, Blue; band 3, Green; band 2, Red; band 1).

Figure 4-2 Photograph of the study area. Forest structure varies. Some area has thick mid-storey vegetation (top) or understorey vegetation (middle) and other area is more open (bottom).

the population grows, change in land use, such as land clearing for grazing, and conversion of native forest to plantations is causing terrestrial habitat loss or modification.

Subdivision of land for residential or industrial development in areas of high vegetation conservation value has become an issue. This is the major threat to biodiversity in this area (The Cradle Coast Natural Resource Management Committee, 2005). An assessment of the present state of ecological structure in forests is useful in forming and implementing a conservation strategy.

4.3 LiDAR data

LiDAR data was acquired over the study area using a RIEGL LMS-Q560 sensor in February 2007. The data was custom flown by Airborne Research Australia for the Landscape Logic project supported by the Australian Commonwealth Environment Research Fund. This is a full waveform system. Table 4-1 shows the specifications for this data acquisition. The data provided was decomposed in up to six returns for this study. The scan angle for this mission was set to ± 22.5º. The flying height was 500 m above the ground, yielding an individual return footprint of approximately 20 cm in diameter. For this study, the pulse repetition frequency was 100 kHz and the wavelength of interaction was 1550 nm. The overall survey was coordinated using static and rapid static GPS methods. This was undertaken to establish a small accurate network of control points to position the field sites and validate the LiDAR positional accuracy.

Table 4-1 Specifications for the data acquisition.

Sensor	RIEGL LMS-Q560
System	Full waveform
Pulse repetition frequency	100 kHz
Scan angle	± 22.5º
Platform altitude	500 m
Beam divergence angle	0.5 mrad
Footprint	20 cm
Pulse width at half maximum	4ns
Pulse energy	8µJ
Wavelength	1550 nm
Acquisition date	February 2007

4.4 Field work to support full waveform LiDAR

Fieldwork was conducted in February 2008. It was conducted in an anniversary (one year) of the data capture. It was unfortunate to have one year time difference between LiDAR data acquisition and fieldwork. However, no major logging or bush fires were confirmed by the research team during this period and the forest condition was similar.

In this fieldwork, ecological structural information was collected with a newly developed method for validation of the LiDAR data. The LiDAR data contains highly accurate 3D information, therefore precise and yet practical quantitative method in the field is required. The collected field variables include canopy, low vegetation (vegetation up to 1 m from the ground), bare ground, grass and litter cover, Leaf Area Index (LAI) for low vegetation, tree top height and height to the first branch. The detailed method is explained in the following sections.

4.4.1 Field plots

Fig. 4-3 illustrates an example of a plot. At each site a 25 m radius circular plot (0.2 ha) was established by defining a centre point and taking a hand-held GPS (eTrex of GARMIN Corporation) measurement. This includes a possibility of an average x, y positional error of ± 5.5 m. The study sites are all natural forests. Some sites have very dense mid- and understorey vegetation, which restricts field survey. The hand-held GPS is the only GPS instrument we can use in this context, since other techniques such as Real Time Kinematic (RTK) and rapid static are not logistically possible. A 0.2 ha sample area was chosen since this is a manageable area in natural forests for detailed survey and an equivalent to a survey site (i.e. two survey plots) utilised in 'Biometric' (Gibbons et al., 2004). A circular plot was used since it is easier to set up a plot in the field.

In this method, five transects, running from East to West, parallel to each other were deployed in each plot. Assessment points were located every 7 m along each transect comprising a total of 27 assessment points in each plot. Assessment areas of a 3.5 m radius circle at each assessment point were used for ground and low vegetation cover assessment. In this way, the survey covers most areas within a plot and measurements are carried out systematically reducing a sampling bias within a plot and between plots.

Fourteen plots were established and surveyed in the study area (Fig. 4-4). The plot locations were selected by Landscape Logic project team scientists in terms of the plant community and the degree of human disturbance. All plots were established in natural forests/remnant forest patches of *Eucalyptus amygdalina* coastal forest and woodland, and without any silvicultural practice. They are the representative of the plant community in this region.

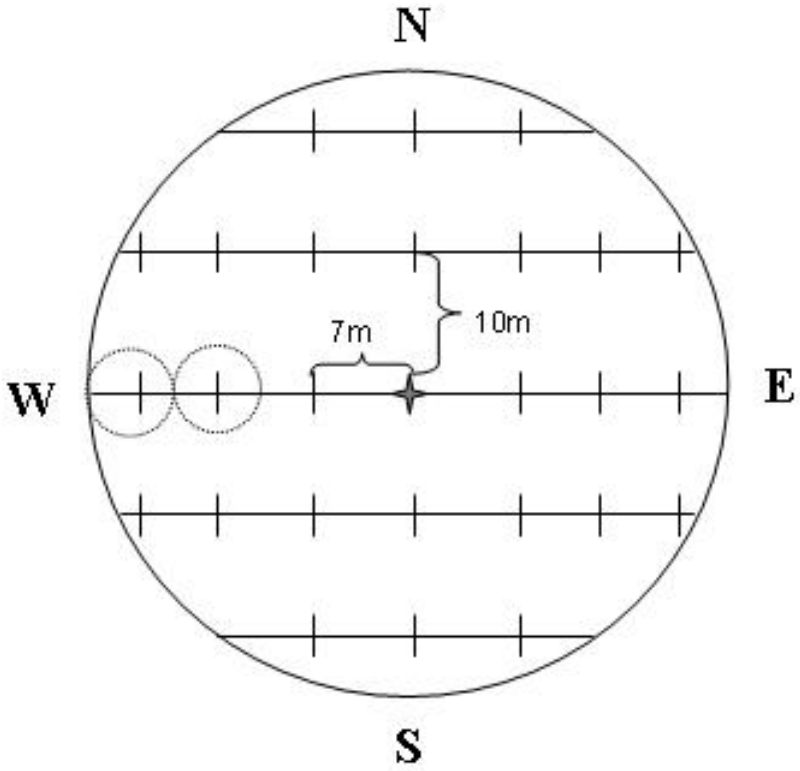

Figure 4-3 Each field plot comprises five transects running from East to West, parallel to each other yielding 27 assessment points for each (0.2 ha) plot. Small circles (only two shown for clarity) indicate the 3.5 m radius assessment areas for understorey cover measurement (these were recorded for each assessment point).

4.4.2 Canopy cover

Canopy Cover (*CC*) as a percentage was recorded in two ways. The first method (*CC_1*) assessed only photosynthetic elements and was conducted in situ with the aide of benchmarked reference photographs (Walker and Hopkins, 1990) at each assessment point. This is the similar approach taken by 'Habitat Hectares' (Parks et al., 2003), TASVEG VCA (Michaels, 2006) and 'Biometric' (Gibbons et al., 2004), which were explained in Section 2.2.2.2.

The second method (*CC_2*) assessed both photosynthetic and non-photosynthetic facets. Vertical images from a 1.7 m vantage point at each assessment point were taken by Canon

Figure 4-4 Surveyed plots. Fourteen plots were established and surveyed in the study area in February 2008.

EOS20D digital camera. The proportion of photosynthetic and non-photosynthetic facets in these images was visually assessed later in the laboratory to calculate *CC*. The assessment process is similar to those of 'Habitat Hectares' (Parks et al., 2003), TASVEG VCA (Michaels, 2006) and 'Biometric' (Gibbons et al., 2004), however, this method includes non-photosynthetic facets as well as photosynthetic facets in the calculation. This

assessment is important when compared to LiDAR analysis since laser pulses interact with both woody components (non-photosynthetic) and foliage (photosynthetic).

4.4.3 Low vegetation

In this research, low vegetation (*Low veg*) is defined as vegetation up to 1 m from the ground to assess understorey vegetation. Assessment of *Low veg* was carried out in two ways. The first method utilises visual estimation of projected cover of *Low veg* in a 3.5 m radius assessment area at each assessment point.

The second method measures the LAI for *Low veg*. This was measured using the LAI2000 Plant Canopy Analyzer of LI-COR, Inc. at each assessment point. Above-canopy (i.e. at 1 m from the ground) and below-canopy (i.e. on the ground) of *Low veg* readings were obtained at five zenith angles (0-13˚, 16-28˚, 32-43˚, 47-58˚ and 61-74˚) simultaneously, which assesses LAI of *Low veg* within an approximately 3 m radius circular area. It should be noted that the LAI values recorded using this instrument include non-leaf elements such as stems and branches.

4.4.4 Ground cover

Bare ground cover, grass cover and litter cover were recorded visually as a percentage within a 3.5 m radius of each assessment point. This followed the standard approach in 'Habitat Hectares' (Parks et al., 2003), TASVEG VCA (Michaels, 2006) and 'Biometric' (Gibbons et al., 2004), however the number of assessments were greater than the existing methods in the same way as the assessment of canopy cover.

4.4.5 Coarse woody debris

Coarse woody debris (CWD) on the ground (defined as woody components ≥ 10 cm in diameter) was recorded noting diameter and length of every woody element on each transect within a plot. The values of diameter and length are used later for volume calculation of CWD. The total volume is considered appropriate in representing the amount of CWD, as seen in published studies (e.g. Jonsson and Jonsson, 2007; Pesonen et al., 2008).

4.4.6 Tree height

Tree top height and the height to the first branch were measured using a Total Station, TCR705 (Leica Geosystems) for every tree within a plot. Diameter at breast height (DBH) was also recorded using a measuring tape. This quantitative measurement is particularly important when making comparisons to the LiDAR data. To make the most of accurate 3D information from the LiDAR data, quantitative tree height measurement is critical.

4.4.7 Derived field variables

To assess the structural information of the LiDAR data, field variables were calculated. Canopy, bare ground, grass, litter and low vegetation cover information and LAI values from each assessment point were summed for each (0.2 ha) plot and presented as a mean. To quantify the amount of CWD, the total volume of CWD was calculated for each plot. Tree height information was used to calculate vertical canopy depth by subtracting the

height to the first branch from tree top height. Canopy depth was weighted by DBH and divided into two categories (vegetation between 1 m and 5 m, and vegetation greater than 5 m). Weighted canopy depth was summed in these categories in each plot. It should be noted that the height to the first branch was not recorded for all trees due to the field of view being obscured at times. In this case, canopy depth was estimated using the regression model (Fig. 4-5) derived from other tree height information which recorded the height to the first branch. To quantify the gap (i.e. openings) in high canopy stratum, the sum of DBH weighted canopy depth in vegetation greater than 5 m was subtracted from the sum of DBH weighted canopy depth in vegetation between 1 m and 5 m. A high value for this index is indicative of large gaps in the high canopy stratum.

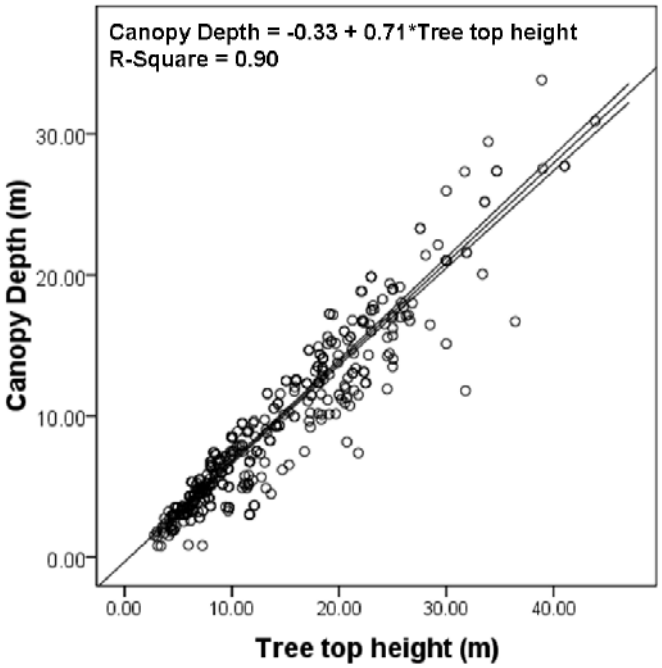

Figure 4-5 Linear regression between field measured tree top height and canopy depth with 95% mean prediction interval.

4.5 Conclusion

In this chapter, a background for a LiDAR full waveform system experiment was provided. The study area located in the Rubicon catchment of the Cradle Coast Region of Tasmania, Australia was described. The LiDAR system used in this experiment is a full waveform system and its specifications of data acquisition were summarised. This LiDAR data contains highly accurate and more detailed 3D information than the conventional discrete return systems. Therefore precise and yet practical quantitative methods in the field were required to validate the information derived from the LiDAR data. New fieldwork protocols developed specifically for this LiDAR experiment were detailed and derived field variables were also explained.

CHAPTER 5 FOREST STRUCTURE ANALYSIS FOR LIDAR FULL WAVEFORM SYSTEM EXPERIMENT

5.1 Introduction

The importance of forest structure information as a surrogate of biodiversity was discussed in Section 2.2. The application of LiDAR technology for extracting forest attributes was reviewed in Section 2.4.5.2 and 2.4.5.3. The utility and potential of conventional discrete return systems for biodiversity were evaluated in Chapter 3. In this chapter, a LiDAR full waveform system experiment is conducted to examine whether full waveform system data can provide more detailed forest structure information. An eight category forest characterisation scheme derived from the LiDAR data is proposed to characterise the ecological structure of a dry Eucalypt forest landscape, and validated using field derived variables presented in Section 4.4.

The contents of this chapter have been substantially published as Miura, N. and Jones, S.D., 2010. Characterizing forest ecological structure using pulse types and heights of airborne laser scanning. Remote Sensing of Environment, 114(5): 1069-1076.

5.2 Forest vertical stratification

Since the light environment is the primary constraint on energy partition and processing (photosynthesis) in forests, a vertical stratification is a logical first-order simplification of

the vegetation structure. A vertical stratification is also used in the definition of forests internationally (e.g. Intergovernmental Panel on Climate Change, 2003). The study area has structurally complex forests dominated by *Eucalyptus amygdalina* with heathy, sedgy and shrubby understorey variants (Harris and Kitchener, 2005). The definition of forest and woodland in terms of vertical stratification of vegetation in this area can be found in Harris and Kitchener (2005). This defines the forest and woodland as single stem trees greater than 5 m in height with more than 5 % projected canopy cover in the area. Although the TASVEG VCA (Michaels, 2006) assesses large trees by referring to the bench mark DBH and does not have the definition for forests in terms of height, defining forests using the 5 m height threshold is considered a critical step in determining the TASVEG ecological vegetation community type (Michaels, pers. comm.). For some understorey life form categories, TASVEG VCA (Michaels, 2006) has definitions using height. This is summarised in Table 5-1. For example, it defines tree (sub-canopy) or large shrub as woody plants greater than 2 m in height, medium shrub/small shrub as woody plants up to 2 m in height, large tussock grass as a robust grass greater than 30 cm in height and medium to small tussock grass as a grass between 5 cm and 30 cm in height.

In this analysis, a 1 m and 5 m threshold was chosen for the vertical stratification of vegetation in terms of simplifying these vegetation categories. The minimum vertical resolution of the LiDAR data is also an important consideration. The minimum pulse interaction gap between two adjacent interactions is approximately 50 cm for this data. Therefore it is not sensible to define a forest vertical stratification with classes less than 50 cm. Vegetation up to 1 m in height includes all grass categories of the TASVEG VCA (Michaels, 2006). Similarly, vegetation between 1 m and 5 m in height includes all shrub categories. Vegetation greater than 5 m in height represents the canopy of forests. It is considered that integrated vegetation categories could show forest structure in this area.

Table 5-1 Understorey life form categories that have height definitions in the TASVEG VCA (After Michaels, 2006).

Life Form	Definitions
Immature tree	Tree canopy species greater than 2m in height but less than two thirds of the mature canopy height
Tree (sub-canopy) or large shrub	Woody plants greater than 2 m in height that never form part of tree canopy
Medium shrub/small shrub	Woody plants up to 2 m in height
Tussock grass	A robust grass, usually with more than one flower stalk and large numbers of leaves arising from a common, often broad base or clump, greater than 5 cm in height.
Large tussock grass	A robust grass, usually with more than one flower stalk and large numbers of leaves arising from a common, often broad base or clump, greater than 30 cm in height
Medium to small tussock grass	A grass, usually with more than one flower stalk and large numbers of leaves arising from a common, often broad base or clump, between 5 cm and 30 cm in height
Non-tussock grass	A grass with leaves arranged along single, erect flower stalks, which in turn arise from rhizomes or stolons, greater than 5 cm in height
Medium to small sedge/ruch/sagg/lily	A small sedge or rush or lily with erect flower stalks, from 5 cm to 30 cm in height
Ground fern and Fern allies	A fern-like non-flowering plant, usually with several to many fronds arising from a common base, and usually growing to less than 1m in height

5.3 Methods

5.3.1 Registration between LiDAR data and field plots

The hand-held GPS measurements used to locate the plots include a possibility of an average x, y positional error of ± 5.5 m as discussed in Section 4.4.1. To compensate for this GPS error, and to obtain a better registration between LiDAR data and the field plot area, the plots were manually relocated when necessary. First, 25 m radius plot circles were created using the plot centre coordinates derived from GPS. The plot circles were then placed over LiDAR point cloud using TerraScan software. Individual trees and paths in the forest were visible in the viewer. The location of them was used to find true location of the plots. The plots were shifted manually if necessary. The maximum shifting of the plots were found to be approximately 1.5-2.0 m in this dataset.

5.3.2 Proposed forest characterisation scheme

In order to create a scheme to characterise forest ecological structure, the LiDAR point cloud data was first classified into four vertical layers; *Ground*, Low vegetation (*Low veg*, 0-1 m from the ground), Medium vegetation (*Medium veg*, 1-5 m from the ground) and High vegetation (*High veg*, >5 m) using TerraScan software of Terrasolid, Ltd. This is shown in Fig. 5-1(a). In this process, ground returns were defined first as *Ground* using the progressive Triangular Irregular Network (TIN) densification algorithm (Axelsson, 1999). The height above the ground for each return was calculated by subtracting the TIN height from its height value. Subsequently, LiDAR returns from each of these layers were sorted into "Types". In this study, four types of LiDAR returns are defined. Type 1 are singular returns, which is to say that only one return was recorded from each emitted pulse of energy. Type 2 are first of many returns, that is, part of the pulse of incident energy has interacted with a plant facet and been reflected back to the sensor but much of the energy has continued through the tree interacting with other structural elements along its path. Type 3 are intermediate returns, which are the subsequent interactions of the pulse described in Type 2. Type 4 are the last of many returns, which is the last returned pulse back to the sensor from an incident pulse. This is shown in Fig. 5-1(b). The total number of returns over a sample plot, T is expressed:

$$T = \sum_{i=1}^{i=4} \sum_{j=1}^{4} R_{ij} \qquad (5\text{-}1)$$

Where R denotes the LiDAR returns, i denotes the classified four layers (1 = *High veg*, 2 = *Medium veg*, 3 = *Low veg* and 4 = *Ground*) and j denotes the return types (1 = Type 1, 2 = Type 2, 3 = Type 3 and 4 = Type 4).

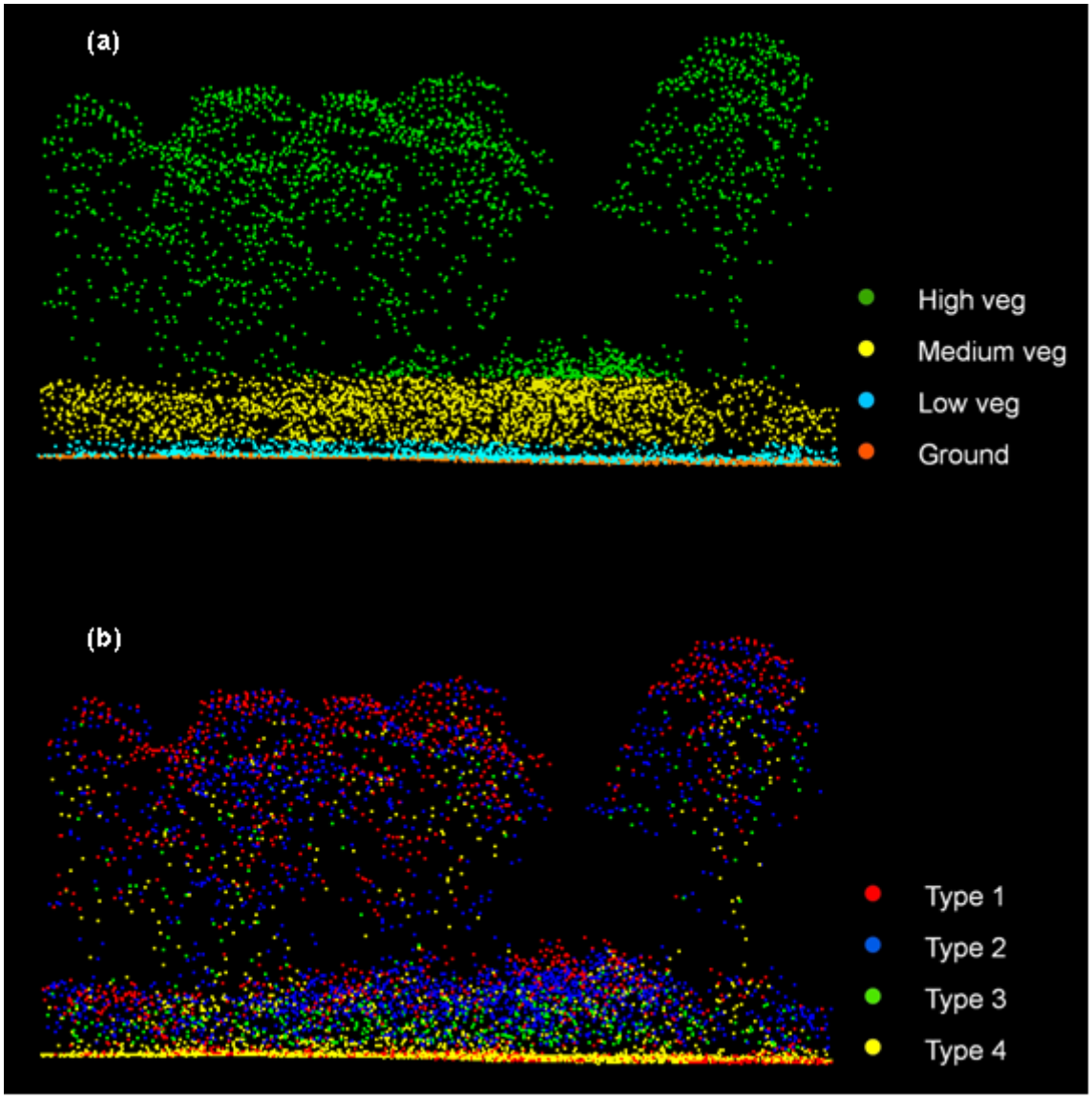

Figure 5-1 LiDAR point cloud classification. (a) LiDAR point cloud data was first classified into four layers; *Ground*, Low vegetation (*Low veg*, 0-1 m from the ground), Medium vegetation (*Medium veg*, 1-5 m from the ground) and High vegetation (*High veg*, >5 m). (b) Four types of LiDAR returns; Type 1 (singular returns), Type 2 (first of many returns), Type 3 (intermediate returns) and Type 4 (last of many returns).

The number of returns for each Type was calculated for each of the four layers. This number was divided by the total number of returns in each plot, resulting in a ratio. Type 1 and Type 2 returns are the result of the first interaction with objects, which suggests that there is opening above this pulse interaction (that is, no interaction above these points). The number of returns in *Low veg*, *Medium veg* and *High veg* layers suggests the presence

of vegetation in each of these strata. Of particular importance is the presence of Type 3 and Type 4 returns in *High veg* strata, since these indicate the presence of a vertically dense canopy. Using the calculated ratios, the following forest characterisation scheme is proposed. This is shown in Table 5-2. Where:

1) Category 1 comprises Type 1 returns from the *Ground* layer; this represents openings above the ground, O_G:

$$O_G = \frac{R_{41}}{T} \tag{5-2}$$

2) Category 2 comprises Type 1 and Type 2 from the *Low veg* layer; this represents openings above low vegetation, O_L:

$$O_L = \frac{R_{31} + R_{32}}{T} \tag{5-3}$$

3) Category 3 contains all return types (Type 1, 2, 3 & 4) from the *Low veg* layer; this indicates the presence of understorey vegetation, V_L:

$$V_L = \frac{R_{31} + R_{32} + R_{33} + R_{34}}{T} = \frac{\sum_{j=1}^{4} R_{3j}}{T} \tag{5-4}$$

4) Category 4 comprises Type 1 and Type 2 from the *Medium veg* and *High veg* layers; this represents canopy cover, *CC*:

$$CC = \frac{(R_{21} + R_{22}) + (R_{11} + R_{12})}{R_{41} + (R_{31} + R_{32}) + (R_{21} + R_{22}) + (R_{11} + R_{12})} \tag{5-5}$$

Since the canopy projected area is calculated, only Type 1 and Type 2 returns are used in this equation. It is noted that points lower than 1.7 m from the ground were excluded in this calculation to match with the field measurement in canopy cover.

5) Category 5 comprises Type 1 and Type 2 returns from the *Medium veg* layer; this represents openings above medium vegetation, O_M:

$$O_M = \frac{R_{21} + R_{22}}{T} \tag{5-6}$$

6) Category 6 contains all return types (Type 1, 2, 3 & 4) from the *Medium veg* layer; this indicates the presence of mid-storey vegetation, V_M:

$$V_M = \frac{R_{21} + R_{22} + R_{23} + R_{24}}{T} = \frac{\sum_{j=1}^{4} R_{2j}}{T} \tag{5-7}$$

7) Category 7 contains all return types (Type 1, 2, 3 & 4) from the *High veg* layer; this indicates the presence of high trees, V_H:

$$V_H = \frac{R_{11} + R_{12} + R_{13} + R_{14}}{T} = \frac{\sum_{j=1}^{4} R_{1j}}{T} \tag{5-8}$$

8) As a refinement of category 7, category 8 quantifies the vertical density of the high tree canopy using only Type 3 and Type 4 returns from the *High veg* layer; this suggests vertically dense canopy of high trees, D_H:

$$D_H = \frac{R_{13} + R_{14}}{T} \tag{5-9}$$

Table 5-2 Forest characterisation scheme (FCS).

Category		Description	LiDAR return ratio
1	O_G	opening above the ground	*Ground* Type 1
2	O_L	opening above low vegetation	*Low veg* Types 1 and 2
3	V_L	presence of understorey vegetation	*Low veg* total (Types 1, 2, 3 and 4)
4	CC	canopy cover	*Medium veg* Types 1 and 2 and *High veg* Types 1 and 2
5	O_M	opening above medium vegetation	*Medium veg* Types 1 and 2
6	V_M	presence of mid-storey vegetation	*Medium veg* total (Types 1, 2, 3 and 4)
7	V_H	presence of high trees	*High veg* total (Types 1, 2, 3 and 4)
8	D_H	vertically dense canopy of high trees	*High veg* Types 3 and 4

Note that while LiDAR derived V_H measures the amount of foliage in the high canopy stratum regardless of the spatial distribution of the canopy, LiDAR derived D_H estimates the vertical density of the high canopy stratum and LiDAR derived CC measures the horizontal density of foliage in medium and high canopy strata, using different laser pulse return properties. This is further demonstrated in Fig. 5-2. In these simplified forest structures, LiDAR derived V_H is the same between A and B since V_H includes all types of returns in *High veg* stratum. LiDAR derived D_H is greater in B because D_H uses only Type 3 and 4 in *High veg* stratum. On the other hand, LiDAR derived CC is greater in A since CC is computed with only Type 1 and 2 in *Medium* and *High veg* strata.

This scheme was subsequently compared to the field variables to validate its utility in characterising ecological structure.

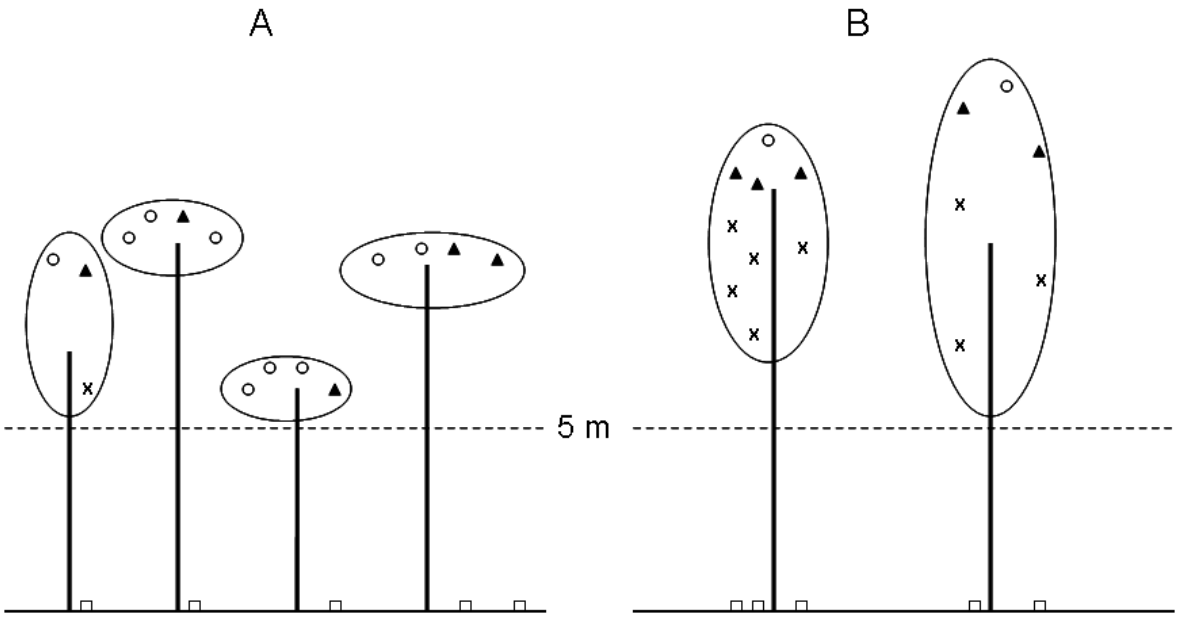

Figure 5-2 Illustration of forest characterisation scheme for different forest structures A (sparse foliage or low optical canopy depth) and B (dense foliage or high optical canopy depth). LiDAR returns are symbolised circles as Type 1, triangles as Type 2, crosses as Type 3 and squares as Type 4. V_H is the same between A and B, however D_H is greater in B and *CC* is greater in A.

5.4 Results

The LiDAR derived variables were compared to field derived variables over 14 plots in the study area. LiDAR derived V_L (category 3; presence of understorey vegetation) was a good predictor of field recorded LAI for vegetation less than 1 m ($R^2 = 0.82$, $P < 0.05$), and exhibited a moderate correlation with field recorded *mean Low veg cover* ($R^2 = 0.58$, $P < 0.05$) shown respectively in Fig. 5-3(a) and (b). As can be seen in Fig. 5-3(a), LiDAR derived V_L and *Field LAI for Low veg* were significantly correlated across a range of LAI values. Comparison between LiDAR derived V_L and field recorded *mean Low veg cover* show a similar trend but reveals that plot 13a was underestimated in the LiDAR.

Fig. 5-3(c) and (d) illustrate LiDAR derived *CC* (category 4; canopy cover) was significantly correlated with the two ground-based measures of *CC*

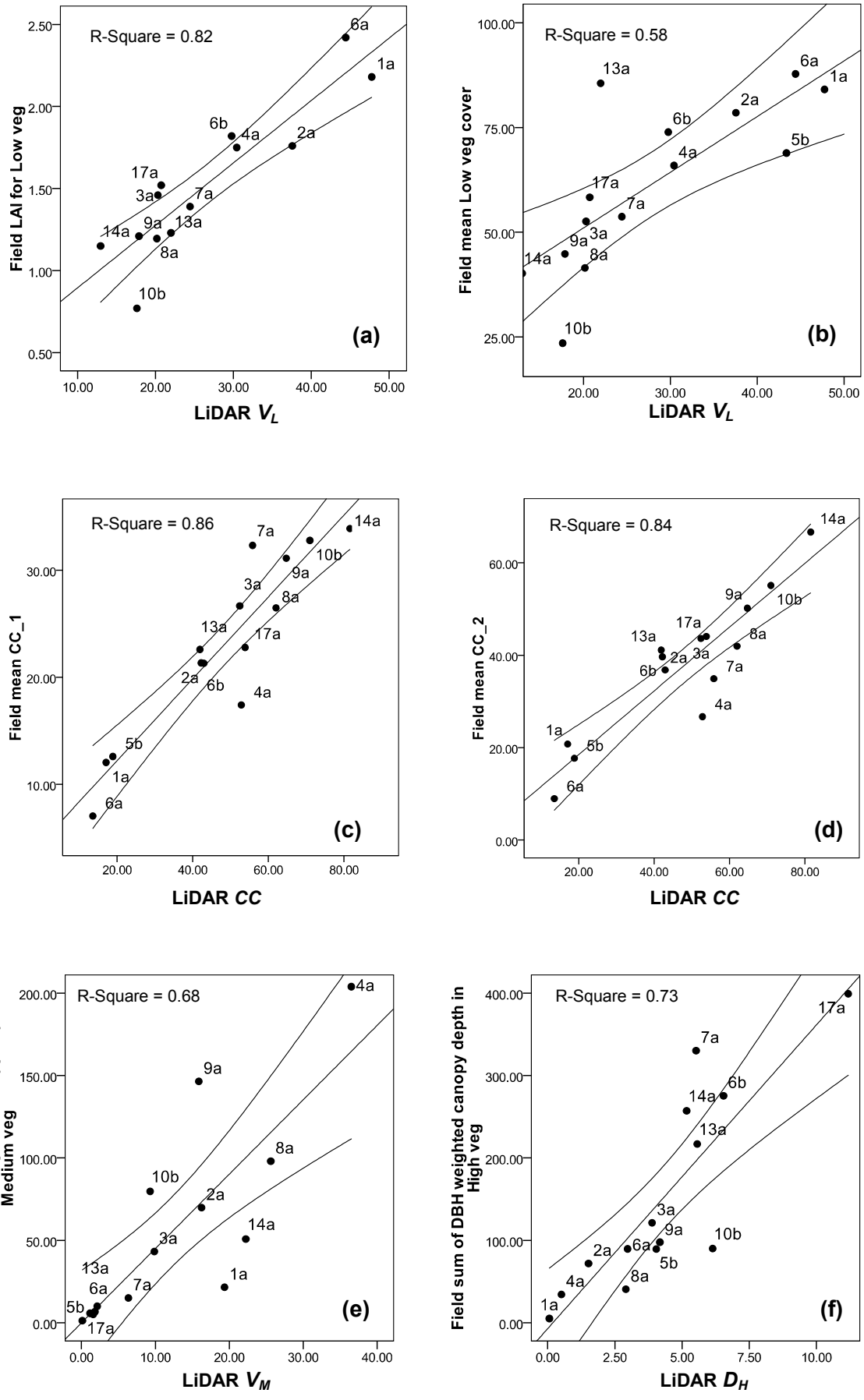
R-Square = 0.82
Field LAI for Low veg
LiDAR V_L
(a)
R-Square = 0.58
Field mean Low veg cover
LiDAR V_L
(b)
R-Square = 0.86
Field mean CC_1
LiDAR CC
(c)
R-Square = 0.84
Field mean CC_2
LiDAR CC
(d)
R-Square = 0.68
Field sum of DBH weighted canopy depth in Medium veg
LiDAR V_M
(e)
R-Square = 0.73
Field sum of DBH weighted canopy depth in High veg
LiDAR D_H
(f)

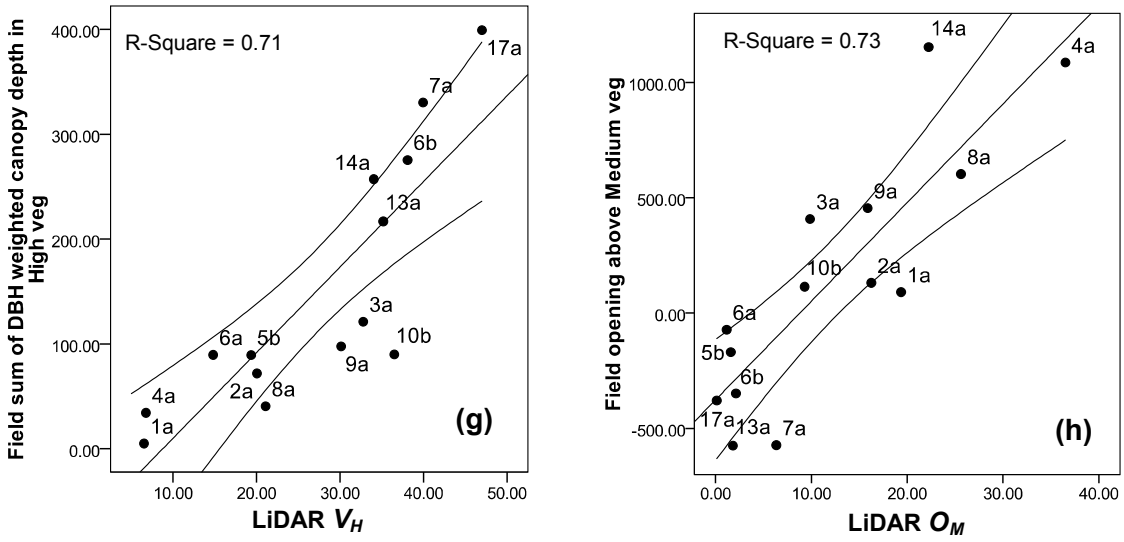

Figure 5-3 Linear regression results between LiDAR derived Forest Characterisation Scheme (FCS) categories and field variables with 95 % mean prediction interval. The labels are surveyed plot names.

(photosynthetic/photosynthetic and non-photosynthetic), with $R^2 = 0.86$ and 0.84, $P < 0.05$ respectively. As displayed in Fig. 5-3(c) and (d), *LiDAR CC* and *Field CC* were highly correlated across a broad range of *CC* values. It was noted that, in absolute terms, the ground-based measures consistently reported a lower *CC* than LiDAR derived measures.

LiDAR derived V_M (category 6; presence of mid-storey vegetation) displayed a good correlation with field derived *sum of DBH weighted canopy depth in Medium veg* ($R^2 = 0.68$, $P < 0.05$). This is shown in Fig. 5-3(e). LiDAR derived D_H (category 8; vertically dense canopy of high trees) and LiDAR derived V_H (category 7; presence of high trees) showed strong correlations with field derived *sum of DBH weighted canopy depth in High veg* with $R^2 = 0.73$ and 0.71, $P < 0.05$ respectively. These are displayed in Fig. 5-3(f) and (g). Again, these associations were observed across a range of canopy depths in both medium vegetation (1-5 m) and high vegetation (> 5 m).

LiDAR derived O_M (category 5; opening above medium vegetation) was strongly correlated with field derived *opening above Medium veg* with $R^2 = 0.73$, $P < 0.05$ (Fig. 5-3(h)).

LiDAR derived O_G (category 1; opening above the ground) and O_L (category 2; opening above low vegetation) showed some correlations with field variables (Table 5-3). Field measured *total volume of CWD* was positively correlated with LiDAR derived O_G (R = 0.542, $P < 0.05$) and LiDAR derived D_H (R = 0.609, $P < 0.05$). In other words, where there is a vertically dense canopy in the high tree layer and an opening above the ground, more CWD is expected. The two ground-based measures of *CC* have negative correlations with LiDAR derived O_G (R = -0.674 and -0.679, $P < 0.01$ respectively) and O_L (R = -0.909 and -0.896, $P < 0.01$ respectively). This suggests that there are fewer openings above the ground and low vegetation where canopy cover is high.

Table 5-3 Pearson correlation coefficients between LiDAR derived variables and field variables.

	Field total volume of CWD	Field mean CC_1	Field mean CC_2
LiDAR Opening above Ground (O_G)	.542(*)	-.674(**)	-.679(**)
LiDAR Opening above Low veg (O_L)	0.196	-.909(**)	-.896(**)
LiDAR vertically dense canopy of high trees (D_H)	.609(*)	0.396	0.455

**. Correlation is significant at the 0.01 level (2-tailed).

*. Correlation is significant at the 0.05 level (2-tailed).

5.5 Discussion

Of the eight proposed FCS categories, all showed good association when compared against field-based metrics. LiDAR derived *CC* and the two field measured *CC* assessments all

displayed strong positive correlations. Interestingly, the two different assessment methods of canopy cover, described in Section 4.4.2, showed similar results (R^2 = 0.86 and 0.84). One would expect higher correlation between *LiDAR CC* and *Field CC_2*, since both variables measure all perturbing canopy objects from laser pulse or sun light, while *Field CC_1* measures only the photosynthetic portion of these objects. In our study site, the vegetation community of the canopy strata is evergreen and dominated by an erectophyle Eucalypt species. The ratio of leaf area to non-photosynthetic elements (stems and branches) should be consistent unless there is defoliation caused by disease. In fact, further investigation revealed that *CC_1* and *CC_2* were significantly correlated with each other presenting a Pearson Correlation Coefficient value 0.903 ($P < 0.01$). In terms of *CC* values, *Field CC* reports a consistently lower absolute value than *LiDAR CC*. It is possible that ground based measurements misrepresent "true" *CC* to some degree, as field derived measures are based on twenty seven independent observations over a 0.2 ha plot area, while LiDAR derived measures are based on more than seven thousand returns in the same 0.2 ha plot. It is expected then that the LiDAR derived estimates would be more capable of assessing *CC* at a landscape scale.

The proposed LiDAR derived FCS categories demonstrated the ability of characterising spatial distribution of the canopy. LiDAR derived *CC* estimates the horizontal density of foliage in medium and high canopy strata and showed high correlation with field measured canopy cover in this strata (Fig. 5-3(c) and (d)). LiDAR derived D_H measures the vertical density of the high canopy stratum and is well correlated with the field measured canopy depth in this stratum (Fig. 5-3(f)). However, D_H did not display significant correlation with field measured canopy cover (Table5-3). As D_H measures the vertical density of the canopy, this also explains why D_H did not show the correlation with *Field CC* (Table 5-3), which is more dependent on the horizontal distribution of the canopy.

Some anomalies are noteworthy, however, if only to illustrate the sensitivity of the proposed technology and method. In the comparison between LiDAR derived V_L and field recorded *mean Low veg cover*, plot 13a was underestimated using the LiDAR technique. Plot 13a has grass and blackberry dominated understorey. It was noted in the field that the southern half of the plot was covered with very short (grazed) grass (Fig. 5-4). This could lead to misclassification of LiDAR returns. The grass is too short to be classified as *Low veg* and the LAI2000 is not designed to measure such low vegetation.

In terms of estimating CWD volume, LiDAR derived O_G and D_H have some potential. The positive correlations between these variables suggest that in a forest where large amount of CWD is found, large trees with vertically dense canopies and gaps from the ground to canopy are present. This is considered logical in natural forests since when a mature tree dies and falls, it will create a gap in this area. The relationship between CWD volume and the canopy gap also fits with the findings of Pesonen et al. (2008). These authors found that the standard deviation in height pulses was the most significant predictor for CWD volume, and explained that higher variations in height distribution would result from gaps, i.e. tree falls.

5.6 Conclusion

In conclusion, the proposed FCS method has the ability to characterise some elements of the ecological structure of a dry Eucalypt forest landscape. Regression analysis showed LiDAR derived variables were good predictors of field recorded variables across a range of forest structural types. The proposed scheme demonstrated the potential of different laser pulse return properties from a full waveform LiDAR to provide information on the

Figure 5-4 Photograph of plot 13a. The top photograph is the southern area of the plot, which was covered with very short (grazed) grass. The bottom photograph is the northern area of the plot. The camera was set at the height of 0.5 m from the ground.

complexity of habitat structure in an efficient and cost-effective manner. Detailed forest structure information can be extracted. In terms of Spies (1998) proposed components of forest structure (Table 2-1), the FCS effectively reports on all elements of component 1 (foliage) as well as elements of component 4 (tree boles), the volume of fallen trees (component 7) and potentially the biomass element of component 8 (Shrub, Herb, and Moss Layers). The FCS however is 'tuneable' to any designed 3D ecological characterisation scheme. It is anticipated that the FCS may have wide applicability in characterising forest structure over a range of scales from patch to landscape although this assertion clearly requires further investigation.

CHAPTER 6 INTENSITY EXPLORATORY ANALYSIS FOR LIDAR FULL WAVEFORM SYSTEM EXPERIMENT

6.1 Introduction

The proposed forest characterisation scheme (FCS) method, using a LiDAR full waveform system, to characterise forest structure was demonstrated in Chapter 5. This chapter poses the question: can the return intensity of a full waveform system be used to provide further forest structure information? Furthermore, is this information common too, or distinct from the point density information?

To date, the utility of LiDAR intensity has been limited due to difficulties with calibration and associated problems in interpretation as described in Section 2.4.4.1. The potential to use intensity from LiDAR discrete return systems for recovering forest structure information was shown in Chapter 3. In this chapter, the return intensity of a LiDAR full waveform system is explored. Since the Tasmanian study site contains forests that are structurally more complex than those from the previous discrete return system experiment, more variation in return intensity is expected. There has been little research to date on intensity response of full waveform data from forested landscape.

In this experiment, the return intensity of LiDAR full waveform system is statistically examined first. Then the modified algorithm with LiDAR discrete return system experiment (Chapter 3) is applied to LiDAR full waveform system to examine whether LiDAR intensity of this system can also recover forest structure variables. Finally, a modified FCS is applied incorporating return intensity into this algorithm to test whether it can enhance the ability to extract forest structure information.

6.2 Methods

6.2.1 Intensity data

The LiDAR data used in this analysis is full waveform system data described in Section 4.3. Note that the data provided was already decomposed in up to six discrete returns. For extracting individual return pulses from waveform signals, a Gaussian Pulse Fitting (GPF) method was used with the default advanced parameters in the RiANALYZE 560 software of RIEGL (RIEGL, 2006). Therefore, the intensity data analysed in this chapter were not full waveform signals but the individual peak amplitude (i.e. intensity) of the determined return pulses. The detailed decomposition process of this method is found in Wagner et al. (2008; 2006). In this analysis, the intensity values were used as sensor outputs without any calibration.

6.2.2 Intensity statistics

In order to have better understanding of LiDAR intensity response from the forested landscape, the return intensity was stratified and statistically examined. The LiDAR point cloud data was first classified into four vertical layers; *Ground*, Low vegetation (*Low veg*, 0-1 m from the ground), Medium vegetation (*Medium veg*, 1-5 m from the ground) and High vegetation (*High veg*, >5 m), and then LiDAR returns from each of these layers were sorted into Types as described in Section 5.3.2. Mean and standard deviation of each type in the four layers were calculated for each plot and analysed.

6.2.3 The application of algorithm developed using LiDAR discrete return system

The LiDAR discrete return system experiment demonstrated the potential of LiDAR intensity (mean and standard deviation), which were vertically stratified using range information and classified utilising return properties, to recover forest structure variables (Chapter 3). The combination of mean and standard deviation of first return intensity from the ground were also found to be useful to differentiate forest structural types (Chapter 3). In this chapter, these algorithms were applied to LiDAR full waveform data. The LiDAR intensity variables, which were vertically stratified using range information and classified according to return properties as explained in Section 6.2.2, were compared with field variables (see Section 4.4) to examine whether there is any correlation. The combination of mean and standard deviation of first return intensity from the ground was also tested to determine if it can differentiate forest structural types in the study area for the LiDAR full waveform experiment (see Section 4.2).

6.2.4 The application of FCS derived from LiDAR full waveform system

A modified FCS was applied incorporating return intensity into this algorithm. Hopkinson and Chasmer (2007; 2009) estimated canopy fractional cover by calculating the ratio of the sum of all canopy level return intensities to the sum of total return intensity, and achieved a high correlation with fractional cover recovered from ground-based digital hemispherical photography. This algorithm, the 'intensity ratio' method (Hopkinson and Chasmer, 2009) was applied to all categories of FCS. The sum of all return intensity over a sample plot, T_{Int} is expressed:

$$T_{Int} = \sum_{i=1}^{i=4} \sum_{j=1}^{4} R_{Int\,ij} \quad (6\text{-}1)$$

Where R_{Int} denotes LiDAR return intensity, i denotes the classified four layers (1 = *High veg*, 2 = *Medium veg*, 3 = *Low veg* and 4 = *Ground*) and j denotes the return types (1 = Type 1, 2 = Type 2, 3 = Type 3 and 4 = Type 4).

The sum of intensity for each Type was calculated for each of the four layers. This sum was divided by the sum of all return intensity in each plot, resulting in a ratio. Consequently, all categories of FCS are expressed as follows.

1) Category 1 comprises Type 1 return intensity from the *Ground* layer; O_{GInt}:

$$O_{GInt} = \frac{R_{Int\,41}}{T_{Int}} \quad (6\text{-}2)$$

2) Category 2 comprises Type 1 and Type 2 return intensity from the *Low veg* layer; O_{LInt}:

$$O_{LInt} = \frac{R_{Int\,31} + R_{Int\,32}}{T_{Int}} \quad (6\text{-}3)$$

3) Category 3 contains intensity of all return types (Type 1, 2, 3 & 4) from the *Low veg* layer; V_{LInt}:

$$V_{LInt} = \frac{R_{Int\,31} + R_{Int\,32} + R_{Int\,33} + R_{Int\,34}}{T_{Int}} = \frac{\sum_{j=1}^{4} R_{Int\,3j}}{T_{Int}} \quad (6\text{-}4)$$

4) Category 4 comprises Type 1 and Type 2 return intensity from the *Medium veg* and *High veg* layers; CC_{Int}:

$$CC_{Int} = \frac{\left(R_{Int21} + R_{Int22}\right) + \left(R_{Int11} + R_{Int12}\right)}{R_{Int41} + \left(R_{Int31} + R_{Int32}\right) + \left(R_{Int21} + R_{Int22}\right) + \left(R_{Int11} + R_{Int12}\right)} \quad (6\text{-}5)$$

5) Category 5 comprises Type 1 and Type 2 return intensity from the *Medium veg* layer; O_{MInt}:

$$O_{MInt} = \frac{R_{Int21} + R_{Int22}}{T_{Int}} \quad (6\text{-}6)$$

6) Category 6 contains intensity of all return types (Type 1, 2, 3 & 4) from the *Medium veg* layer; V_{MInt}:

$$V_{MInt} = \frac{R_{Int21} + R_{Int22} + R_{Int23} + R_{Int24}}{T_{Int}} = \frac{\sum_{j=1}^{4} R_{Int2j}}{T_{Int}} \quad (6\text{-}7)$$

7) Category 7 contains intensity of all return types (Type 1, 2, 3 & 4) from the *High veg* layer; V_{HInt}:

$$V_{HInt} = \frac{R_{Int11} + R_{Int12} + R_{Int13} + R_{Int14}}{T_{Int}} = \frac{\sum_{j=1}^{4} R_{Int1j}}{T_{Int}} \quad (6\text{-}8)$$

8) Category 8 contains only Type 3 and Type 4 return intensity from the *High veg* layer; D_{HInt}:

$$D_{HInt} = \frac{R_{Int13} + R_{Int14}}{T_{Int}} \quad (6\text{-}9)$$

This intensity version of the scheme was subsequently compared to the field variables (see

Section 4.4) to examine whether it can enhance utility of FCS in characterising ecological structure.

6.3 Results

6.3.1 Mean and standard deviation of intensity

Fig. 6-1(left) illustrates mean intensity for each Type for the four vertical strata in each plot. It demonstrates some return intensity characteristics. Type 1 returned highest intensity in every vegetation stratum, followed by Type 4, Type 2 and Type 3 in this order (Fig. 6-1, left). In terms of the four vegetation layers, *High veg* stratum returns lowest intensity in all plots (Fig. 6-1, left). Mean intensity was found to be slightly higher in *Medium veg* stratum than in *High veg* stratum (Fig. 6-1, left). *Ground* stratum returned the highest intensity (Fig. 6-1, left). It is noted that *Ground* and *Low veg* strata had similar trend and mean intensity values (Fig. 6-1, left). The difference in mean intensity between types was found to be small in *High veg* stratum, and elevated in *Medium veg*, *Low veg* and *Ground* strata in this order (Fig. 6-1, left). Distinctive peaks were found in Plot 10b and 17a in every stratum (Fig. 6-1, left). Plot 5b in *Medium veg* stratum and Plot 13a in *Low veg* and *Ground* strata also displayed high intensity values (Fig. 6-1, left).

Fig. 6-1(right) shows standard deviation of intensity for each Type for the four vertical strata in each plot. The standard deviation of Type 1 and Type 4 had similar range values in *Ground* and *Low veg* strata. These were found to be higher than the standard deviation of Type 2 and Type 3 in *Low veg* and *Medium veg* strata (Fig. 6-1, right). In *High veg* stratum, all types exhibited a similar range of standard deviations (Fig. 6-1, right). Type 2 and Type

3 showed a similar range of standard deviation in all strata except *Ground* which contains no Type 2 and Type 3 (Fig. 6-1, right).

6.3.2 Correlation with field variables

Table 6-1 shows the Pearson correlation coefficients between LiDAR intensity variables (mean and standard deviation of intensity for each Type in the four vegetation strata) and field variables. Several variables displayed significant correlations. For example, *standard deviation of Ground Type 1* and *Low veg Type 1* were highly negatively correlated with *Field LAI for Low veg* ($R = -0.828$ and $R = -0.853$, $P < 0.01$ respectively) and with *Field mean Low veg cover* ($R = -0.722$, $P < 0.01$ and $R = -0.608$, $P < 0.05$ respectively), and positively correlated with *Field CC-1* and *Field CC-2* ($R = 0.811$ and $R = 0.757$, $R = 0.673$ and $R = 0.717$, $P < 0.01$ respectively). *Standard deviation of High veg Type 1* showed significant and positive correlation with *Field total volume of CWD* ($R = 0.785$, $P < 0.01$), *Field mean tree height* ($R = 0.698$, $P < 0.01$) and *Field sum of DBH weighted canopy depth in High veg* ($R = 0.723$, $P < 0.01$).

6.3.3 Combination of mean and standard deviation of first return intensity from the ground

Fig. 6-2 shows the scatter plot of first return intensity from ground stratum (*Mean Ground Type 1*) and standard deviation of first return intensity from ground stratum (*SD Ground Type 1*). The results did not display the trend found in the LiDAR discrete return system experiment (Section 3.7.4), but showed different classification potential. Plots in group A

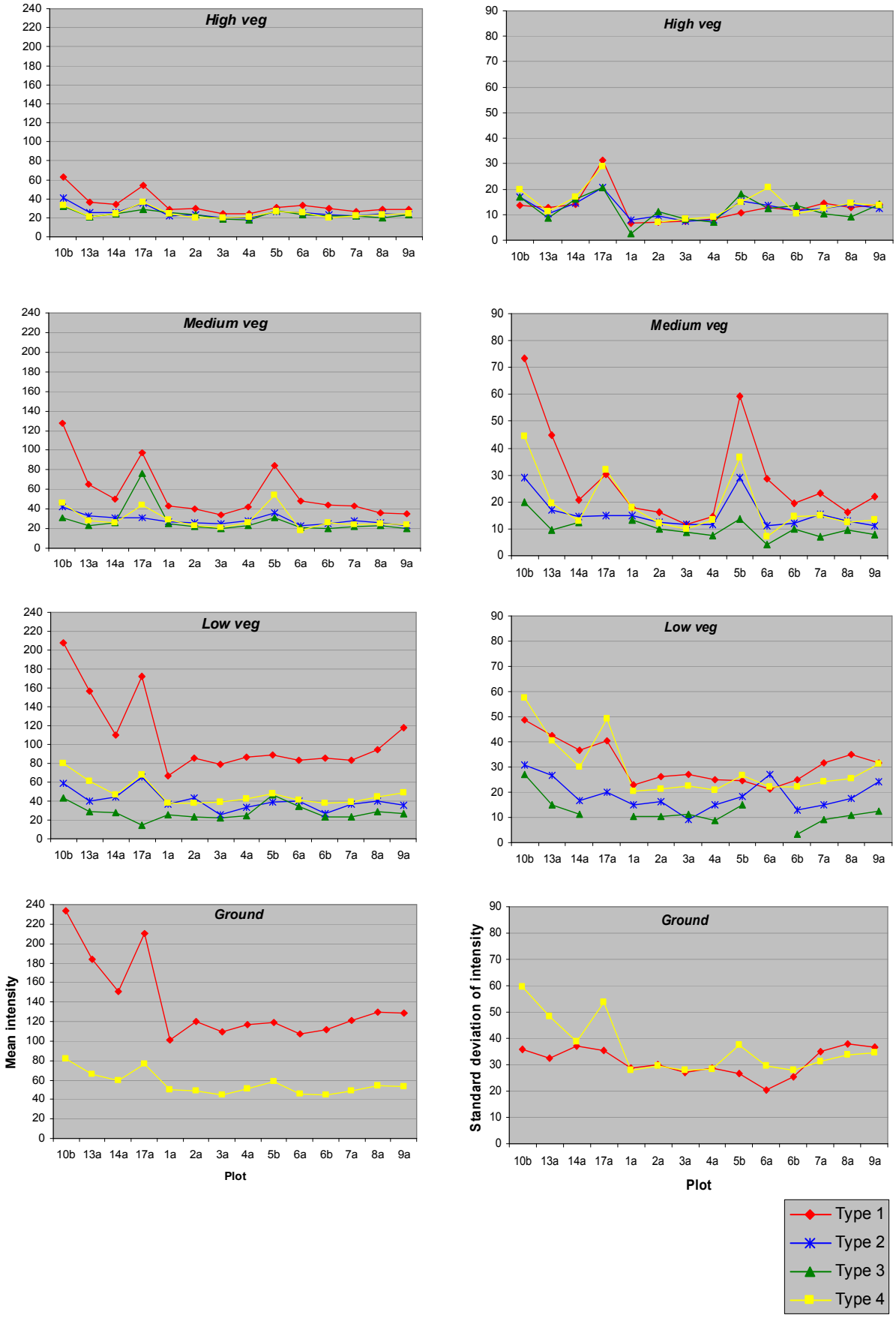

Figure 6-1 Mean intensity (left) and standard deviation of intensity (right) for each Type for *Ground*, *Low veg*, *Medium veg* and *High veg* in each plot.

Table 6-1 Pearson correlation coefficients between LiDAR intensity variables and field variables.

	Field LAI for Low veg	Field total volume of CWD	Field mean CC_1	Field mean CC_2	Field mean bare ground cover	Field mean grass cover	Field mean litter cover	Field mean Low veg cover	Field mean tree height	Field opening above Medium veg	Field sum of DBH weighted canopy depth in High veg	Field sum of DBH weighted canopy depth in Medium veg
Mean Ground Type 1	-.652*	0.403	0.438	.546*	0.176	0.163	-0.163	-0.459	0.363	-0.185	0.380	-0.077
Mean Ground Type 4	-.615*	0.449	0.326	0.439	0.111	0.094	-0.126	-0.441	0.369	-0.147	0.277	-0.061
Mean Low veg Type 1	-.649*	0.389	0.423	0.527	0.165	0.248	-0.196	-0.453	0.336	-0.193	0.320	-0.020
Mean Low veg Type 2	-0.326	.596*	0.173	0.279	-0.066	-0.031	-0.022	-0.324	0.321	-0.141	0.295	-0.139
Mean Low veg Type 3	-0.274	-0.088	-0.162	-0.192	-0.198	-0.087	0.127	-0.163	-0.204	0.006	-0.448	-0.037
Mean Low veg Type 4	-.611*	0.430	0.328	0.422	0.154	0.190	-0.192	-0.444	0.341	-0.201	0.241	-0.043
Mean Medium veg Type 1	-0.433	0.473	0.101	0.179	-0.026	0.031	-0.034	-0.317	0.447	-0.314	0.225	-0.239
Mean Medium veg Type 2	-.598*	0.129	0.203	0.238	0.056	-0.127	0.029	-0.354	0.236	-0.150	0.088	-0.146
Mean Medium veg Type 3	-0.105	.806**	0.005	0.138	0.056	0.050	-0.092	-0.123	.692**	-0.256	0.530	-0.268
Mean Medium veg Type 4	-0.462	0.413	-0.041	0.018	-0.075	-0.139	0.163	-0.235	0.521	-0.252	0.118	-0.204
Mean High veg Type 1	-0.414	0.487	0.222	0.349	-0.005	0.065	-0.053	-0.371	0.369	-0.256	0.287	-0.200
Mean High veg Type 2	-0.454	0.460	0.233	0.335	-0.039	-0.021	0.060	-0.432	0.341	-0.239	0.237	-0.197
Mean High veg Type 3	-0.225	0.397	0.026	0.109	-0.302	-0.231	0.336	-0.263	0.330	-0.300	0.127	-0.334
Mean High veg Type 4	-0.282	.650*	0.102	0.176	-0.001	-0.079	0.040	-0.403	0.428	-0.178	0.284	-0.180
SD Ground Type 1	-.828**	-0.126	.811**	.757**	0.338	-0.290	0.285	-.722**	-0.002	0.211	0.262	0.285
SD Ground Type 4	-.630*	0.464	0.356	0.459	0.123	0.155	-0.143	-0.425	0.404	-0.242	0.344	-0.156
SD Low veg Type 1	-.853**	0.162	.673**	.717**	0.323	0.055	-0.065	-.608*	0.214	-0.085	0.371	0.002
SD Low veg Type 2	-0.266	0.345	0.015	0.053	-0.254	0.452	-0.315	-0.116	-0.012	-0.214	-0.076	-0.003
SD Low veg Type 3	-.691*	0.319	0.268	0.270	0.189	-0.075	-0.094	-0.489	-0.170	-0.049	-0.261	0.033
SD Low veg Type 4	-.639*	0.426	0.415	0.506	0.180	0.156	-0.131	-0.478	0.381	-0.232	0.344	-0.095
SD Medium veg Type 1	-0.484	0.271	0.029	0.035	-0.137	0.101	-0.021	-0.219	0.272	-0.360	0.013	-0.239
SD Medium veg Type 2	-.570*	0.102	0.049	0.023	-0.069	-0.228	0.211	-0.292	0.214	-0.238	-0.069	-0.216
SD Medium veg Type 3	-0.515	-0.240	0.250	0.372	-0.005	-0.464	0.384	-0.429	0.072	0.033	-0.143	-0.076
SD Medium veg Type 4	-0.498	0.342	0.087	0.124	-0.036	-0.125	0.135	-0.329	0.456	-0.307	0.120	-0.184
SD High veg Type 1	-0.239	.785**	0.224	0.281	0.048	0.209	-0.079	-0.253	.698**	-0.313	.723**	-0.268
SD High veg Type 2	-0.375	.655*	0.213	0.266	-0.090	-0.014	0.189	-0.426	.533*	-0.229	0.484	-0.284
SD High veg Type 3	-0.396	.548*	0.253	0.344	-0.061	0.042	0.273	-0.390	.537*	-0.155	0.510	-0.223
SD High veg Type 4	-0.286	.746**	0.174	0.228	0.080	0.237	-0.116	-0.370	0.460	-0.145	0.504	-0.183

**. Correlation is significant at the 0.01 level (2-tailed).

*. Correlation is significant at the 0.05 level (2-tailed).

(Fig. 6-2) have a high canopy cover and low LAI/cover for low vegetation. Plots in group B (Fig. 6-2) have low canopy cover and high LAI/cover for low vegetation. Plot 6a has similar site characteristics with group B, however displayed very low mean and standard deviation of first return intensity from ground stratum. Plot 10b, 13a and 17a were found to have little in common in terms of plot characteristics except they have high mean intensity values. Plot 10b has high canopy cover and low LAI/cover for low vegetation, while Plot 13a has high to moderate canopy cover and high cover for low vegetation, and Plot 17a has high canopy cover and moderate LAI/cover for low vegetation.

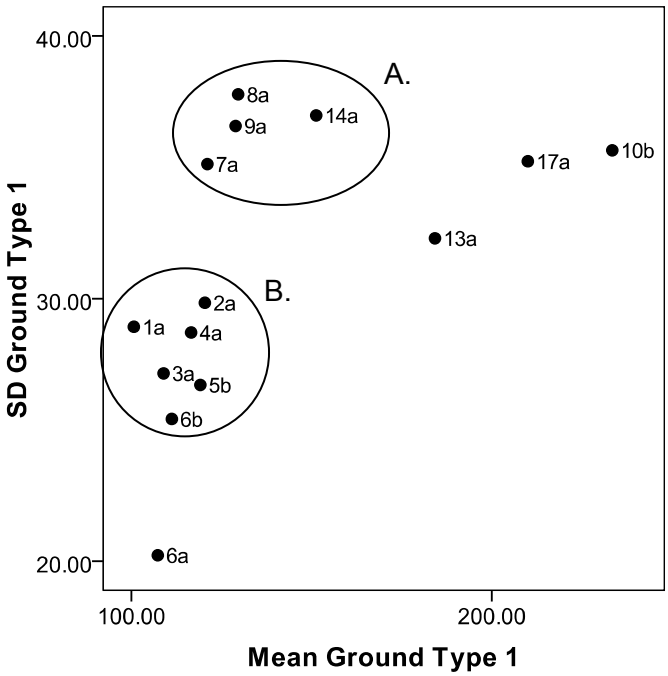

Figure 6-2 Scatter plot of first return intensity from ground stratum (Mean Ground Type 1) and standard deviation of first return intensity from ground stratum (SD Ground Type 1). Labels are surveyed plot names. Plots can be classified into three groups; group A, B and other.

Table 6-2 Pearson correlation coefficients between LiDAR derived intensity version of FCS categories and field variables.

	Field total volume of CWD	Field mean CC_1	Field mean CC_2
LiDAR intensity Opening above Ground (O_{GInt})	.566(*)	-.405	-.445
LiDAR intensity Opening above Low veg (O_{LInt})	0.180	-.896(**)	-.879(**)
LiDAR intensity vertically dense canopy of high trees (D_{HInt})	.408	.605(*)	.637(*)

**. Correlation is significant at the 0.01 level (2-tailed).

*. Correlation is significant at the 0.05 level (2-tailed).

6.3.4 FCS intensity

Fig. 6-3 presents linear regression results between LiDAR derived intensity version of FCS categories and field variables. LiDAR intensity derived V_{LInt} (category 3; presence of understorey vegetation) showed good correlation with *Field LAI for Low veg* ($R^2 = 0.692$, $P < 0.05$, Fig.6-3(a)) and moderate correlation with field recorded *mean Low veg cover* ($R^2 = 0.56$, $P < 0.05$, Fig 6-3(b)). Fig. 6-3(c) and (d) displayed that LiDAR intensity derived CC_{Int} (category 4; canopy cover) were moderately correlated with two field measures of *CC* ($R^2 = 0.514$ and $R^2 = 0.577$, $P < 0.05$ respectively). LiDAR intensity derived V_{MInt} (category 6; presence of mid-storey vegetation) also displayed moderate correlation with field derived *sum of DBH weighted canopy depth in Medium veg* ($R^2 = 0.555$, $P < 0.05$). This is shown in Fig. 6-3(e). LiDAR intensity derived D_{HInt} (category 8; vertically dense canopy of high trees) showed a good correlation with field derived *sum of DBH weighted canopy depth in High veg* with $R^2 = 0.636$, $P < 0.05$ (Fig. 6-3(f)). LiDAR intensity derived V_{HInt} (category 7; presence of high trees) was moderately correlated with *sum of DBH weighted canopy depth in High veg* with $R^2 = 0.465$, $P < 0.05$ (Fig. 6-3(g)). LiDAR intensity derived O_{MInt} (category 5; opening above medium vegetation) was strongly correlated with field derived *opening above Medium veg* with $R^2 = 0.773$, $P < 0.05$ (Fig. 6-

3(h)).

Table 6-2 displays the Pearson correlation coefficients between LiDAR derived intensity version of FCS categories and the field variables. LiDAR intensity derived O_{GInt} (category 1; opening above the ground) was positively correlated with field measured *total volume of CWD* (R = 0.566, P < 0.05). The two field measures of *CC* showed a negative correlation with LiDAR intensity derived O_{LInt} (category 2; opening above low vegetation) with R = -0.896 and R = -0.879, P < 0.01 respectively and positive correlation with LiDAR intensity derived D_{HInt} (category 8; vertically dense canopy of high trees) with R = 0.605 and R = 0.637, P < 0.05 respectively.

6.4 Discussion

Intensity information classified according to return types and vertical strata contained important and distinct response from the forested landscape. In terms of return types, Type 1 returned the highest intensity in every vegetation stratum when compared to other types. This is expected since Type 1 returns are singular returns and result only from the first interaction with objects. They therefore contain the highest return energy. This supports previous findings from the discrete return system experiment (Section 3.7.3) and Moffiet et al. (2005). The difference in returned intensity between vegetation layers (Fig. 6-1) could result from the different composition of components present in each layer. Fig. 6-4 illustrates typical spectral reflectance curves for vegetation, dry soil and water. The LiDAR system, RIEGL LMS-Q560 sensor, used in this study operates at a wavelength of 1550 nm. At this wavelength, the reflectance of an individual green leaf is approximately 30 %, and less than that of dry soil (approximately 45 %). Since *High veg* stratum contains the

canopy (mainly leaves of high trees), less reflectance from this stratum is expected compared to *Ground* stratum at this wavelength. Furthermore, multiple scattering of laser pulses occurs in *High veg* stratum where the average facet size will be much smaller due to leaves. Therefore only low intensity values are recorded for returns from this stratum. It is likely that *Medium* and *Low veg* strata have more components, such as shrubs, as well as leaves of trees. Therefore laser pulses might interact more with larger and more substantial woody materials and stronger intensity values are returned. In fact, the standard deviation of intensity for Type 1 in *Medium* and *Low veg* strata (Fig. 6-1, right) showed greater variation than that in *High veg* stratum. This means that these strata are most likely heterogeneous and contains various reflective mediums. It was noted that *Low veg* and *Ground* strata have similar range and trend of intensity values (Fig. 6-1, left). This could be due to misclassification of LiDAR returns. *Low veg* stratum might contain some *Ground* points. It is always challenge to obtain highly accurate terrain in densely vegetated areas and over uneven grounds. Improvements in point classification accuracy would perhaps emphasise the differences between *Low veg* and *Ground* strata. However, robust methods to distinguish these strata could not be developed in the time frame of this research. Distinct high values were found in mean intensity for plots, 10b, 13a, 17a and 5b (Fig. 6-1, left). The high standard deviation of intensity for these plots means the intensity values are very noisy (Fig. 6-1, right). However, logical explanation for these high values could not be found.

The intensity variables calculated for each type in the four vegetation layers showed some correlations with field variables (Table 6-1). The results between *standard deviation of Ground Type 1* and *Field LAI for Low veg*, *Field mean Low veg cover* and the two measures of field *CC* suggest that where canopy cover is high, LAI/cover for low vegetation is low and the single (first) return standard deviation of intensity in the ground

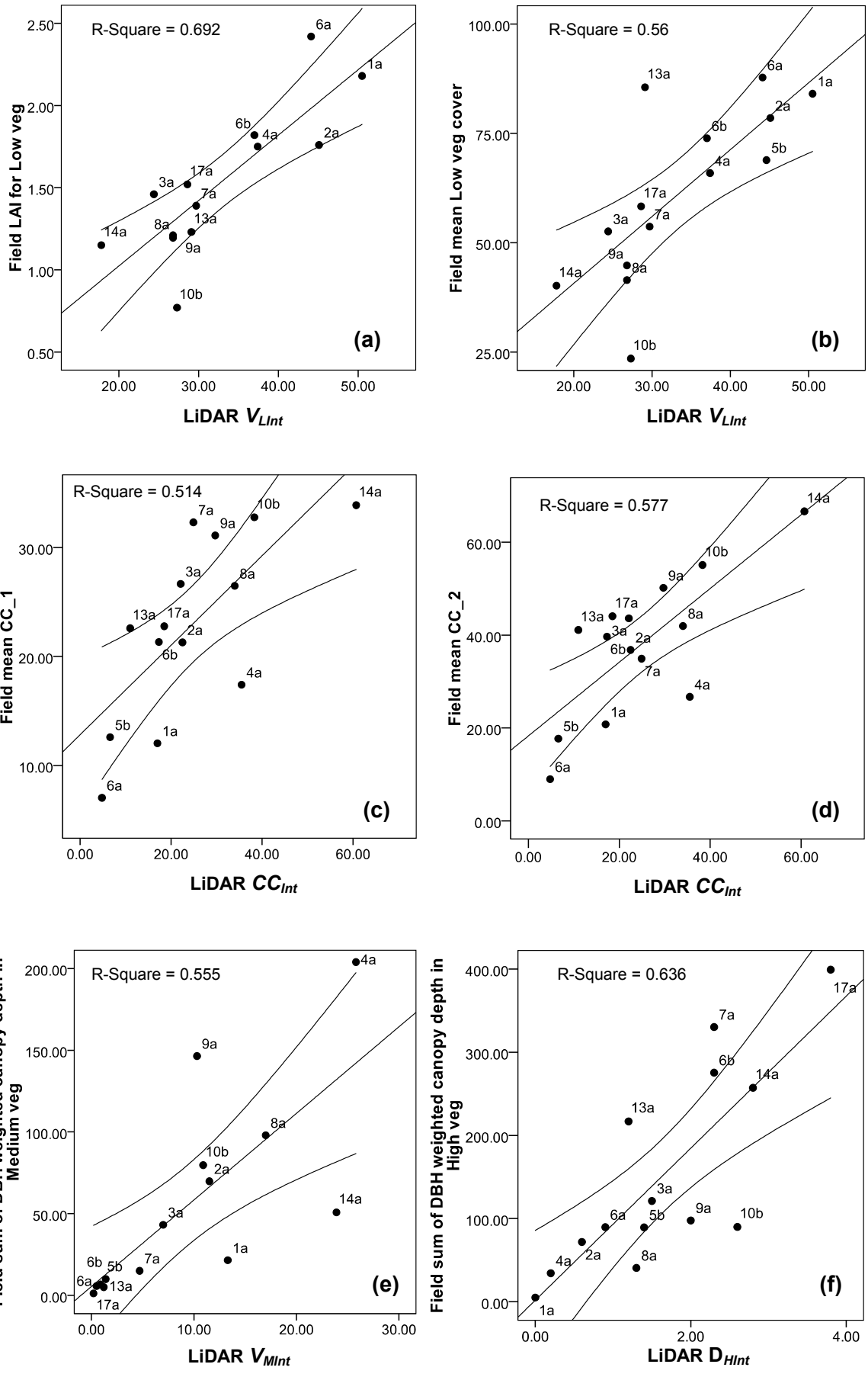
R-Square = 0.692
Field LAI for Low veg
LiDAR V_{LInt}
(a)
R-Square = 0.56
Field mean Low veg cover
LiDAR V_{LInt}
(b)
R-Square = 0.514
Field mean CC_1
LiDAR CC_{Int}
(c)
R-Square = 0.577
Field mean CC_2
LiDAR CC_{Int}
(d)
R-Square = 0.555
Field sum of DBH weighted canopy depth in Medium veg
LiDAR V_{MInt}
(e)
R-Square = 0.636
Field sum of DBH weighted canopy depth in High veg
LiDAR D_{HInt}
(f)

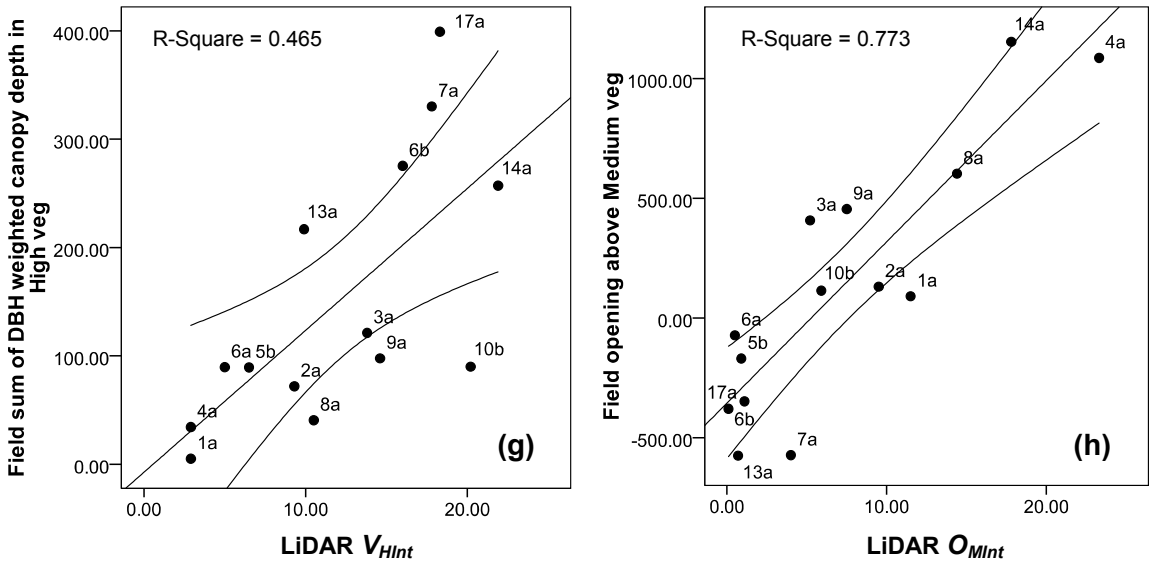

Figure 6-3 Linear regression results between LiDAR derived intensity version of FCS categories and field variables with 95 % mean prediction interval. The labels are surveyed plot names.

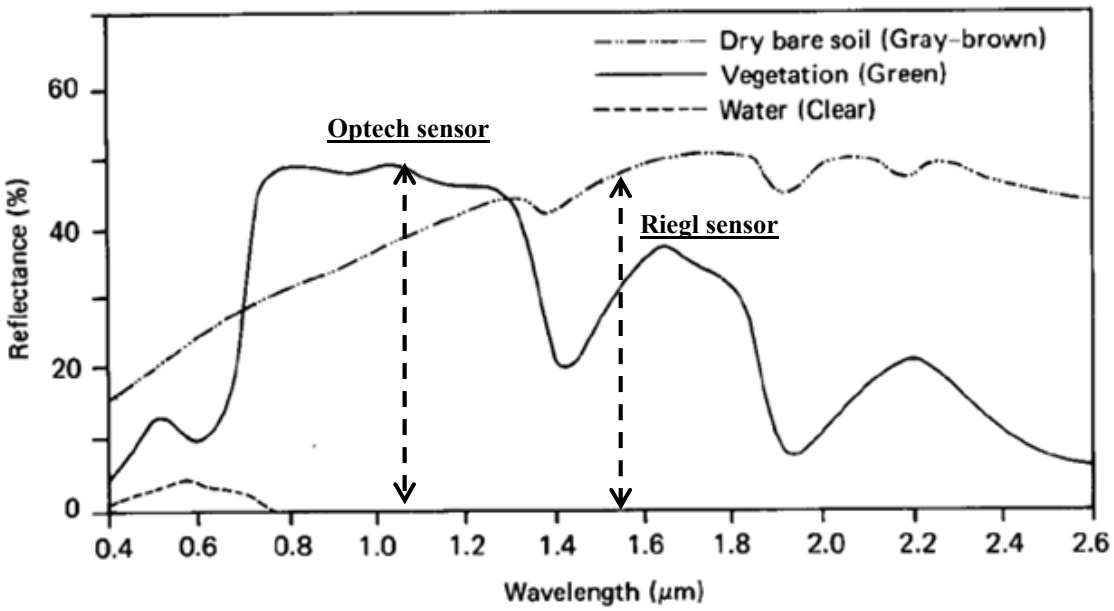

Figure 6-4 Typical spectral reflectance curves for vegetation, dry soil and water (After Davis et al., 1978). Arrows show the wavelength for Optech Inc. ALTM and RIEGL LMS-Q560 sensors operation.

stratum is high. In other words, where the canopy is horizontally dense, low vegetation does not grow thickly and the ground is more likely heterogeneous. The same trend was found in the results between *standard deviation of Low veg Type 1* and field variables (Table 6-1). This trend is different from the results found in the LiDAR discrete return system experiment (Section 3.7.1 and 3.7.2), where the results indicate where the canopy is dense, grass does not grow thickly and the ground is more likely homogeneous. Since the two experiments were conducted in different study sites where forest structures differ significantly, diverse outcomes are possible. This means that analysis using intensity variables could be site specific. The results between *Standard deviation of High veg Type 1* and field variables (Table 6-1) indicate that where trees are tall, canopy is vertically dense or fallen trees are abundant, the high canopy stratum is more likely to be heterogeneous. This partially fits with the result found in Section 5.4, which showed significant positive correlation between LiDAR derived D_H (category 8; vertically dense canopy of high trees) and *Field total volume of CWD* (Table 5-3). *Standard deviation of High veg Type 1* can be a good predictor for CWD, mean tree height and the canopy depth in high canopy stratum. Table 6-1 displayed other significant correlations between intensity variables and field variables, however no physical explanation was found, as reported in Pesonen et al. (2008), who noted the relationship between the intensity and CWD volume. Further study and careful interpretation is required for intensity analysis.

The combination of mean and standard deviation of first return intensity from the ground demonstrated the potential of differentiating forest structural types; sparse canopy with few fallen trees or dense canopy with many fallen trees (Section 3.7.4). The same combination in this experiment, however, did not show the same ability. The possible reasons are the difference in study sites and in systems used. In fact, in the study site for the LiDAR full waveform system experiment, more CWD are likely found in the area where large trees

with vertically dense canopies and gaps from the ground to canopy are present (Section 5.5). Different LiDAR variable combinations may be required to recover the same structural variable in a different forest landscape. Figure 6-2 displayed the potential to classify different forest structural types; high canopy cover and low LAI/cover for the low vegetation, and low canopy cover and high LAI/cover for the low vegetation. However, this plot characteristic can be obtained using the original FCS easily rather than utilising additional intensity information.

The intensity version of FCS presented promising results (Table 6-2 and Fig. 6-3). Category 1, 2 and 8 of intensity version of FCS displayed similar trends with the original FCS (Table 5-3), although the degree of significance were slightly different between corresponding results (Table 6-2). Category 3 to 8 of the intensity version of FCS showed notably similar trends with FCS (Fig. 5-2). This is shown in Fig. 6-3. However, most of the linear regression R^2 values between intensity version of FCS and field variables displayed slightly less correlation than those of the original FCS. In particular, LiDAR derived CC_{Int} showed considerably lower correlations with the two measures of field *CC* ($R^2 = 0.514$ and $R^2 = 0.577$, $P < 0.05$ respectively), compared to significant correlations of LiDAR derived *CC* ($R^2 = 0.86$ and 0.84, $P < 0.05$ respectively). This is contrary to the findings of Hopkinson and Chasmer (2009). These authors estimated the fractional cover across multiple forest ecozones using four methods; a canopy cover-to-total first returns ratio, a canopy-to-total return ratio, an intensity return ratio and a Beer's Law modified intensity ratio, and found that intensity-based models were better predictors. The difference in vegetation species and forest structure in study sites might be one reason for the different outcomes. Another reason may be the difference in LiDAR systems used. Hopkinson and Chasmer (2009) utilised Optech Inc. ALTM sensors which are discrete return systems and operate at a wavelength of 1064 nm. RIEGL LMS-Q560 sensor used in this study operates

at a wavelength of 1550 nm. The difference in the wavelength would cause the different intensity response. At a wavelength of 1064 nm, green vegetation generally reflects approximately 50 % of incident energy and dry soil reflects approximately 35 % of the energy (Fig. 6-4). However the reflectance of vegetation drops nearly half, approximately 30 % and the reflectance of dry soil increases up to approximately 45 % at 1550 nm (Fig. 6-4). In our dataset, the returned intensity from canopy strata (*Medium veg* and *High veg*) could be too low and the returned intensity from ground stratum (*Ground*) could be too high to compute canopy cover properly due to weaker spectral reflectance of vegetation and stronger reflectance of the soil at wavelength of 1550 nm. It might be optimal to utilise a wavelength of 1064 nm for recovering green vegetation attributes such as canopy cover. However, this needs further study to conclude. The selection of sensor with appropriate wavelength for the study would be critical to use intensity information. Different sensor and landscape combinations might work to recover particular forest structural information. To account for the utility of intensity variables, further application and comparison of intensity version of FCS are required.

6.5 Conclusion

In this chapter, the return intensity of a LiDAR full waveform system was explored to examine whether the intensity variables can give an insight into forest structure attributes. The exploratory analysis of mean and standard deviation of intensity classified into types and vegetation strata revealed that each return type in the four vegetation strata has distinct response characteristics. Type 1 returned the highest intensity compared to other types regardless of vegetation strata. This was followed by Type 4, 2 and 3 in this order.

Returned intensity and its variation were relatively low in the high canopy stratum. The highest returned intensity was observed in the ground strata followed by the low and medium vegetation strata in this order. Higher intensity variation was found in the medium and low vegetation strata. These characteristics would be helpful information to understand the intensity response from forested landscape at a given wavelength. Improvements in point classification accuracy might be required for better interpretation since the possibility of misclassification of the ground points was found. The correlation between intensity variables and field variables suggested that standard deviation of Type 1 intensity in the ground and the low vegetation strata have the potential to recover LAI/cover for low vegetation and canopy cover. Similarly, standard deviation of Type 1 intensity in the high canopy stratum displayed the potential to recover CWD amount, mean tree height and canopy depth in the high canopy stratum. However, many of significant correlations found in the analysis defy physical explanation at this time. It was noted that the analysis using intensity variables could be site specific. Further study and careful interpretation are required. The algorithm of the LiDAR discrete return system experiment to use the combination of mean and standard deviation of first return intensity from the ground for forest structural type classification did not work the same way in this analysis. The intensity version of FCS clearly showed the potential of recovering field variables, however it did not enhance the ability of the original FCS. It was noted that the selection of sensor with an appropriate wavelength for the study would be critical to use intensity information. Further application of intensity version of FCS is required to account for the utility of intensity variables. It is concluded that the original FCS is better option to recover forest structure variables at this stage.

CHAPTER 7 APPLICATION OF FOREST CHARACTERISATION SCHEME

7.1 Introduction

In this chapter, applications of the previously proposed LiDAR based scheme for characterising the ecological structure of a dry Eucalypt forest landscape (FCS) are presented. In Section 7.2, the robustness of LiDAR derived FCS is examined by comparing two LiDAR datasets of the same area. The scheme is also tested for compatibility with commonly used field-based biodiversity metrics. This is discussed in Section 7.3.

7.2 Applicability of forest characterisation scheme for a different LiDAR dataset

7.2.1 Introduction

Previously proposed FCS categories (see Chapter 5) allowed for quantification of gaps (above bare ground, low vegetation and medium vegetation), canopy cover and its density as well as the presence of various canopy strata (low, medium and high). The scheme demonstrated the potential of full waveform LiDAR to provide information on the complexity of habitat structure. This section asks the question: does this scheme work equally well using a different LiDAR dataset? It is increasingly common for natural resource managers to have multiple LiDAR datasets acquired using different sensors or the same sensor with different sensor configurations.

It has been reported that different sensors (Næsset, 2009), flying altitude (Goodwin et al., 2006; Morsdorf et al., 2008; Næsset, 2004; Næsset, 2009), pulse repetition frequencies (Chasmer et al., 2006; Næsset, 2005; Næsset, 2009) and scan angle (Goodwin et al., 2006; Holmgren et al., 2003) all may affect the point cloud configuration and attributes derived from a forest landscape. In studies using discrete return systems, Næsset (2004; 2009) and Goodwin et al. (2006) concluded that the different flying altitude was not a major influence in recovering forest biophysical properties, however Goodwin et al. (2006) suggests that higher flying altitude can reduce the first and last return combinations because of the larger footprint size and an insufficient intensity of the laser energy being returned to the sensor. A smaller proportion of multiple returns was also reported in higher pulse repetition frequency systems due to reduced output energy in emitted laser pulses (Næsset, 2009). Holmgren et al. (2003) demonstrated a scanning angle effect in canopy returns. These authors reported that the proportion of canopy hits was increased off nadir when the scanning angle reaches a critical value for a particular tree species. Similar findings were reported by Morsdorf et al. (2008) and Goodwin et al. (2007). The method of decomposing full waveform may also have an impact on return properties that can be indentified (Wagner et al., 2006). Therefore, it is important to examine the robustness of any proposed scheme using the different datasets.

In this section, the previously proposed FCS is applied to LiDAR data of the same area acquired under different specifications and validated using field variables to examine the wide applicability and robustness of the proposed scheme.

7.2.2 Methods

7.2.2.1 LiDAR data

Two LiDAR datasets were used in this study. The initial LiDAR data (LiDAR07) was acquired over the study area using a RIEGL LMS-Q560 sensor in February 2007, which was described in Section 4.3. This data was used to develop the forest characterisation scheme. An additional LiDAR data (LiDAR08) was provided by the State Government of Tasmania through the Department of Primary Industries and Water. This was acquired using LiteMapper 5600 sensor in March 2008 by the Antarctic Climate & Ecosystems Cooperative Research Centre as part of its Climate Futures for Tasmania project. These are independently acquired datasets flown by different operators with similar LiDAR systems. The specifications for both sensors are summarized in Table 7-1. Note that in both specifications the LiDAR systems have the same pulse energy and similar pulse width at half maximum. LiDAR08 has a slightly higher pulse repetition frequency (120 kHz), wider scan angle (± 30º) and higher platform altitude (800 m) than LiDAR07 (100 kHz, ± 22.5º and 500 m, respectively). Although this study utilised full waveform LiDAR systems, each data provided was already decomposed in up to six discrete returns by respective data providers. For this process, it was confirmed that a Gaussian Pulse Fitting (GPF) method for LiDAR07 and a Gaussian Pulse Estimation (GPE) method for LiDAR08 were used with the default advanced parameters in RiANALYZE 560 software of RIEGL (RIEGL, 2006). The accuracy of these methods is nearly identical (RIEGL, 2006).

7.2.2.2 Field data

The same field data collected in February 2008 and computed, which was presented in

Section 4.4, were used for this analysis.

Table 7-1 Specifications for the two LiDAR data acquisition.

LiDAR data	LiDAR07	LiDAR08
Sensor	RIEGL LMS-Q560	LiteMapper 5600 (LMS-Q560)
System	Waveform	Waveform
Pulse repetition frequency	100 kHz	120 kHz
Scan angle	± 22.5º	± 30º
Platform altitude	500 m	800 m
Beam divergence angle	0.5 mrad	0.5 mrad
Footprint	20 cm	25 cm
Pulse width at half maximum	4ns	5ns
Pulse energy	8μJ	8μJ
Wavelength	1550 nm	1550 nm
Acquisition date	February 2007	March 2008

7.2.2.3 Forest characterisation scheme (FCS)

The FCS proposed in Chapter 5 was applied to LiDAR08 and subsequently compared to the field variables. Then the results of LiDAR08 were compared to the results of LiDAR07 to examine applicability and robustness of FCS using the different LiDAR dataset. It should be noted that LiDAR derived O_G (category 1; opening above the ground) and O_L (category 2; opening above low vegetation) were compared with field derived CC according to existing correlations (see Table 5-3).

7.2.3 Results

The comparison between the LiDAR derived structural characterisation scheme and the

field data is shown in Fig. 7-1. LiDAR derived O_G (category 1; opening above the ground) displayed moderate correlations with field derived *CC* for both LiDAR07 (Fig. 1(a); R^2 = 0.454, $P < 0.05$) and LiDAR08 (Fig. 1(b); R^2 = 0.524, $P < 0.05$). LiDAR derived *CC* (category 4; canopy cover) was significantly correlated with field derived *CC* for both LiDAR07 (Fig. 1(g); $R^2 = 0.856$, $P < 0.05$) and LiDAR08 (Fig. 1(h); $R^2 = 0.826$, $P < 0.05$). LiDAR derived O_M (category 5; opening above medium vegetation) presented high correlations with field derived *opening above Medium veg* for both LiDAR07 (Fig. 1(i); R^2 = 0.731, $P < 0.05$) and LiDAR08 (Fig. 1(j); R^2 = 0.694, $P < 0.05$). LiDAR derived V_M (category 6; presence of mid-storey vegetation) and the field derived *sum of DBH weighted canopy depth in Medium veg* showed a good correlation for LiDAR07 (Fig. 1(k); R^2 = 0.677, $P < 0.05$) and a moderate correlation with LiDAR08 (Fig. 1(l); $R^2 = 0.460$, $P < 0.05$). LiDAR derived V_H (category 7; presence of high trees) was well correlated with field derived *sum of DBH weighted canopy depth in High veg* for both LiDAR07 (Fig. 1(o); R^2 = 0.710, $P < 0.05$) and LiDAR08 (Fig. 1(p); $R^2 = 0.649$, $P < 0.05$).

LiDAR derived O_L (category 2; opening above low vegetation), V_L (category 3; presence of understorey vegetation) and D_H (category 8; vertically dense canopy of high trees) exhibited high correlations with field derived variables for LiDAR07 (Fig. 1(c); $R^2 = 0.826$, (e); $R^2 = 0.823$ and (m); $R^2 = 0.729$, $P < 0.05$, respectively). On the other hand, the same categories for LiDAR08 showed similar trends to LiDAR07, however exhibited much weaker and not significant correlations (Fig. 1(d); $R^2 = 0.297$, (f); $R^2 = 0.241$ and (n); R^2 = 0.307, $P < 0.05$, respectively).

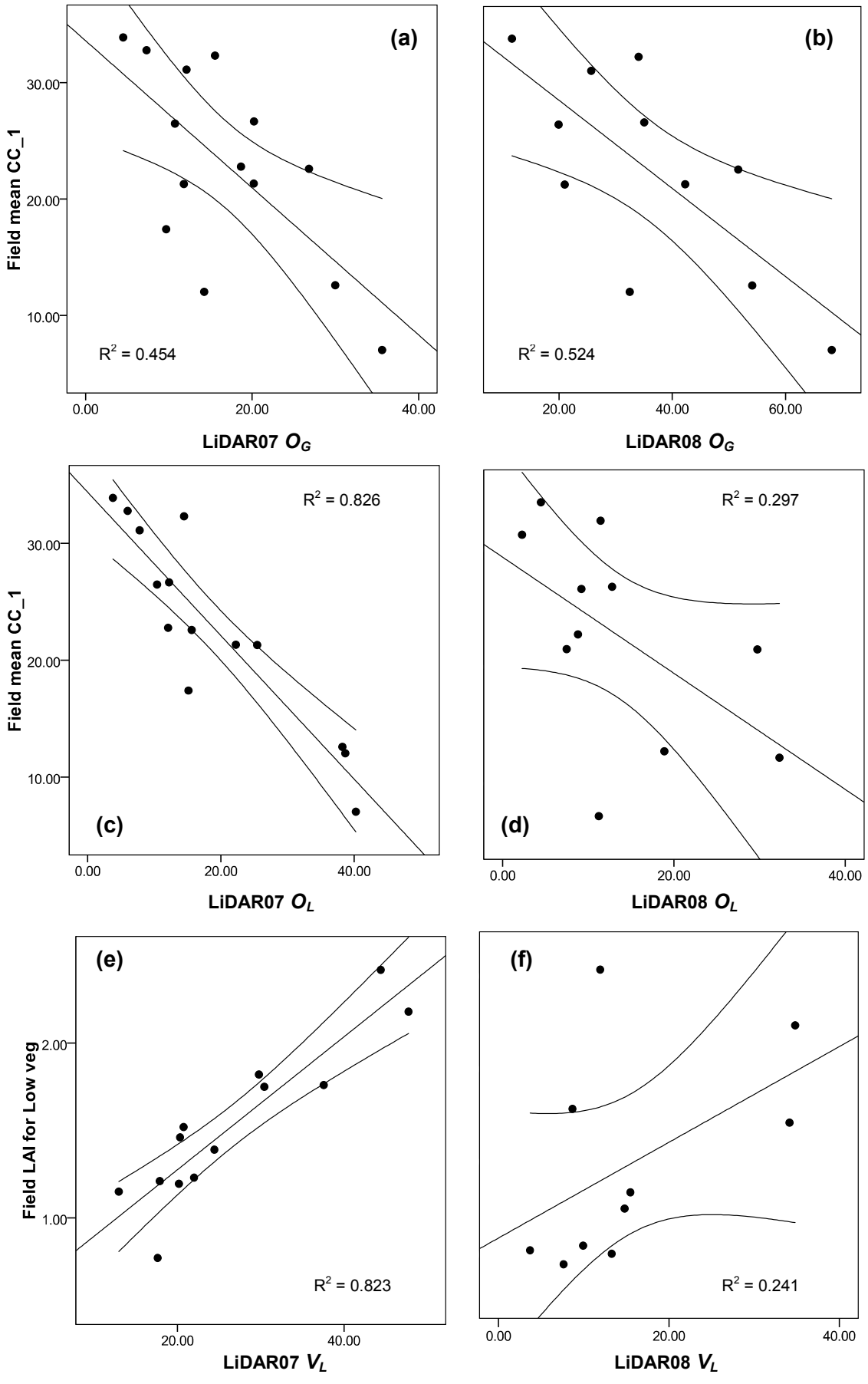
(a)
(b)
(c)
(d)
(e)
(f)
Field mean CC_1
Field LAI for Low veg
30.00
20.00
10.00
2.00
1.00
0.00
20.00
40.00
60.00
R² = 0.454
R² = 0.524
R² = 0.826
R² = 0.297
R² = 0.823
R² = 0.241
LiDAR07 O_G
LiDAR08 O_G
LiDAR07 O_L
LiDAR08 O_L
LiDAR07 V_L
LiDAR08 V_L

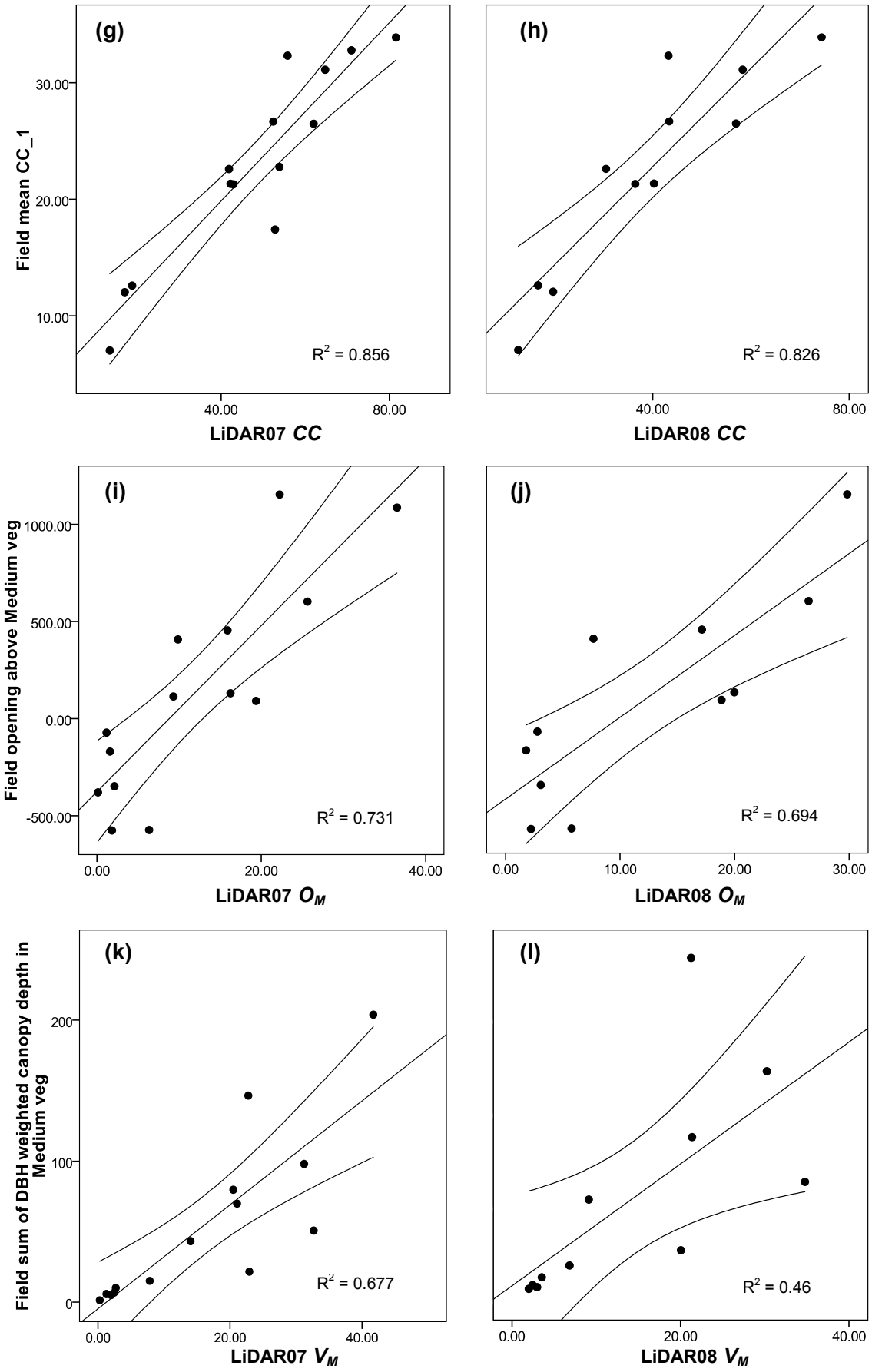
(g)
Field mean CC_1
30.00
20.00
10.00
R² = 0.856
40.00
80.00
LiDAR07 CC
(h)
R² = 0.826
40.00
80.00
LiDAR08 CC
(i)
Field opening above Medium veg
1000.00
500.00
0.00
-500.00
R² = 0.731
0.00
20.00
40.00
LiDAR07 O_M
(j)
R² = 0.694
0.00
10.00
20.00
30.00
LiDAR08 O_M
(k)
Field sum of DBH weighted canopy depth in Medium veg
200
100
0
R² = 0.677
0.00
20.00
40.00
LiDAR07 V_M
(l)
R² = 0.46
0.00
20.00
40.00
LiDAR08 V_M

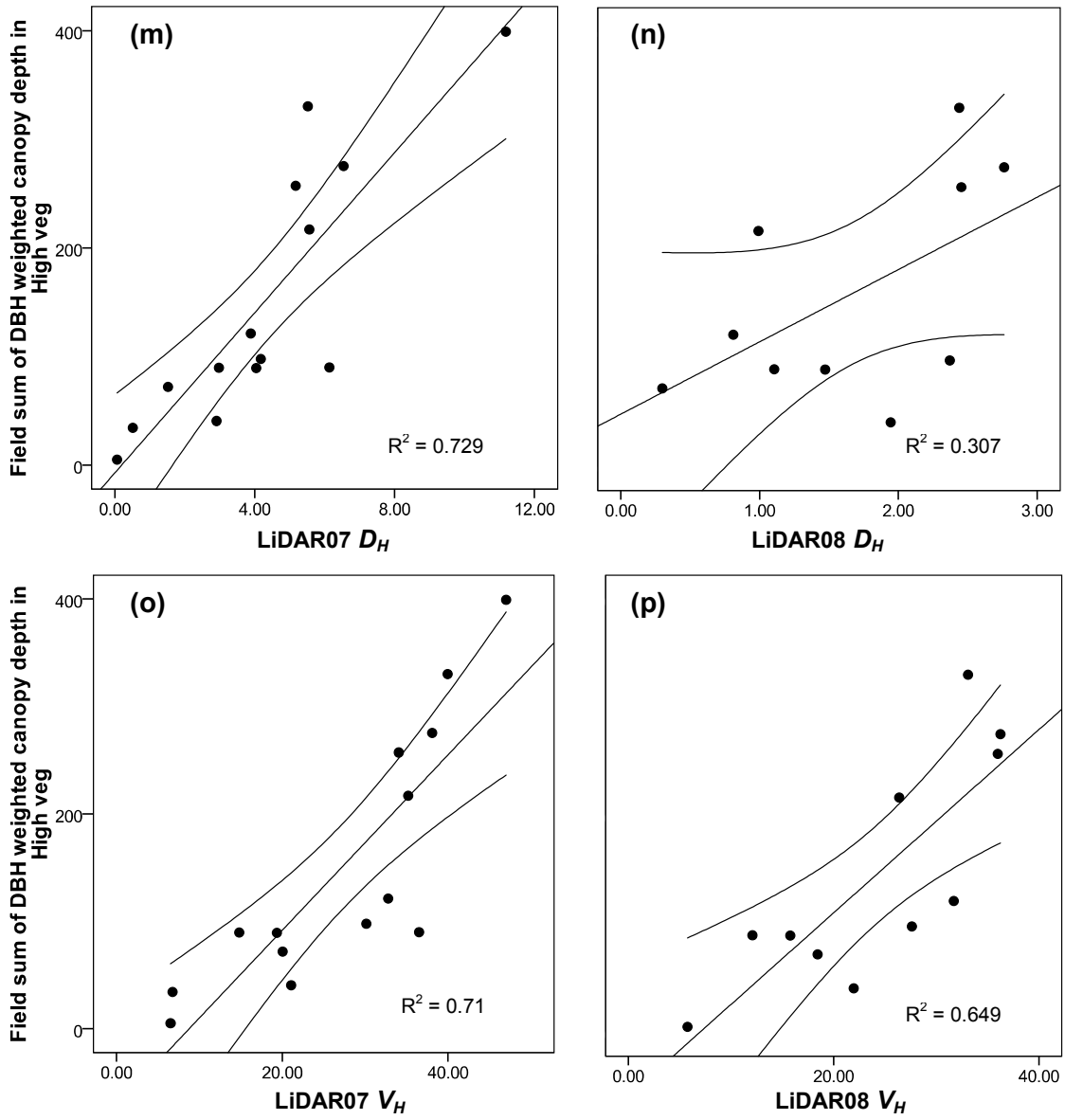

Figure 7-1 Linear regression results between LiDAR derived Forest Characterisation Scheme categories of LiDAR07 and LiDAR08 and field variables with 95 % mean prediction interval.

7.2.4 Discussion

The results suggest that Category 1 (opening above the ground), 4 (canopy cover), 5 (Opening above medium vegetation), 6 (presence of mid-storey vegetation) and 7 (presence of high trees) are robust and resilient to the different specifications (Table 7-1) of these two LiDAR data acquisitions. Category 2 (opening above low vegetation), 3

(presence of understorey vegetation) and 8 (vertically dense canopy of high trees) are considered somewhat susceptible to changes in sensor configurations. Since calculations of these categories used all types of *Low veg* and Type 3 and 4 of *High veg*, it is possible that these particular return type ratios were affected by the difference in LiDAR data acquisitions.

Note also that LiDAR07 and LiDAR08 use different methods for the decomposition of the waveform data and have different flying altitudes, pulse repetition frequencies and scan angles. The method of decomposing the waveform has been reported to potentially impact return properties (Wagner et al., 2006), however, this is unlikely to be the case for our datasets, since the two methods are similar and report an identical level of accuracy.

LiDAR08 was derived at higher flying height, higher pulse repetition frequency and wider scan angle than LiDAR07. Previous studies using discrete return systems have reported that these specifications may affect the point cloud configuration and attributes derived from a forest landscape (e.g. Goodwin et al., 2006; Næsset, 2009). In our datasets, LiDAR08 displayed more Type 1 and less Type 2, 3 and 4 than LiDAR07 (Fig 7-2). In another words, LiDAR08 has more singular returns and less multiple returns. Since the comparison of mean intensity for each plot between LiDAR07 and LiDAR08 showed consistently lower intensity in LiDAR08 (Fig. 7-3), it is likely that the increased pulse repetition frequency for LiDAR08 caused a reduction in energy per emitted laser pulse, resulting in a smaller portion of multiple returns; as reported by Næsset (2009).

Comparing the proportion of total returns in the four strata: *Ground*, *Low veg*, *Medium veg* and *High veg*, for each plot between LiDAR07 and LiDAR08, it was found that the proportion of total returns for LiDAR08 was consistently larger in *Ground* stratum and

smaller in *Low veg* stratum, while it was nearly identical between the two datasets in *Medium veg* and *High veg* strata respectively (Fig. 7-4). Fig. 7-5 shows the proportion of each return type for each plot in *Ground*, *Low veg*, *Medium veg* and *High veg* strata for LiDAR07 and LiDAR08. In *Ground* stratum, the proportion of Type 4 exhibited a similar range in both the LiDAR07 and LiDAR08; however the proportion of Type 1 was found to be much larger in LiDAR08 (Fig. 7-5). In *Low veg* stratum, the proportion of all types was found to be smaller in LiDAR08 (Fig. 7-5). In particular, the proportion of Type 4 was found to be much smaller (Fig. 7-5). In the *Medium veg* and *High veg* strata, it was found that the proportion of Type 1 was larger in LiDAR08, while the proportion of Type 2 was larger in LiDAR07 (Fig. 7-5). In these strata, the proportion of Type 3 and 4 was found to be much smaller in LiDAR08 (Fig. 7-5). In particular, the proportion of Type 3 was close to 0 % in most plots (Fig. 7-5). These results suggest an insufficient proportion of returns in the *Low veg* stratum, particularly a reduced number of Type 4 interactions, and this may explain the reason for weaker correlation with field variables in Category 2 (opening above low vegetation; O_L) and Category 3 (presence of understorey vegetation; V_L). Another consideration is that the scarce proportion of Type 3 in *High veg* stratum may explain the poor correlation with field variables in Category 8 (vertically dense canopy of high trees; D_H).

In terms of the flying altitude, its effect on the portion of single/multiple returns in LiDAR08 may be mitigated since the footprint sizes are similar between LiDAR07 and LiDAR08. Morsdorf et al. (2008) suggested that the vertical separation of objects was dependent on flying altitude contrary to the understanding that minimum vertical distance between objects will increase with an increase only in pulse width (Baltsavias, 1999). In either case, this effect may not be profound since the minimum separation distance of objects within an emitted pulse is fairly small, approximately 30 cm in LiDAR08

(Eichstaedt, pers. comm.).

It has been reported that a greater scan angle (off nadir) increases the proportion of canopy returns (e.g. Holmgren et al., 2003). However, our datasets did not show this effect, with minimal differences in the proportion of returns in *Medium veg* and *High veg* strata (Fig. 7-4) between different scan angles noted. Furthermore, the FCS Category 4 (canopy cover; *CC*) worked equally well using the wider scanning angle of LiDAR08. The effect of scanning angle was not observed in this study.

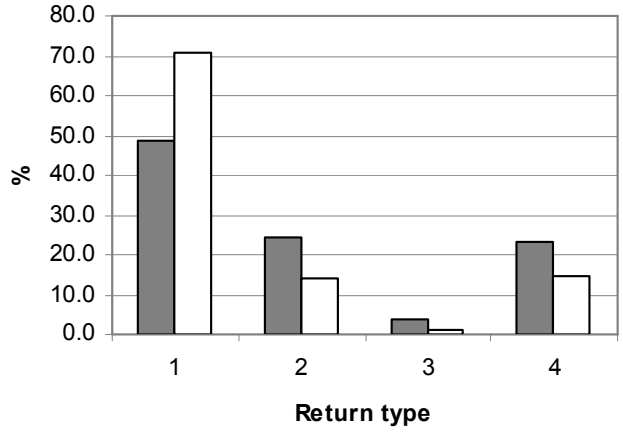

Figure7-2 Proportion of each return type in LiDAR07 (grey bars) and LiDAR08 (white bars).

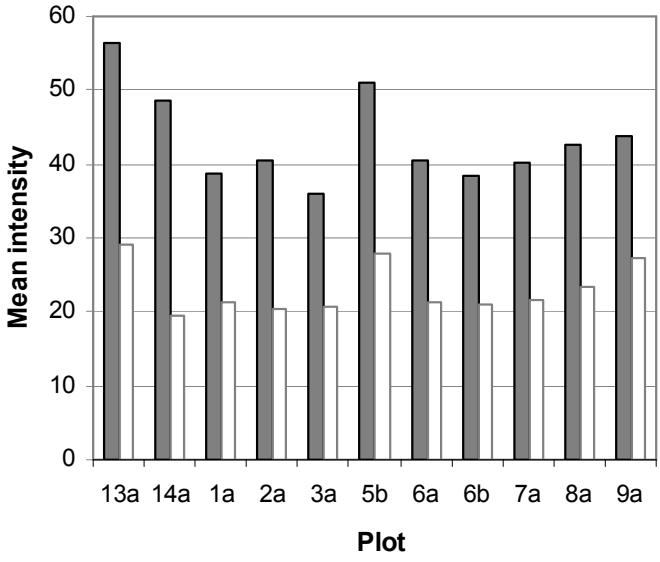

Figure7-3 Mean intensity for each plot in LiDAR07 (grey bars) and LiDAR08 (white bars).

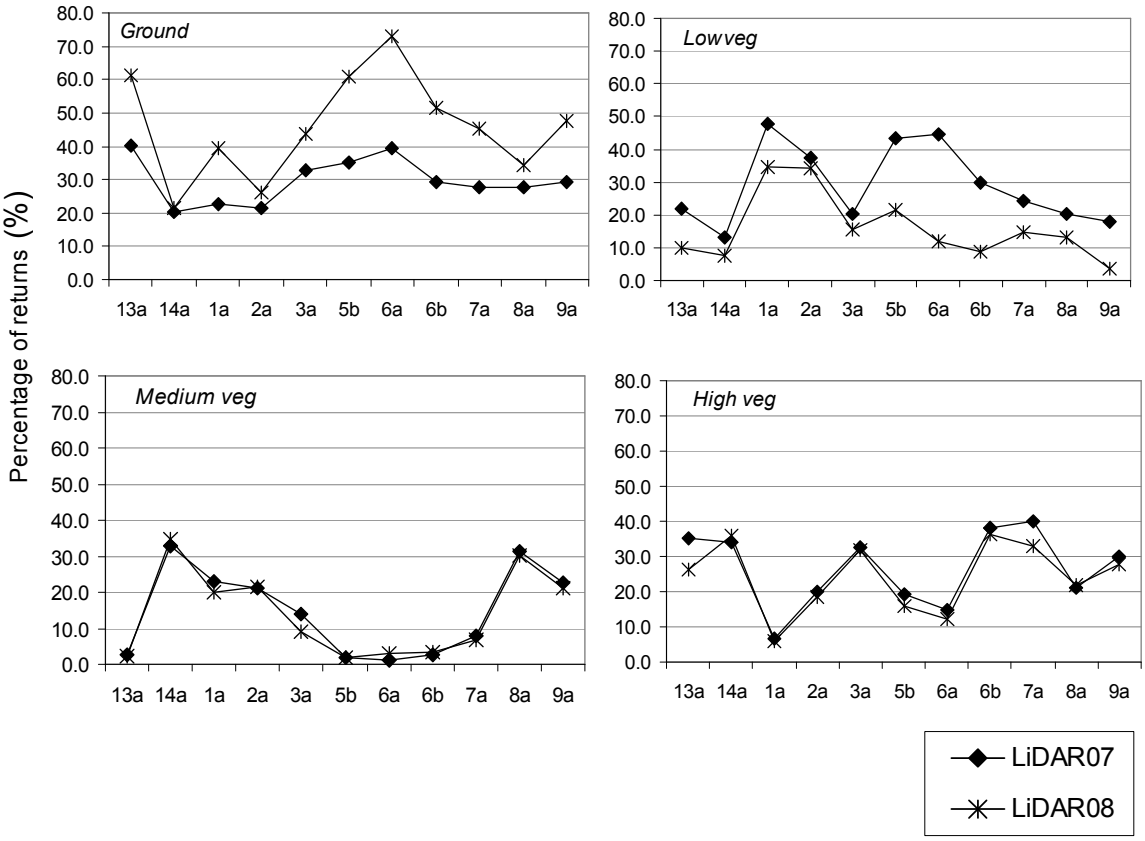

Figure 7-4 Proportion of total returns for each plot in *Ground*, *Low veg*, *Medium veg* and *High veg* strata for LiDAR07 and LiDAR08.

7.2.5 Summary of applicability of forest characterisation scheme for a different LiDAR dataset

As a result of this multiple dataset comparison, it was concluded the FCS Category 1 (opening above the ground; O_G), Category 4 (canopy cover; CC), Category 5 (opening above medium vegetation; O_M), Category 6 (presence of mid-storey vegetation; V_M) and Category 7 (presence of high trees; V_H) were robust and resilient to the LiDAR data acquired under different specifications. Category 2 (opening above low vegetation; O_L), Category 3 (presence of understorey vegetation; V_L) and Category 8 (vertically dense canopy of high trees; D_H) were found somewhat susceptible to changes in sensor configurations, especially variations in the pulse repetition frequency. To maintain a good

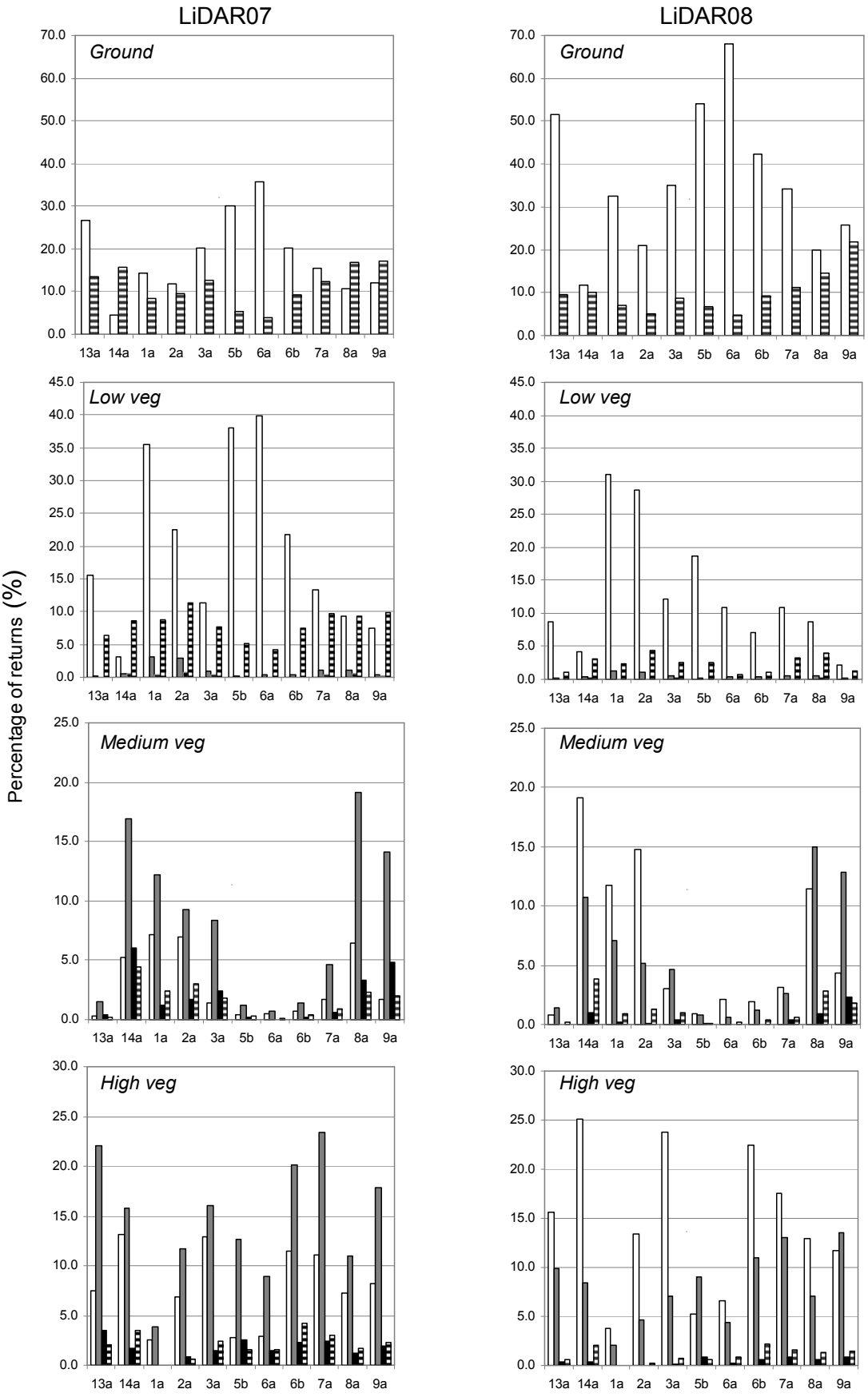

Figure 7-5 Proportion of each return type; Type 1 (white bars), Type 2 (grey bars), Type 3 (black bars) and Type 4 (stripe bars), for each plot in *Ground*, *Low veg*, *Medium veg* and *High veg* strata for LiDAR07 and LiDAR08.

performance for all categories of the forest characterisation, obtaining sufficient multiple returns by setting an appropriate pulse repetition frequency is the key. Next step would be to test this scheme in different forest ecosystems.

7.3 Applicability of LiDAR based forest characterisation scheme for field-based biodiversity metrics

7.3.1 Introduction

Traditional vegetation assessment methods require costly fieldwork and are often laborious, having a subjective element such as comparison to the benchmark in the case of assessment methods in Australia. Therefore an efficient and cost-effective assessment tool to compliment these surveys would be ideal (Section 2.2.2). The proposed forest characterisation scheme (FCS) aimed to quantitatively measure surrogates of biodiversity and variables widely utilised in vegetation monitoring systems in Australia. The proposed FCS was validated against a custom made ground sampling method and showed promising results (Chapter 5). This rises a question: can the proposed FCS directly be incorporated into and complement traditional survey methods? In this section, the previously proposed FCS is tested for compatibility with commonly used field-based biodiversity metrics.

7.3.2 Methods

7.3.2.1 LiDAR data

LiDAR data acquired in February 2007 using a RIEGL LMS-Q560 sensor was used for

this study. The specification of data acquisition is described and listed in Section 4.3 and Section 7.2.2.1. This data was used to develop the FCS presented in Chapter 5. Eight categories of the FCS are compared with commonly used field-based biodiversity metrics to examine their compatibility.

7.3.2.2 Field-based biodiversity metrics

Fieldwork was conducted in February 2007, which was synchronised with the LiDAR data acquisition date, by the Landscape Logic project team members. In this fieldwork, native vegetation condition was assessed using the 'BioMetric' tool (Gibbons et al., 2004). As presented in Section 2.2.2, this survey method is a plot based and measures indigenous plant species, native overstorey, midstorey and ground cover, exotic plant cover, the number of trees with hollows, regeneration, total length of fallen logs and number of stems in specified diameter classes. Assessed variables and methods used in this fieldwork are summarised in Table 7-2. These measurements are scored against the bench mark and integrated to produce site values. Although the site value may be a good indication of native vegetation condition, scoring methods are locally specific and the integrating process may lose much of the detailed information. In terms of biodiversity assessments, the utility of the site values would be limited since they are comprehensive scores and do not provide individual quantitative measurements which are often required for ecological applications such as habitat suitability models. It is also difficult to compare different forests in different geographical regions where the bench mark system is not utilised. The universal quantitative variables such as the percent cover of canopy and LAI would be able to provide more utility. Furthermore, the site values are computed based on individual assessments of the variables. It is considered more important to investigate individual

variables. In this study, individual variables of field measurements such as overstorey cover are used for comparison with LiDAR based FCS.

7.3.2.3 Comparison between LiDAR based forest characterisation scheme and field-based biodiversity metrics

Nine sites were selected due to availability of both LiDAR and field datasets. One site consists of two 20 m ×50 m field plots and a 0.2 ha LiDAR plot (Fig. 7-6). To compare with the FCS, field data was calculated. *Overstorey* cover and *Midstorey* cover were assessed at 20 points within the two plots. These percentage covers were summed and the mean was computed. *Shrub*, *Grass* and *Ground species* cover were recorded as presence or absence at 100 points within the two plots. They were converted into percent cover calculating as the total number of presence divided by the total number of points measured (Gibbons et al., 2004). *Logs* are computed as a total length and total volume in the two plots. *Crown closure* was ranked according to the recorded classes; dense, mid-dense, sparse, very sparse and isolated. Mean ranking was calculated for the two plots. The rest of the variables were excluded from the comparison due to lack of equivalent categories in the FCS.

7.3.3 Results

Field-based *Overstorey* showed positive, but not strong correlation with LiDAR derived *CC* ($R^2 = 0.29$, $P < 0.05$) and moderate correlation with V_H ($R^2 = 0.42$, $P < 0.05$). This is shown in Fig. 7-7(a) and (b) respectively. Field-based *Midstorey* (Fig. 7-7(c)) did not

Table 7-2 Assessment variables and methods for the fieldwork in February 2007. The methodology follows the BioMetric vegetation condition assessment methods (Gibbons et al., 2004).

Variable	Sampling unit	Assessment method
Native species richness	20m x 20m quadrat	Record the number of species found in each of the five listed life-forms (canopy, mid-storey, shrubs, grasses and ground species). Note the dominant canopy species across the site and any other dominant species.
Stumps and dead trees	20m x 50m plot	Record the number of dead trees and stumps within the plot area.
Hollow-bearing trees	20m x 50m plot	Record the number of trees present with at least one hollow. Hollows must be at least 5cm in diameter, have visible depth and be at least 1m above the ground.
Crown closure	20m x 50m plot	The general level of tree crown closure across the plot area is recorded using defined classes; dense (tree crowns touching to overlapping), mid-dense (tree crowns touching to slightly separated), sparse (tree crowns clearly separated), very sparse (tree crowns well separated) and isolated (tree crowns >100m apart).
Tree diameter classes	20m x 50m plot	Record the number of tree stems present within given dbh classes. Classes used in this project are: <5cm, 5-20cm, 20-40cm, 40-60cm, 60-80cm >80cm. If a tree has multiple stems, measure the largest stem.
Regeneration	20m x 50m plot	Regeneration is measured as the percentage of canopy species present at the site that are regenerating. Regeneration is taken as tree stems with a diameter <5cm.
Logs	20m x 50m plot	Record the length and diameter of logs within the plot area. Logs must have a diameter greater than 10cm and be at least 50cm long. Only those parts of the log lying within the plot are measured.
Overstorey cover	50m transect	Estimate percent cover at 10 intervals (every 5m) along the transect. Canopy cover and health and mid-storey cover can be estimated using the visual guides provided. The average percent cover is then calculated from these point assessments.
Overstorey health	50m transect	
Midstorey cover	50m transect	
Shrub cover	50m transect	At 50 points (every 1m) along the transect, record the presence or absence of each life-form. Percent cover is the calculated as the total number of present divided by the total number of points measured.
Grass cover	50m transect	
Ground species cover	50m transect	
Exotic species cover	50m transect	
Organic litter cover	50m transect	
Exposed rock	50m transect	
Bare ground	50m transect	

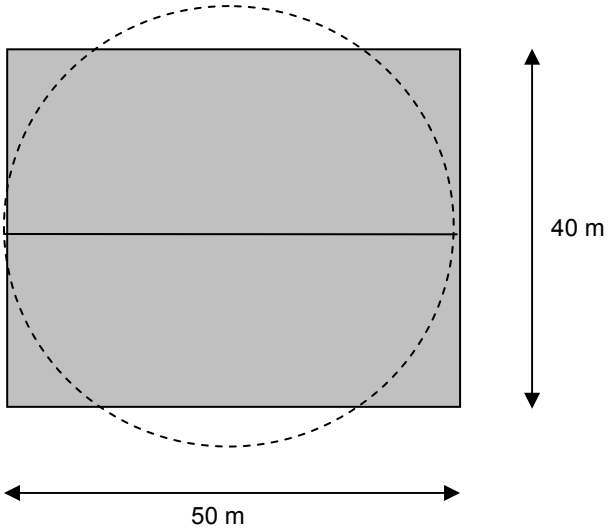

Figure 7-6 Two 20 m × 50 m field plots (grey area) and a 0.2 ha LiDAR plot (dashed circle).

exhibit strong correlation with LiDAR V_M ($R^2 = 0.21$, $P < 0.05$). Field-based *Shrub* was moderately correlated with LiDAR derived V_L ($R^2 = 0.42$, $P < 0.05$). This is displayed in Fig. 7-7(d). As shown in Fig. 7-7(e) and (f), field-based *Grass* and *Ground species* were not correlated with LiDAR derived V_L ($R^2 = 0.26$ and $R^2 = 0.22$ respectively, $P < 0.05$). Field-based *Crown closure* did not exhibit correlation with LiDAR derived *CC* (Table 7-3).

Table 7-4 displayed correlation between field-based total length of *Logs* and all of FCS categories. None of the correlations was significant between these variables. Field-based total volume of *Logs* was also not significantly correlated with any of the FCS categories (Table 7-5).

Table 7-3 Correlation between field-based *Crown Closure* and LiDAR derived *CC*.

			LiDAR *CC*
Spearman's rho	*Crown closure*	Correlation Coefficient	0.225

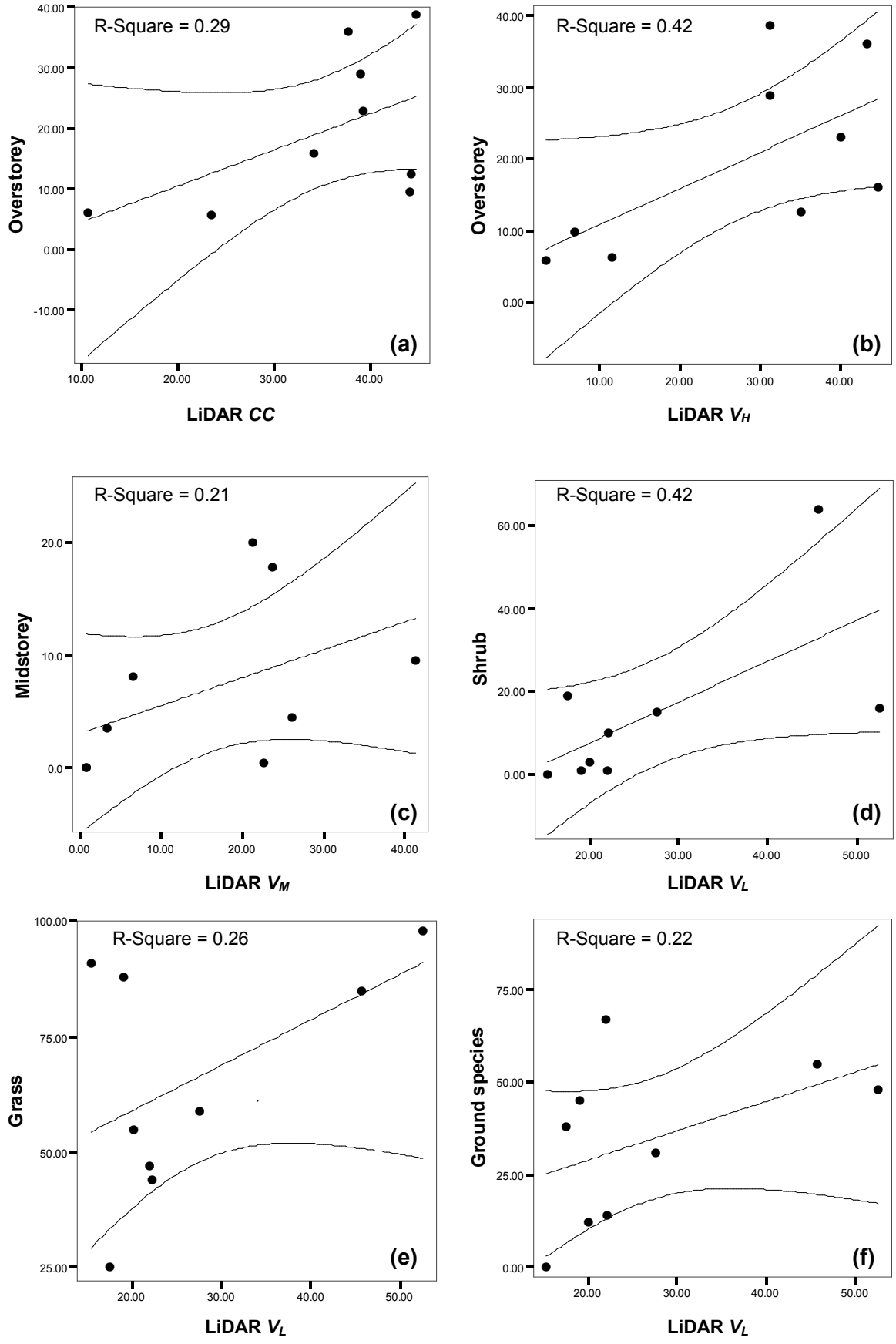

Figure 7-7 Linear regression results between LiDAR derived FCS and field variables (percentage cover) with 95% mean prediction interval.

Table 7-4 Correlation between field-based total length of *Logs* and LiDAR derived forest characterisation scheme categories.

		LiDAR O_G	LiDAR O_L	LiDAR V_L	LiDAR CC	LiDAR O_M	LiDAR V_M	LiDAR V_H	LiDAR D_H
Total length of *Logs*	Pearson Correlation	-0.440	-0.489	-0.422	0.539	0.313	0.288	0.177	0.145

Table 7-5 Correlation between field-based total volume of *Logs* and LiDAR derived FCS.

		LiDAR O_G	LiDAR O_L	LiDAR V_L	LiDAR CC	LiDAR O_M	LiDAR V_M	LiDAR V_H	LiDAR D_H
Total volume of *Logs*	Pearson Correlation	-0.190	-0.314	-0.353	0.263	-0.332	-0.273	0.485	0.212

7.3.4 Discussion

None of the field-based variables was significantly correlated with the FCS categories. Considering the strong correlation between the FCS categories and field variables presented in Chapter 5, the weak association in the results could be explained by the field-based biodiversity metric used in this analysis. *Overstorey* measurement showed a moderate correlation with LiDAR derived V_H, but a weak correlation with LiDAR derived *CC* (Fig. 7-7(b) and (a) respectively). In the field methodology of BioMetric Tool (Gibbons et al., 2004), *Overstorey* is defined as the cover of tallest woody stratum above 1 m. The "tallest woody stratum" is site dependant and prone to observer bias. LiDAR derived *CC* measures all projected vegetation coverage above 1.7 m and LiDAR derived V_H estimates the amount of foliage greater than 5 m. Compared to the clear definition of LiDAR derived variables, the field-based variable includes a large amount of uncertainty in what is assessed. It is likely that *Overstorey* measures only a part of what LiDAR derived *CC* and V_H assess. However, it is not possible to quantify this, therefore making comparison difficult. A more quantitative and objective approach is required for the field-based

biodiversity metric.

This would be also true for the comparison between *Midstorey* and LiDAR derived V_M (Fig. 7-7(c)). LiDAR derived V_M estimates the amount of foliage between 1 m and 5 m from the ground. On the other hand, the field-based variable, *Midstorey* measures vegetation cover between overstorey stratum and 1 m in height. Since the overstorey stratum varies, it is hard to identify "below the overstorey stratum" and keep consistency in the measurement.

For *Shrub*, *Grass* and *Ground species*, the definition of vertical stratification is the same as LiDAR derived V_L, which is the vegetation up to 1 m from the ground. Although the field-based variables assess the individual vegetation component separately while LiDAR derived V_L measures all vegetation in the stratum, the computation method in the field-based variables seems more problematic than the difference in assessed vegetation. The percentage cover of *Shrub*, *Grass* and *Ground species* is calculated as the total number of presence divided by the total number of points measured. This conversion of the qualitative data into quantitative data can be quite misleading, because the presence of particular vegetation at assessment points does not necessarily inform how much the particular vegetation covers at that point. It could be easily overestimated. In fact, the sum of *Shrub*, *Grass* and *Ground species* cover exceeds 100 % in some sites. The comparison based on this calculation may not be reliable.

Crown closure represents the degree of tree crowns interlocking/separation in a plot. It assesses the same element with LiDAR derived *CC*, which is horizontal projected coverage of canopy. However, the correlation between them was quite weak or absent (Table 7-3). *Crown closure* was assessed on a plot basis. One can imagine that the canopy is overlapping each other in some areas as well as being separated in other areas within a plot.

Selecting only one class out of five *Crown closure* classes for a plot is very subjective. It could be misinterpreted.

Neither the total length nor volume of *Logs* displayed significant correlation with LiDAR derived FCS categories as the total volume of CWD showed in Chapter 5. The reason of the weak association is difficult to identify.

7.3.5 Summary of applicability of LiDAR based forest characterisation scheme for field-based biodiversity metrics

In conclusion, LiDAR based FCS was not compatible with commonly used field-based biodiversity metrics. As discussed above, the main reason is considered to be that the field-based biodiversity metrics utilised in this study were assessed in more qualitative and subjective way compared to LiDAR derived quantitative and objective measurements. The field-based biodiversity metrics include important qualitative assessments such as *Native species richness*, *Hollow-bearing trees* and *Regeneration*, which are variables LiDAR derived FCS is not capable of measurement. However, refinement in field methodology would be necessary for measuring structural variables to maximise the utility of LiDAR derived FCS in their metrics. Quantitative ground-based measurements, using equipment such as laser rangefinders and the LAI2000 Plant Canopy Analyser, are highly complementary to LiDAR assessments (Section 4.4 and Chapter 5). It is recommended to incorporate their use into the condition monitoring systems themselves.

7.4 Conclusion

LiDAR sensors are evolving quickly, existing sensors are upgraded frequently and the number of available datasets is increasing rapidly. Analysis of multi-temporal LiDAR datasets is particularly important when the datasets are acquired with different sensors or the same sensor with different sensor configurations. This is since these differences may affect point cloud configurations and attributes derived from forested landscapes. In Section 7.2, the applicability and robustness of a LiDAR based FCS was examined using datasets acquired with different sensor specifications. As a result of this multiple dataset comparison, it is concluded the FCS Category 1 (opening above the ground; O_G), Category 4 (canopy cover; *CC*), Category 5 (opening above medium vegetation; O_M), Category 6 (presence of mid-storey vegetation; V_M) and Category 8 (presence of high trees; V_H) were robust and resilient to the LiDAR data acquired under different specifications. Category 2 (opening above low vegetation; O_L), Category 3 (presence of understorey vegetation; V_L) and Category 7 (vertically dense canopy of high trees; D_H) were found somewhat susceptible to changes in sensor configurations, especially variations in the pulse repetition frequency. It is reported that the increased pulse repetition frequency causes a reduction in energy per emitted laser pulse, resulting in a smaller portion of multiple returns (Næsset, 2009). To maintain a good performance for all categories of the forest characterisation, obtaining sufficient multiple returns by setting an appropriate pulse repetition frequency is the key.

Traditional vegetation assessment methods require costly fieldwork and are often laborious, therefore an efficient and cost-effective assessment tool to compliment these surveys would be ideal. The proposed FCS aimed to quantitatively measure surrogates of biodiversity and variables widely utilised in vegetation monitoring systems in Australia.

The analysis of compatibility, of this LiDAR derived scheme, with commonly used field-based biodiversity metrics suggested that LiDAR based FCS was not compatible with commonly used field-based biodiversity metrics due to the qualitative and subjective survey methods of these field-based metrics. Refinement in field methodology would be necessary for measuring structural variables to maximise the utility of LiDAR derived FCS in their metrics. Quantitative ground-based measurements, using equipment such as laser rangefinders and the LAI2000 Plant Canopy Analyser, are highly complementary to LiDAR assessments. It is recommended to incorporate their use into the condition monitoring systems themselves. It would be then relatively simple to modify field-based biodiversity metrics, such as 'Habitat Hectares' (Parks et al., 2003) in Victoria, the 'Biometric' tool (Gibbons et al., 2004) in New South Wales and TASVEG VCA (Michaels, 2006) in Tasmania, to include a LiDAR derived total sample of woody/vegetation structural variables, given that suitable LiDAR datasets exist or are planned in all of these states in Australia. The field-based biodiversity metrics include important qualitative assessments such as *Native species richness*, *Hollow-bearing trees* and *Regeneration* in 'Biometric' tool (Gibbons et al., 2004), which are variables LiDAR derived FCS is not capable of measurement. Field survey would still be required. However, the combination of the LiDAR derived FCS and field-based biodiversity metrics could minimise costly fieldwork saving laborious process, and allow efficient, quantitative total sampling assessment with high-spatial coverage in these vegetation condition monitoring systems.

CHAPTER 8 THE UTILITY OF LIDAR FOR LANDSCAPE BIODIVERSITY ASSESSMENT

8.1 Introduction

This thesis investigated the potential of Light Detection and Ranging (LiDAR) to inform landscape biodiversity assessments. The objective of this research was to develop a robust, quantifiable and repeatable method able to measure a surrogate of biodiversity. In particular, the ability of LiDAR technology to recover forest structure information was examined. In this chapter, research questions are restated and discussed. The results and findings presented in this thesis are comprehensively evaluated. The utility of LiDAR for landscape biodiversity assessments is assessed as well as a future research agenda set. Accordingly, the following research questions were posed.

1. What, if any, forest structure information can be extracted from data produced by a LiDAR discrete return system?

2. Does a LiDAR full waveform system provide additional or higher quality forest structure information?

3. Can LiDAR intensity values be used to recover forest structure information?

4. Can the utility of LiDAR compliment traditional ecological survey methods?

In order to address these questions, experiments using LiDAR discrete return (Chapter 3) and full waveform systems (Chapter 5, 6, and 7) were conducted following a

comprehensive literature review (Chapter 2). The background and a new fieldwork protocol for the full waveform system experiments were also described (Chapter 4). An eight category forest characterisation scheme (FCS) derived from a LiDAR full waveform system was proposed and validated using field derived variables (Chapter 5). Intensity variables derived from LiDAR full waveform were explored to determine their utility (Chapter 6). The applicability of the proposed scheme was also examined by comparing two independent LiDAR full waveform datasets of the same area and by comparing the LiDAR derived FCS to commonly used field-based biodiversity metrics (Chapter 7).

8.2 What, if any, forest structure information can be extracted from data produced by a LiDAR discrete return system?

Conventional LiDAR discrete (first and last) return systems are the most commonly deployed airborne laser scanning systems and are widely available to natural resource managers. In this thesis, a conventional discrete return system was examined to determine whether forest structure information can be extracted from the data (Chapter 3). As a result of the LiDAR discrete return system experiment, it was concluded that conventional discrete return systems can be used to recover forest structure information for forests with an ecologically simple structure (i.e. single tree species with no mid- and understorey vegetation except grass and relatively flat terrain). If the study site includes structurally complex forests, it would be better options to use the latest discrete (multiple) return systems or full waveform systems.

LiDAR intensity, vertically stratified using range information, has potential to recover canopy cover, grass cover and the amount of fallen trees. The combination of LiDAR

intensity mean and standard deviation can be used to differentiate forest structural types in this study area; sparse canopy with few fallen trees or dense canopy with many fallen trees. Utilising standard deviation of intensity as a variable could be one solution in using intensity data since it avoids the intensity calibration issues. It was noted that first returns are better variables for a conventional discrete (first and last) return system analysis, since last returns were affected by the amount of remaining energy in the pulse and did not show significant correlation with field variables as the first returns displayed. In terms of data preparation, it is recommended that LiDAR point data should be accompanied by information regarding its return properties such as singular returns or first of many returns since this information could have the impact on the results.

8.3 Does a LiDAR full waveform system provide additional or higher quality forest structure information?

An eight category forest characterisation scheme (FCS) was created using pulse return types and range information from a full waveform LiDAR (Chapter 5). The proposed FCS successfully showed the potential to quantitatively measure surrogates of biodiversity. This method allows for quantification of the vertical gap structure (i.e. gaps above bare ground, low vegetation and medium vegetation), canopy cover and its vertical density as well as the presence of various canopy strata (low, medium and high). Regression analysis showed all LiDAR derived variables were good predictors of field recorded variables (e.g. R^2 = 0.86, $P < 0.05$ between LiDAR derived canopy cover and field derived canopy cover) across a range of forest structural types. The proposed scheme demonstrated the potential of different laser pulse return properties from a full waveform LiDAR to provide

information on the complexity of habitat structure in an efficient and cost-effective manner.

The FCS was further evaluated using an independently acquired full waveform LiDAR dataset of the same area with a slightly different system specification (Section 7.2). Analysis of multi-temporal LiDAR datasets is particularly important when the datasets are acquired with different sensors or the same sensor with different sensor configurations. This is since these differences may affect point cloud configurations and attributes derived from forested landscapes. As a result of this multiple dataset comparison, it was concluded the FCS Category 1 (opening above the ground; O_G), Category 4 (canopy cover; CC), Category 5 (opening above medium vegetation; O_M), Category 6 (presence of mid-storey vegetation; V_M) and Category 7 (presence of high trees; V_H) were robust and resilient to the LiDAR data acquired under different specifications. Category 2 (opening above low vegetation; O_L), Category 3 (presence of understorey vegetation; V_L) and Category 8 (vertically dense canopy of high trees; D_H) were found somewhat susceptible to changes in sensor configurations, especially variations in the pulse repetition frequency. To maintain a good performance for all categories of the forest characterisation, obtaining sufficient multiple returns by setting an appropriate pulse repetition frequency is the key.

8.4 Can LiDAR intensity values be used to recover forest structure information?

The utility of LiDAR intensity to provide forest structure information was examined in the two experiments. First experiment using a LiDAR discrete return system showed the potential of intensity (mean and standard deviation) variables to recover forest structure

information for forests with an ecologically simple structure as described in Chapter 3.

The second experiment using a LiDAR full waveform system over structurally more complex forests (Chapter 6) suggested that the standard deviation of Type 1 intensity in the ground and the low vegetation strata have the potential to recover LAI/cover for low vegetation and canopy cover. Similarly, standard deviation of Type 1 intensity in the high canopy stratum displayed the potential to recover CWD amount, mean tree height and canopy depth in the high canopy stratum. The standard deviation of intensity seems to be a useful variable in the full waveform system experiment as well as in the discrete return system experiment. However, many of the other significant correlations found between intensity variables and field variables defy physical explanation at this time. It was noted that the analysis using intensity variables could be site specific and therefore not generally applicable. The algorithm of the LiDAR discrete return system experiment to use the combination of mean and standard deviation of first return intensity from the ground for forest structural type classification did not show the same classification results in this analysis. The intensity version of FCS clearly showed the potential of recovering field variables. Although the results were encouraging, in terms of reporting new structural information content, it would have to be concluded that little new information can be recovered using this technique. It did not enhance the ability of the original FCS. As such, this author can not recommend complicating the FCS method to incorporate intensity at this stage. It was noted that the selection of a sensor with an appropriate wavelength for the study would be critical to use the intensity information. Further investigation of intensity version of FCS is required to account for the utility of intensity variables.

8.5 Can the utility of LiDAR compliment traditional ecological survey methods?

The utility of LiDAR can compliment traditional ecological survey methods. Traditional vegetation assessment methods require costly fieldwork and are often laborious and logistically difficult, therefore an efficient and cost-effective assessment tool to compliment these surveys would be ideal. The proposed FCS has the potential to quantitatively measure surrogates of biodiversity and variables widely utilised in vegetation condition monitoring systems such as 'Habitat Hectares' (Parks et al., 2003) in Victoria, the 'Biometric' tool (Gibbons et al., 2004) in New South Wales and TASVEG VCA (Michaels, 2006) in Tasmania, Australia, in an efficient and cost-effective manner.

However, an analysis of compatibility of this LiDAR derived scheme with commonly used field-based biodiversity metrics (Section 7.3) suggested that LiDAR based FCS was not compatible with commonly used field-based biodiversity metrics due to qualitative and subjective survey methods of these field-based metrics. Therefore, refinement in field methodology would be necessary for measuring structural variables to maximise the utility of LiDAR derived FCS in their metrics. Quantitative and objective ground-based measurements are required. For example, the fieldwork protocols developed in this thesis used equipment such as laser rangefinders and the LAI2000 Plant Canopy Analyser, and found that they were highly complementary to LiDAR assessments. It is recommended to incorporate their use into the condition monitoring systems themselves. It would be then relatively simple to modify the above mentioned field-based biodiversity metrics to include a LiDAR derived total sample of woody/vegetation structural variables, given that suitable LiDAR datasets exist or are planned in all of these states in Australia. The field-based biodiversity metrics include important qualitative assessments such as *Native species*

richness, *Hollow-bearing trees* and *Regeneration* in 'Biometric' tool (Gibbons et al., 2004), which are variables LiDAR derived FCS is not capable of measurement. Field survey would still be required. However, the combination of the LiDAR derived FCS and field-based biodiversity metrics could minimise costly fieldwork saving laborious process, and allow efficient, quantitative total sampling assessment with high-spatial coverage in these vegetation condition monitoring systems.

8.6 Future research

This study demonstrated how LiDAR technology (conventional discrete return system and full waveform systems) can be used to derive forest structure information for landscape biodiversity assessment. The method proposed in this study is versatile, repeatable and quantitative, which can provide useful information to inform decisions and conservation strategies. There are several other areas which could further extend this work.

The FCS is 'tunable' to any designed 3D ecological characterisation scheme. It is anticipated that the FCS may have wide applicability in characterising forest structure over different forested landscape. Current restrictions on separating vertical vegetation strata include the minimum vertical resolution of the LiDAR data (i.e. the minimum pulse interaction gap between two adjacent interactions), which was approximately 50 cm in our dataset. It was not sensible to define a forest vertical stratification with classes less than 50 cm in this study. However, this could be improved by using different data processing methods. The minimum vertical resolution of the LiDAR full waveform data depends on decomposition methods of points from the waveform rather than the sensor setting. It is possible to achieve better than 30 cm of the minimum vertical resolution with improved

decomposition methods (Eichstaedt, pers. comm.). The robustness of FCS could be further tested. More applications of the intensity version of FCS are also required to determine the utility of LiDAR intensity.

The data synthesis approach may be another topic to explore. LiDAR data contains information on height of the illuminated objects, which has been primarily utilized in constructing 3D models. On the other hand, high-resolution satellite or airborne optical sensor data has spectral information which has been mainly used for classification. If both data sources are merged and used for characterising the object, it would extend application potential greatly.

The proposed FCS in this thesis showed the potential to provide information on the complexity of habitat structure. This 3D information could be used to develop habitat suitability models for the species living in the environment where closed canopy exists, i.e. optical sensors cannot provide information underneath the canopy, or where ground-based survey is logistically difficult. For example, eastern barred bandicoot (*Perameles gunni*) in Tasmania is a species facing a high risk of extinction in the medium term future, as listed in the Environment Protection and Biodiversity Conservation Act 1999 (Australian Government, 1999) in Australia. This small marsupial mainly lived in the native grasslands and grassy woodlands of the Midlands in Tasmania, however these habitats were already cleared for agriculture and grazing (Department of Primary Industries and Water Government of Tasmania, 2009). Identifying their suitable habitat and implementing a conservation strategy is critical. The proposed FCS could provide information on their key habitat, presence and amount of understorey vegetation even in woodlands and forests, in an efficient and cost-effective manner and would help in identifying conservation priorities. The FCS would present wide applicability in ecological research and could provide a rich

contribution to biodiversity assessments.

This thesis has provided a robust, versatile, and repeatable methodology to quantitatively measure a surrogate of biodiversity, i.e. forest structure information, in natural forests using LiDAR technology. The practical utility of conventional LiDAR discrete return systems and the potential of the latest LiDAR full waveform systems to recover forest structure information have been both presented with current limitations and possible future work. The potential of LiDAR technology to compliment traditional vegetation survey methods has also been discussed with suggestions. It is hoped that the information provided from this thesis will help in forming conservation strategies and contribute to maintaining biodiversity in our world.

REFERENCES

Ackermann, F., 1999. Airborne laser scanning--present status and future expectations. ISPRS Journal of Photogrammetry and Remote Sensing, 54(2-3): 64-67.

Ahern, L. et al., 2003. Biodiversity Action Planning landscape Plans for the Boulburn Broken CMA, Sheppartion Irrigation Region - North Zones, Department of Sustainability and Environment, Victoria, Goulburn Broken Catchment Management Authority.

Airborne Laser Survey Working Group, 2004. Handbook of Airborne Laser Survey. Association of Precise Survey & Applied Technology, Tokyo.

Anderson, J. et al., 2006. The use of waveform lidar to measure northern temperate mixed conifer and deciduous forest structure in New Hampshire. Remote Sensing of Environment, 105(3): 248-261.

Anderson, J.E. et al., 2008. Integrating waveform lidar with hyperspectral imagery for inventory of a northern temperate forest. Remote Sensing of Environment, 112(4): 1856-1870.

Angel, E., 2003. Interactive Computer Graphics A Top-Down Approach with OpenGL. Addison Wesley, NY, 559-593 pp.

Australian Government, 1999. Environment Protection and Biodiversity Conservation Act 1999. Office of Legislative Drafting and Publishing, Attorney General's Department, Canberra

Axelsson, P., 1999. Processing of laser scanner data--algorithms and applications. ISPRS Journal of Photogrammetry and Remote Sensing, 54(2-3): 138-147.

Bacon, P.E., Stone, C., Binns, D.L., Edwards, D.E. and Leslie, D.J., 1993. Inception Report on Development of Watering Strategies to Maintain the Millewa Group of River Red Gum (Eucalyptus camaldulensis), Research Division, Forestry Commission of New South Wales, Sydney.

Baltsavias, E.P., 1999. Airborne laser scanning: basic relations and formulas. ISPRS Journal of Photogrammetry and Remote Sensing, 54(2-3): 199-214.

Bauer, M.E., Daughtry, C.S.T., Biehl, L.L., Kanemasu, E.T. and Hall, F.G., 1986. Field Spectroscopy of Agricultural Crops. Geoscience and Remote Sensing, IEEE Transactions on, GE-24(1): 65-75.

Bourgeron, P.S., 1983. 3. Spatial aspects of vegetation structure. In: F.B. Golley (Editor), Tropical rain forest ecosystems: Structure and function. Ecosystems of the World 14A. Elsevier Scientific Publishing Company, New York.

Bradbury, R.B. et al., 2005. Modelling relationships between birds and vegetation structure using airborne LiDAR data: a review with case studies from agricultural and woodland environments. Ibis, 147(3): 443-452.

Brandtberg, T., 2007. Classifying individual tree species under leaf-off and leaf-on conditions using airborne lidar. ISPRS Journal of Photogrammetry and Remote Sensing, 61(5): 325-340.

Brandtberg, T., Warner, T.A., Landenberger, R.E. and McGraw, J.B., 2003. Detection and analysis of individual leaf-off tree crowns in small footprint, high sampling density lidar data from the eastern deciduous forest in North America. Remote Sensing of Environment, 85(3): 290-303.

Brunig, E.F., 1983. 4. Vegetation structure and growth. In: F.B. Golley (Editor), Tropical rain forest ecosystems: Structure and function. Ecosystems of the World 14A. Elsevier Scientific Publishing Company, New York.

Cain, S.A., Castro, G.M.d.O., Pires, J.M. and Silva, N.T.d., 1956. Application of some phytosociological techniques to Brazilian rain forest. American Journal of Botany, 43(10).

Canadian Council of Forest Ministers, 2003. Defining Sustainable Forest Management in Canada: Criteria and indicators 2003. Canadian Forest Service, Natural Resources Canada, Ontario.

Catling, P.C. and Burt, R.J., 1995. Studies of the Ground-Dwelling Mammals of Eucalypt Forests in South-Eastern New South Wales: the Effect of Habitat Variables on Distribution and Abundance. Wildlife Research, 22(3): 271-288.

Chasmer, L., Hopkinson, C., Smith, B. and Treitz, P., 2006. Examining the influence of changing laser pulse repetition frequencies on conifer forest canopy returns. Photogrammetric Engineering and Remote Sensing, 72(12): 1359-1367.

Chen, J.M. and Black, T.A., 1992. Defining leaf-area index for non-flat leaves. Plant Cell and Environment, 15: 421-429.

Chong, J., 2003. Analysis and Management of Unseasonal Surplus Flows in the Barmah-Millewa Forest. Technical report 03/2, Cooperarive Research Center for Catchment Hydrology.

Coops, N. et al., 2007. Estimating canopy structure of Douglas-fir forest stands from discrete-return LiDAR. Trees - Structure and Function, 21(3): 295-310.

Curran, P.J., 1985. Principles of Remote Sensing. Longman, England.

Danson, F.M., Morsdorf, F. and Koetz, B., 2009. 13 Airborne and Terrestrial Laser Scanning for Measuring Vegetation Canopy Structure. In: G.L. Heritage and A.R.G. Large (Editors), Laser scanning for the environmental sciences. Wiley-Blackwell, Chichester.

Davis, S.M. et al., 1978. Remote sensing: the quantitative approach. McGraw-Hill International Book Co., New York, 405 pp.

Davis, T.A.W. and Richards, P.W., 1933. The vegetation of Morabelli Creek, British Guiana. An ecological study of a limited area of tropical rain forest. I. Journal of Ecology, 21: 350-384.

de Wasseige, C. and Defourny, P., 2002. Retrieval of tropical forest structure characteristics from bi-directional reflectance of SPOT images. Remote Sensing of Environment, 83(3): 362-375.

Department of Primary Industries and Water Government of Tasmania, 2009. Eastern Barred Bandicoot, Native Plants & Animals Tasmania.

Department of Sustainability and Environment, 2004. Vegetation Quality Assessment Manual–Guidelines for applying the habitat hectares scoring method. Version 1.3, Victorian Government Department of Sustainability and Environment, Melbourne.

Devereux, B. and Amable, G., 2009. 4 Airborne LiDAR: Instrumentation, Data Acquisition and Handling. In: A.R.G. Large and G.L. Heritage (Editors), Laser scanning for the environmental sciences. Wiley-Blackwell, Chichester.

Einaudi, F., Schwemmer, G.K., Gentry, B.M. and Abshire, J.B., 2004. LIDAR Past, Present, and Future in Nasa's Earth and Space Science Programs In: G. Pappalardo and A. Amodeo (Editors), 22nd Internation Laser Radar Conference (ILRC 2004). European Space Agency, Matera, Italy, pp. 7.

Eyre, T.J., Kelly, A.L. and Neldner, V.J., 2006. BioCondition: A Terrestrial Vegetation Condition Assessment Tool for Biodiversity in Queensland. Field Assessment Manual. Version 1.5, Environmental Protection Agency, Biodiversity Sciences Unit, Brisbane.

Falkowski, M.J., Evans, J.S., Martinuzzi, S., Gessler, P.E. and Hudak, A.T., 2009. Characterizing forest succession with lidar data: An evaluation for the Inland Northwest, USA. Remote Sensing of Environment, 113(5): 946-956.
Flood, M. and Gutelius, B., 1997. Commercial Implications of Topographic Terrain Mapping Using Scanning Airborne Laser Radar. Photogrammetric Engineering & Remote Sensing, 63: 327-366.
Florence, R.G., 1996. Ecology and silviculture of eucalypt forests. CSIRO Publishing, Collingwood, 413 pp.
Franklin, J.F. et al., 1981. Ecological Characteristics of Old-Growth Douglas-Fir Forests. General Technical Report PNW-118, USDA Forest Service, Portland.
Freudenberger, D., 1999. Guidelines for Enhancing Grassy Woodlands for the Vegetaion Investment Project. A report commissioned by Greening Australia ACT & SE NSW Inc, CSIRO Wildlife Ecology, Canberra, ACT.
Gemmell, F. and Varjo, J., 1999. Utility of Reflectance Model Inversion Versus Two Spectral Indices for Estimating Biophysical Characteristics in a Boreal Forest Test Site. Remote Sensing of Environment, 68(2): 95-111.
Gibbons, I., Ayers, D., Seddon, J., Doyle, S. and Briggs, S., 2004. BioMetric Decision Support Tool Version 1.4. Biodiversity Assessment Tool To Support the NSW Property Vegetation Plan Developer, NSW Department of Environment and Conservation, Camberra.
Goetz, S., Steinberg, D., Dubayah, R. and Blair, B., 2007. Laser remote sensing of canopy habitat heterogeneity as a predictor of bird species richness in an eastern temperate forest, USA. Remote Sensing of Environment, 108(3): 254-263.
Goodwin, N.R., Coops, N.C. and Culvenor, D.S., 2006. Assessment of forest structure with airborne LiDAR and the effects of platform altitude. Remote Sensing of Environment, 103(2): 140-152.
Goodwin, N.R., Coops, N.C. and Culvenor, D.S., 2007. Development of a simulation model to predict LiDAR interception in forested environments. Remote Sensing of Environment, 111(4): 481-492.
Gordon, W.F., Baker, H.G. and Opler, P.A., 1974. Comparative Phenological Studies of Trees in Tropical Wet and Dry Forests in the Lowlands of Costa Rica. The Journal of Ecology, 62(3): 881-919.
Gower, S.T., Kucharik, C.J. and Norman, J.M., 1999. Direct and indirect estimation of leaf area index, f_{APAR}, and net primary production of terrestrial ecosystems. Remote Sensing of Environment, 70: 29-51.
Grubb, P.J., Lloyd, J.R., Pennington, T.D. and Whitmore, T.C., 1963. A Comparison of Montane and Lowland Rain Forest in Ecuador I. The Forest Structure, Physiognomy, and Floristics. The Journal of Ecology, 51(3): 567-601.
Gutiérrez, A.G. et al., 2009. Structural and environmental characterization of old-growth temperate rainforests of northern Chiloé Island, Chile: Regional and global relevance. Forest Ecology and Management, 258(4): 376-388.
Hallé, F., Oldeman, R.A.A. and Tomlinson, P.B., 1978. Tropical Trees and Forests. An Architectural Analysis. Springer-Verlag, Berlin.
Harding, D., 2009. 5. Pulsed Laser Altimeter Ranging Techniques and Implications for Terrain Mapping. In: J. Shan and C.K. Toth (Editors), Topographic Laser Ranging And Scanning: principles and processing. CRC Press, Boca Raton, pp. 173-194.
Harding, D.J., Lefsky, M.A., Parker, G.G. and Blair, J.B., 2001. Laser altimeter canopy height profiles: methods and validation for closed-canopy, broadleaf forests. Remote Sensing of Environment, 76(3): 283-297.

Harris, I. and Rawson, R., 1992. Management Plan for Barmah State Park and Barmah State Forest, Department of Conservation and Environment, Australia.
Harris, S. and Kitchener, A., 2005. From Forest to Fjaeldmark: Descriptions of Tasmania's Vegetation. Department of Primary Industries, Water and Environment, Printing Authority of Tasmania, Hobart.
Heritage, G.L. and Large, A.R.G., 2009. 2 Principles of 3D Laser Scanning. In: A.R.G. Large and G.L. Heritage (Editors), Laser scanning for the environmental sciences. Wiley-Blackwell, Chichester.
Hill, R.A. and Thomson, A.G., 2005. Mapping woodland species composition and structure using airborne spectral and LiDAR data. International Journal of Remote Sensing, 26(17): 3763 - 3779.
Hinsley, S.A., Hill, R.A., Gaveau, D.L.A. and Bellamy, P.E., 2002. Quantifying woodland structure and habitat quality for birds using airborne laser scanning. Functional Ecology, 16(6): 851-857.
Hirata, Y., Furuya, N., Suzuki, M. and Yamamoto, H., 2009. Airborne laser scanning in forest management: Individual tree identification and laser pulse penetration in a stand with different levels of thinning. Forest Ecology and Management, 258(5): 752-760.
Holdridge, L.R., 1970. A system for representing structure in tropical forest associations. In: H.T. Odum and R.F. Pigeon (Editors), A Tropical Rainforest. A Study of Irradiation and Ecology at El Verde, Puerto Rico. US Atomic Energy Commission, Washington, D. C.
Holmgren, J., Nilsson, M. and Olsson, H., 2003. Simulating the effects of lidar scanning angle for estimation of mean tree height and canopy closure. Canadian Journal of Remote Sensing, 29(5): 623-632.
Holmgren, J. and Persson, A., 2004. Identifying species of individual trees using airborne laser scanner. Remote Sensing of Environment, 90(4): 415-423.
Holmgren, J., Persson, Ã. and Söderman, U., 2008. Species identification of individual trees by combining high resolution LiDAR data with multi-spectral images. International Journal of Remote Sensing, 29(5): 1537 - 1552.
Hopkinson, C. and Chasmer, L., 2007. Using Discrete Laser Pulse Return Intensity to Model Canopy Transmittance. The Photogrammetric Journal of Finland, 20(2).
Hopkinson, C. and Chasmer, L., 2009. Testing LiDAR models of fractional cover across multiple forest ecozones. Remote Sensing of Environment, 113(1): 275-288.
Hopkinson, C., Chasmer, L. and Hall, R.J., 2008. The uncertainty in conifer plantation growth prediction from multi-temporal lidar datasets. Remote Sensing of Environment, 112(3): 1168-1180.
Hyde, P. et al., 2005. Mapping forest structure for wildlife habitat analysis using waveform lidar: Validation of montane ecosystems. Remote Sensing of Environment, 96(3-4): 427-437.
HyyppÃ, J. et al., 2008. Review of methods of small-footprint airborne laser scanning for extracting forest inventory data in boreal forests. International Journal of Remote Sensing, 29(5): 1339 - 1366.
HyyppÃ, J. et al., 2009. 12. Forest Inventory Using Small-Footprint Airborne LiDAR. In: J. Shan and C.K. Toth (Editors), Topographic Laser Ranging And Scanning: principles and processing. CRC Press, Boca Raton.
Intergovernmental Panel on Climate Change, 2003. Good Practice Guidance for Land Use, Land-Use Change and Forestry, UNEP. In: J. Penman et al. (Editors). WMO, Institute for Global Environmental Strategies (IGES) for the IPCC

Irish, J.L. and Lillycrop, W.J., 1999. Scanning laser mapping of the coastal zone: the SHOALS system. ISPRS Journal of Photogrammetry and Remote Sensing, 54(2-3): 123-129.
Jonsson, M.T. and Jonsson, B.G., 2007. Assessing coarse woody debris in Swedish woodland key habitats: Implications for conservation and management. Forest Ecology and Management, 242(2-3): 363-373.
Jorgensen, E.E., 2002. Small mammals: consequences of stochastic data variation for modeling indicators of habitat suitability for a well-studied resource. Ecological Indicators, 1(4): 313-321.
Jupp, D.L.B. and Walker, J., 1997. Detecting structural and growth changes in woodlands and forests: the challenge for remote sensing and the role of geometric-optical modeling. In: H.L. Gholz, K. Nakane and H. Shimoda (Editors), The use of remote sensing in the modeling of forest productivity. Kluwer Academic Publishing, Dordrecht, pp. 75-108.
Kato, A. et al., 2009. Capturing tree crown formation through implicit surface reconstruction using airborne lidar data. Remote Sensing of Environment, 113(6): 1148-1162.
Kim, Y. et al., 2009. Distinguishing between live and dead standing tree biomass on the North Rim of Grand Canyon National Park, USA using small-footprint lidar data. Remote Sensing of Environment, 113(11): 2499-2510.
Klinge, H., 1973. Struktur und Artenreichtum des Zentral-amazonischen Regenwaldes. Amazoniana, 4(3): 283-292.
Klinge, H., Rodrigues, W.A., Brunig, E. and Fittakau, E.J., 1975. Biomass and Structure in a Central Amazonian Rain Forest. Springer-Verlag, New York.
Kraus, K. and Pfeifer, N., 1998. Determination of terrain models in wooded areas with airborne laser scanner data. ISPRS Journal of Photogrammetry and Remote Sensing, 53(4): 193-203.
Lévesque, J. and King, D.J., 1999. Airborne Digital Camera Image Semivariance for Evaluation of Forest Structural Damage at an Acid Mine Site. Remote Sensing of Environment, 68(2): 112-124.
Lamonaca, A., Corona, P. and Barbati, A., 2008. Exploring forest structural complexity by multi-scale segmentation of VHR imagery. Remote Sensing of Environment, 112(6): 2839-2849.
Lamprecht, H., 1969. Über Strukturanalysen im Tropenwald. Beih. Z. Schw. Forestverein, 46: 51-61.
Large, A.R.G. and Heritage, G.L., 2009. 1 Laser Scanning - Evolution of the Discipline. In: A.R.G. Large and G.L. Heritage (Editors), Laser scanning for the environmental sciences. Wiley-Blackwell, Chichester.
Lathrop Jr, R.G. and Pierce, L.L., 1991. Ground-based canopy transmittance and satellite remotely sensed measurements for estimation of coniferous forest canopy structure. Remote Sensing of Environment, 36(3): 179-188.
Lefsky, M.A. et al., 1999a. Lidar Remote Sensing of the Canopy Structure and Biophysical Properties of Douglas-Fir Western Hemlock Forests. Remote Sensing of Environment, 70(3): 339-361.
Lefsky, M.A., Cohen, W.B., Parker, G.G. and Harding, D.J., 2002. Lidar remote sensing for ecosystem studies. Bioscience, 52(1): 19-30.
Lefsky, M.A., Harding, D., Cohen, W.B., Parker, G. and Shugart, H.H., 1999b. Surface Lidar Remote Sensing of Basal Area and Biomass in Deciduous Forests of Eastern Maryland, USA. Remote Sensing of Environment, 67(1): 83-98.

Lefsky, M.A., Hudak, A.T., Cohen, W.B. and Acker, S.A., 2005. Patterns of covariance between forest stand and canopy structure in the Pacific Northwest. Remote Sensing of Environment, 95(4): 517-531.
Liang, S., 2004. Quantitative Remote Sensing of Land Surfaces. John Wiley & Sons, Inc., USA.
Lillesand, T.M., Kiefer, R.W. and Chipman, J.W., 2004. REMOTE SENSING AND IMAGE INTERPRETATION. John Wiley & Sons, Inc.
Longman, K.A. and Jenik, J., 1987. Tropical forest and its environment Tropical ecology series. Longman, London
Müller, J., Moning, C., Bässler, C., Heurich, M. and Brandl, R., 2009. Using airborne laser scanning to model potential abundance and assemblages of forest passerines. Basic and Applied Ecology, 10(7): 671-681.
Mac Nally, R., Parkinson, A., Horrocks, G., Conole, L. and Tzaros, C., 2001. Relationships between terrestrial vertebrate diversity, abundance and availability of coarse woody debris on south-eastern Australian floodplains. Biological Conservation, 99(2): 191-205.
Maltamo, M. et al., 2005. Identifying and quantifying structural characteristics of heterogeneous boreal forests using laser scanner data. Forest Ecology and Management, 216(1-3): 41-50.
Marsden, C. et al., 2009. Relating MODIS vegetation index time-series with structure, light absorption and stem production of fast-growing Eucalyptus plantations. Forest Ecology and Management, 259(9): 1741-1753.
McElhinny, C., 2002. Forest and Woodland Structure as Index of Biodiversity: A review, NSW NPWS.
Means, J.E. et al., 1999. Use of Large-Footprint Scanning Airborne Lidar To Estimate Forest Stand Characteristics in the Western Cascades of Oregon. Remote Sensing of Environment, 67(3): 298-308.
Michaels, K., 2006. A Manual for Assessing Vegetation Condition in Tasmania, *Versiton 1.0.* Resource Management and Conservation, Department of Primary Industries, Water and Environment, Hobart.
Moffiet, T., Mengersen, K., Witte, C., King, R. and Denham, R., 2005. Airborne laser scanning: Exploratory data analysis indicates potential variables for classification of individual trees or forest stands according to species. ISPRS Journal of Photogrammetry and Remote Sensing, 59(5): 289-309.
Morsdorf, F., Frey, O., Meier, E., Itten, K.I. and AllgÃöwer, B., 2008. Assessment of the influence of flying altitude and scan angle on biophysical vegetation products derived from airborne laser scanning. International Journal of Remote Sensing, 29(5): 1387 - 1406.
Morsdorf, F., Kötz, B., Meier, E., Itten, K.I. and Allgöwer, B., 2006. Estimation of LAI and fractional cover from small footprint airborne laser scanning data based on gap fraction. Remote Sensing of Environment, 104(1): 50-61.
Muinonen, E., Maltamo, M., Hyppänen, H. and Vainikainen, V., 2001. Forest stand characteristics estimation using a most similar neighbor approach and image spatial structure information. Remote Sensing of Environment, 78(3): 223-228.
Næsset, E., 1997. Estimating timber volume of forest stands using airborne laser scanner data. Remote Sensing of Environment, 61(2): 246-253.
Næsset, E., 2002. Predicting forest stand characteristics with airborne scanning laser using a practical two-stage procedure and field data. Remote Sensing of Environment, 80(1): 88-99.

Næsset, E., 2004. Effects of different flying altitudes on biophysical stand properties estimated from canopy height and density measured with a small-footprint airborne scanning laser. Remote Sensing of Environment, 91(2): 243-255.
Næsset, E., 2005. Assessing sensor effects and effects of leaf-off and leaf-on canopy conditions on biophysical stand properties derived from small-footprint airborne laser data. Remote Sensing of Environment, 98(2-3): 356-370.
Næsset, E., 2009. Effects of different sensors, flying altitudes, and pulse repetition frequencies on forest canopy metrics and biophysical stand properties derived from small-footprint airborne laser data. Remote Sensing of Environment, 113(1): 148-159.
Næsset, E. and Gobakken, T., 2008. Estimation of above- and below-ground biomass across regions of the boreal forest zone using airborne laser. Remote Sensing of Environment, 112(6): 3079-3090.
Næsset, E. and Nelson, R., 2007. Using airborne laser scanning to monitor tree migration in the boreal-alpine transition zone. Remote Sensing of Environment, 110(3): 357-369.
Nelson, R., Keller, C. and Ratnaswamy, M., 2005. Locating and estimating the extent of Delmarva fox squirrel habitat using an airborne LiDAR profiler. Remote Sensing of Environment, 96(3-4): 292-301.
Nelson, R., Krabill, W. and MacLean, G., 1984. Determining forest canopy characteristics using airborne laser data. Remote Sensing of Environment, 15(3): 201-212.
Nelson, R., Krabill, W. and Tonelli, J., 1988. Estimating forest biomass and volume using airborne laser data. Remote Sensing of Environment, 24(2): 247-267.
Noss, R.F., 1990. Indicators for Monitoring Biodiversity: A Hierarchical Approach. Conservation Biology, 4(4): 355-364.
Oliveira-Filho, A.T.D., Ratter, J.A. and Shepherd, G.J., 1990. Floristic composition and community structure of a central Brazilian gallery forest. Flora, 184: 103-117.
Ørka, H.O., Næsset, E. and Bollandsås, O.M., 2009. Classifying species of individual trees by intensity and structure features derived from airborne laser scanner data. Remote Sensing of Environment, 113(6): 1163-1174.
Packalén, P. and Maltamo, M., 2007. The k-MSN method for the prediction of species-specific stand attributes using airborne laser scanning and aerial photographs. Remote Sensing of Environment, 109(3): 328-341.
Parks, D., Newell, G. and Cheal, D., 2003. Assessing the quality of native vegetation: The 'habitat hectares' approach. Ecological Management & Restration, 4(supplement): s29-s38.
Persson, A., Holmgren, J. and Söderman, U., 2002. Detecting and Measuring Individual Trees Using an Airborne Laser Scanner. Photogrammetric Engineering & Remote Sensing, 68(9): 925-932.
Pesonen, A., Maltamo, M., Eerikäinen, K. and Packalèn, P., 2008. Airborne laser scanning-based prediction of coarse woody debris volumes in a conservation area. Forest Ecology and Management, 255(8-9): 3288-3296.
Petrie, G. and Toth, C.K., 2009a. 1. Introduction to Laser Ranging, Profiling, and Scanning. Topographic Laser Ranging And Scanning: principles and processing. CRC Press, Boca Raton.
Petrie, G. and Toth, C.K., 2009b. 3. Terrestrial Laser Scanners. In: J. Shan and C.K. Toth (Editors), Topographic Laser Ranging And Scanning: principles and processing. CRC Press, Boca Raton.

Pfeifer, N. and Mandlburger, G., 2009. 11. LiDAR Data Filtering and DTM Generation. Topographic Laser Ranging And Scanning: principles and processing. CRC Press, Boca Raton.
Psyllakis, J.M. and Gillingham, M.P., 2009. Using forest structure and composition to predict the occurrence of vertebrate species in Douglas-Fir forests of British Columbia. Biological Conservation, 142(7): 1427-1441.
Riaño, D., Meier, E., Allgöwer, B., Chuvieco, E. and Ustin, S.L., 2003. Modeling airborne laser scanning data for the spatial generation of critical forest parameters in fire behavior modeling. Remote Sensing of Environment, 86(2): 177-186.
Riaño, D., Valladares, F., Condés, S. and Chuvieco, E., 2004. Estimation of leaf area index and covered ground from airborne laser scanner (Lidar) in two contrasting forests. Agricultural and Forest Meteorology, 124(3-4): 269-275.
Richards, P.W., 1939. Ecological Studies on the Rain Forest of Southern Nigeria: I. The Structure and Floristic Composition of the Primary Forest. The Journal of Ecology, 27(1): 1-61.
RIEGL, 2006. Airborne Data-Processing Software for Full Waveform Analysis RiANALYZE 560 Version 3.0.8, Austria.
Roberts, S.D. et al., 2005. Estimating individual tree leaf area in loblolly pine plantations using LiDAR-derived measurements of height and crown dimensions. Forest Ecology and Management, 213(1-3): 54-70.
Rosema, A., Verhoef, W., Noorbergen, H. and Borgesius, J.J., 1992. A new forest light interaction model in support of forest monitoring. Remote Sensing of Environment, 42: 23-41.
Rosette, J.A.B., North, P.R.J. and SuÃrez, J.C., 2008. Vegetation height estimates for a mixed temperate forest using satellite laser altimetry. International Journal of Remote Sensing, 29(5): 1475 - 1493.
Schreier, H., Lougheed, J., Tucker, C. and Leckie, D., 1985. Automated measurements of terrain reflection and height variations using an airborne infrared laser system. International Journal of Remote Sensing, 6(1): 101 - 113.
Secretariat of the Convention on Biological Diversity, 2000. Sustaining Life on Earth - How the Convention on Biological Diversity promotes nature and human well-being, Secretariat of the Convention on Biological Diversity.
Secretariat of the Convention on Biological Diversity, 2010. Action for Biodiversity: Towards a society in harmony with nature, Montreal.
Secretariat of the Convention on Biological diversity, U.N.E.P., 2005. Forest Biodiversity.
Seielstad, C., A. and Queen, L., P. , 2003. Using airborne laser altimetry to determine fuel models for estimating fire behavior. Journal of Forestry, 101(4): 10.
Simard, M., Rivera-Monroy, V.H., Mancera-Pineda, J.E., Castañeda-Moya, E. and Twilley, R.R., 2008. A systematic method for 3D mapping of mangrove forests based on Shuttle Radar Topography Mission elevation data, ICEsat/GLAS waveforms and field data: Application to Ciénaga Grande de Santa Marta, Colombia. Remote Sensing of Environment, 112(5): 2131-2144.
Solberg, S. et al., 2009. Mapping LAI in a Norway spruce forest using airborne laser scanning. Remote Sensing of Environment, 113(11): 2317-2327.
Solberg, S., Næsset, E., Hanssen, K.H. and Christiansen, E., 2006. Mapping defoliation during a severe insect attack on Scots pine using airborne laser scanning. Remote Sensing of Environment, 102(3-4): 364-376.
Song, C., 2007. Estimating tree crown size with spatial information of high resolution optical remotely sensed imagery. International Journal of Remote Sensing, 28(15): 3305 - 3322.

Spies, T.A., 1998. Forest Structure: A Key to the Ecosystem. Northwest Science, 72(2).
Sprent, P. and Smeeton, N.C., 2001. Applied nonparametric statistical methods. Chapman & Hall/CRC, Boca Raton, 461 pp.
Stilla, U. and Jutzi, B., 2009. 7. Waveform analysis for Small-Footprint Pulsed Laser Systems. Topographic Laser Ranging And Scanning: principles and processing. CRC Press, Boca Raton.
Stone, J.N. and Porter, J.L., 1998. What is forest Stand Structure and How to Measure it? Northwest Science, 72(2): 2.
Sullivan, T.P., Sullivan, D.S. and Lindgren, P.M.F., 2001. Stand Structure and Small Mammals in Young Lodgepole Pine Forest: 10-Year Results after Thinning. Ecological Applications, 11(4): 1151-1173.
Sun, G., Ranson, K.J., Kimes, D.S., Blair, J.B. and Kovacs, K., 2008. Forest vertical structure from GLAS: An evaluation using LVIS and SRTM data. Remote Sensing of Environment, 112(1): 107-117.
Tanabe, S., Toda, M.J. and Vinokurova, A.V., 2001. Tree shape, forest structure and diversity of drosophilid community: Comparison between boreal and temperate birch forests. Ecological Research, 16(3): 369-385.
The Cradle Coast Natural Resource Management Committee, 2005. Cradle Coast natural Resource Management Strategy, Burnie.
Tomlinson, P.B., 1983. 2. Structural elements of the rain forest. In: F.B. Golley (Editor), Tropical rain forest ecosystems: Structure and function. Ecosystems of the World 14A. Elsevier Scientific Publishing Company, New York.
Tucker, C.J., 1979. Red and Photographic Infrared Linear Combinations for Monitoring Vegetation. Remote Sensing of Environment, 8: 127-150.
van Aardt, J.A.N., Wynne, R.H. and Oderwald, R.G., 2006. Forest volume and biomass estimation using small-footprint lidar-distributional parameters on a per-segment basis. Forest Science, 52(6): 636-649.
Vehmas, M., Eerikäinen, K., Peuhkurinen, J., Packalèn, P. and Maltamo, M., 2009. Identification of boreal forest stands with high herbaceous plant diversity using airborne laser scanning. Forest Ecology and Management, 257(1): 46-53.
Verschuyl, J.P., Hansen, A.J., McWethy, D.B., Sallabanks, R. and Hutto, R.L., 2008. Is the effect of forest structure on bird diversity modified by forest productivity? Ecological Applications, 18(5): 1155-1170.
Vosselman, 2000. Slope based filtering of laser altimetry data, IAPRS XXXIII, B3/2, Amsterdam.
Wagner, W., Hollaus, M., Briese, C. and Ducic, V., 2008. 3D vegetation mapping using small-footprint full-waveform airborne laser scanners. International Journal of Remote Sensing, 29(5): 1433 - 1452.
Wagner, W., Ullrich, A., Ducic, V., Melzer, T. and Studnicka, N., 2006. Gaussian decomposition and calibration of a novel small-footprint full-waveform digitising airborne laser scanner. ISPRS Journal of Photogrammetry and Remote Sensing, 60(2): 100-112.
Walker, J. and Hopkins, M.S., 1990. Vegetation. In: R.C. McDonald, R.F. Isbell, J.G. Speight, J. Walker and M.S. Hopkins (Editors), Australian Soil and Land Survey. Field Handbook. Inkata Press, Melbourne, pp. 58-77.
Wallerman, J. and Holmgren, J., 2007. Estimating field-plot data of forest stands using airborne laser scanning and SPOT HRG data. Remote Sensing of Environment, 110(4): 501-508.

Watson, D.J., 1947. Comparative physiological studies in the growth of field crops: I. Variation in net assimilation rate and leaf area between species and varieties, and within and between years. Annals of Botany, 11(1): 41-76.
Watson, J., Freudenberger, D. and Paull, D., 2001. An Assessment of the Focal-Species Approach for Conserving Birds in Variegated Landscapes in Southeastern Australia. Conservation Biology, 15(5): 1364-1373.
Webb, L.J., Tracey, J.G., Williams, W.T. and Lance, G.N., 1970. Studies in the numerical analysis of complex rain forest communities. V. A comparison of the properties of floristic and physiognomic structural data. Journal of Ecology, 58: 202-232.
Wehr, A., 2009. 4. LiDAR Systems and Calibration. Topographic Laser Ranging And Scanning: principles and processing. CRC Press, Boca Raton.
Wehr, A. and Lohr, U., 1999. Airborne laser scanning--an introduction and overview. ISPRS Journal of Photogrammetry and Remote Sensing, 54(2-3): 68-82.
Wolter, P.T., Townsend, P.A. and Sturtevant, B.R., 2009. Estimation of forest structural parameters using 5 and 10 meter SPOT-5 satellite data. Remote Sensing of Environment, 113(9): 2019-2036.
Yu, X., Hyyppa, J., Kaartinen, H. and Maltamo, M., 2004. Automatic detection of harvested trees and determination of forest growth using airborne laser scanning. Remote Sensing of Environment, 90(4): 451-462.
Yu, X., HyyppÃ, J., Kaartinen, H., Maltamo, M. and HyyppÃ, H., 2008. Obtaining plotwise mean height and volume growth in boreal forests using multi-temporal laser surveys and various change detection techniques. International Journal of Remote Sensing, 29(5): 1367 - 1386.
Zhao, K. and Popescu, S., 2009. Lidar-based mapping of leaf area index and its use for validating GLOBCARBON satellite LAI product in a temperate forest of the southern USA. Remote Sensing of Environment, 113(8): 1628-1645.
Zhao, K., Popescu, S. and Nelson, R., 2009. Lidar remote sensing of forest biomass: A scale-invariant estimation approach using airborne lasers. Remote Sensing of Environment, 113(1): 182-196.
Zimble, D.A. et al., 2003. Characterizing vertical forest structure using small-footprint airborne LiDAR. Remote Sensing of Environment, 87(2-3): 171-182.

APPENDICES

This section contains the appendices referred to throughout the thesis. The appendices are:

Photographic guide used to assess per cent foliage cover

Field data collection fieldwork sheets

1. Photographic guide used to assess per cent foliage cover

The photographic guide was used to assess canopy per cent foliage cover at each assessment point: "canopy cover" in the LiDAR discrete return system experiment (Chapter 3) and "*CC_1*" in the LiDAR full waveform system experiment (Chapter 4). It provides some level of direction to assessors when determining the canopy per cent foliage cover at an assessment point and relate to Eucalypt species, which are dominant in the study areas. The photographic guide is a published guide and has been used widely in Australia.

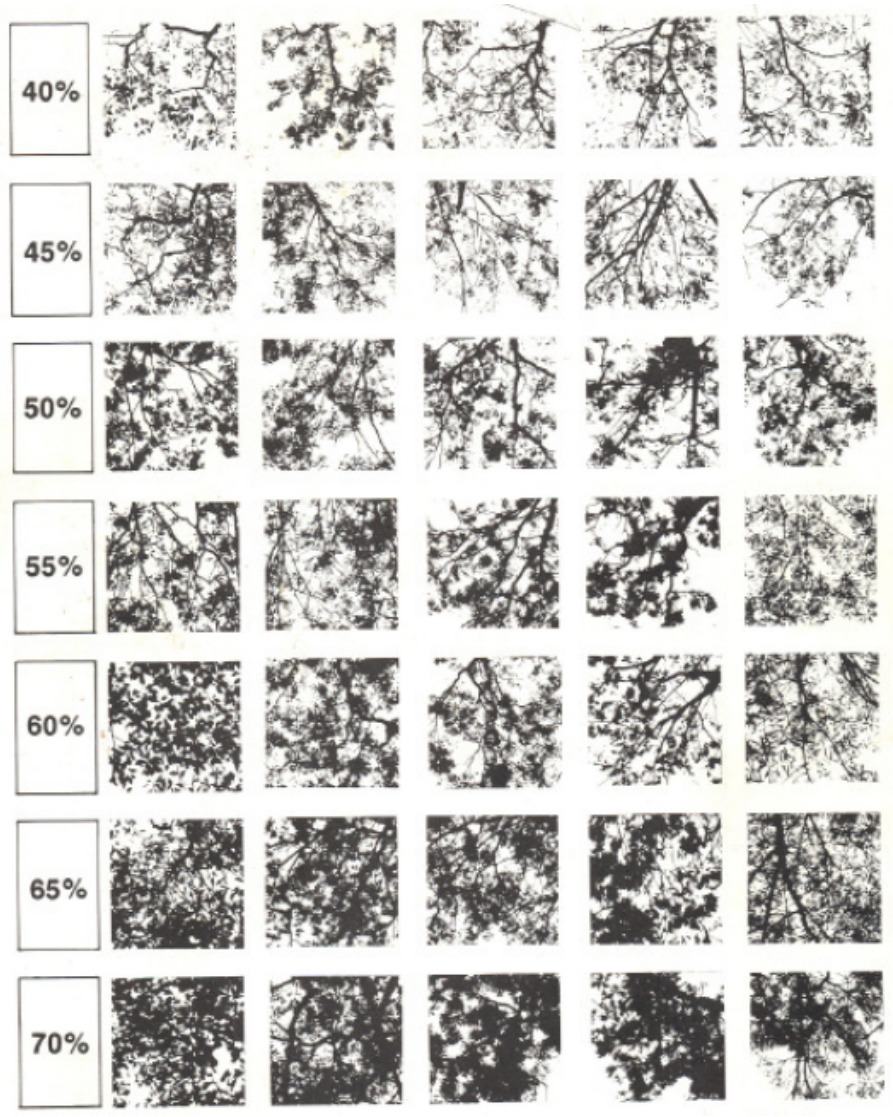

Figure 1 Photographic guide used to assess canopy per cent foliage cover (Walker and Hopkins 1990).

Reference

Walker, J. and Hopkins, M.S., 1990. Vegetation. In: R.C. McDonald, R.F. Isbell, J.G. Speight, J. Walker and M.S. Hopkins (Editors), Australian Soil and Land Survey. Field Handbook. Inkata Press, Melbourne, pp. 58-77.

2. Field data collection fieldwork sheets

The following fieldwork sheets were used to record field data information for each assessment point in a plot for the LiDAR full waveform experiment (Chapter 4). The recorded data in the hardcopy versions of the fieldwork sheets were used to compute field variables later in the lab.

Assessment points

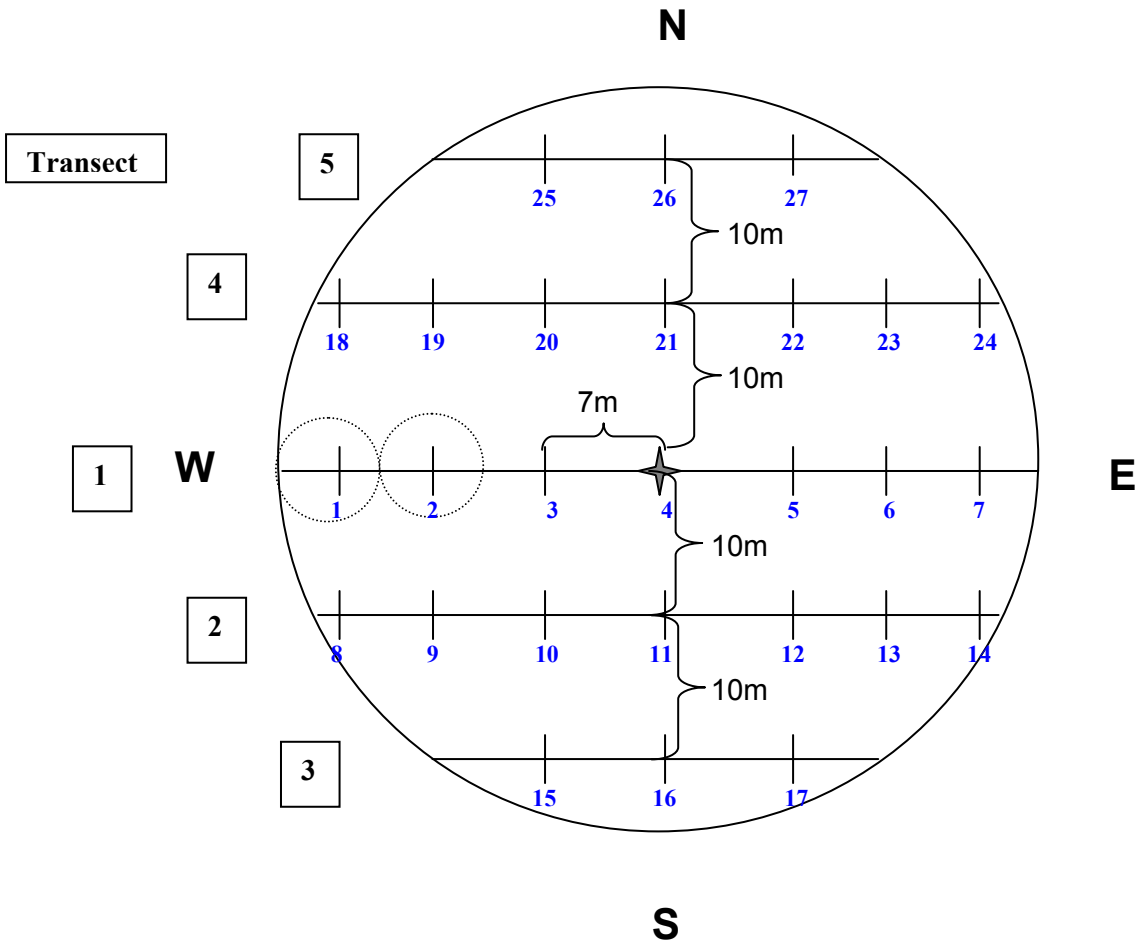

Canopy cover assessment

Site		Date		Weather	
Assessor		Time			

Transect	Point	Photo ID	Coverage %	Comments
1	1			
	2			
	3			
	4			
	5			
	6			
	7			
2	8			
	9			
	10			
	11			
	12			
	13			
	14			
3	15			
	16			
	17			
4	18			
	19			
	20			
	21			
	22			
	23			
	24			
5	25			
	26			
	27			

Foliage density recording

Low veg

Direction	Photo ID	Comments
1		
2		
3		
4		
5		
6		

Medium veg

Direction	Photo ID	Comments
1		
2		
3		
4		
5		
6		

High veg

Direction	Photo ID	Comments
1		
2		
3		
4		
5		
6		

Ground cover (%) assessment

Site		Date		Weather	
Assessor		Time			

Transect	Point	Bare ground	Grass	Litter	Low veg (0-1m)	Comments
1	1					
	2					
	3					
	4					
	5					
	6					
	7					
2	8					
	9					
	10					
	11					
	12					
	13					
	14					
3	15					
	16					
	17					
4	18					
	19					
	20					
	21					
	22					
	23					
	24					
5	25					
	26					
	27					

Coarse Woody debris assessment

Site		Date		Weather	
Assessor		Time			

Transect	Diameter (cm)	Length (m)	Diameter (cm)	Length (m)	Comments
1					
2					
3					
4					
5					

Vegetation height assessment

Site		Date		Weather	
Assessor		Time		GPS	

Direction	Top (m)	1st branch (m)	DBH (cm)	Top	1st branch	DBH
N						
W						
S						
E						

Site memo

Date		Site		Assessor